Evaluation of Platooning Efficiency for Heavy Duty Trucks using Cooperative Adaptive Cruise Control

by

Patrick Smith

A thesis submitted to the Graduate Faculty of
Auburn University
in partial fulfillment of the
requirements for the Degree of
Master of Science

Auburn, Alabama
May 2, 2020

Keywords: Truck Platooning, CACC, Vehicle Automation, Fuel Savings, Coastdown Test, Aerodynamic Drag Reduction

Approved by

David Bevly, Chair, Bill and Lana McNair Endowed Professor of Mechanical Engineering
Mark Hoffman, Assistant Professor of Mechanical Engineering
Brian McAuliffe, Senior Research Officer at National Research Council Canada

Abstract

This thesis presents an evaluation of heavy duty truck platooning efficiency through fuel and coastdown testing. The trucking industry accounts for nearly 70% of the freight shipped in the United States. These heavy duty vehicles travel on average 5x more miles than passenger vehicles and consume billions of gallons of fuel. The trucking industry has a large potential for vehicle automation to achieve benefits such as reduced traffic congestion, increased safety, and reduced fuel consumption and greenhouse gas emissions. Cooperative Adaptive Cruise Control (CACC) is a vehicle automation system that allows two or more vehicles to act cooperatively by using Vehicle to Vehicle communication. This thesis describes a CACC system implemented on two heavy duty trucks to travel in close proximity to each other, or platoon. The main benefit of CACC truck platooning is fuel savings from aerodynamic drag reduction.

The CACC system was evaluated through a series of test campaigns in order to study the benefits of truck platooning. An extensive fuel test was completed on a test track to study the fuel savings in a controlled environment. The nominal, aligned platoon was evaluated and the results were similar in magnitude and trends to prior work. Additionally, mixed traffic scenarios were tested with a forward pattern of passenger vehicles and a heavy duty truck to provide more realistic conditions like those experienced on-road. A novel aerodynamic evaluation, the controlled platoon coastdown, was then completed to quantify the drag area reduction of truck platooning. Previously, prior research described that coastdown testing could not be applied to platoons of vehicles because there is no method to maintain the gap distance between vehicles. In this thesis, the CACC system was modified to maintain the gap distance and complete a platoon coastdown in the lead and following vehicle positions. The drag area reductions for the following vehicle were distinct and significant in magnitude, 17 - 23% for the gap distances tested. The calculated drag reductions were also converted to an estimated fuel savings for comparison to the fuel test, and the results were within about 2% of each other. In an effort to extend this work, a final test campaign was completed for on-road platooning. The highway

fuel test is introduced, and the basic gravimetric results are presented. The fuel savings were lower than expected based on similar track-based tests, but the results are put into context with a study of the amount of traffic and platoon interactions. Future improvements to the CACC system and further evaluations of this truck platooning system are discussed.

Acknowledgments

I would like to thank my family and friends for their support and encouragement during my academic endeavors. I am incredibly blessed to be surrounded by these people over the years. In particular, I am grateful for the love and support of Bridget who most certainly helped me through this process. Also, I have to thank my brother Ryan for previously getting his Masters degree, or I may not have aspired to do the same. The playing field is now level again.

I would also like to thank my advisor, David Bevly, for the oppurtunity to further my education and challenge myself with interesting research projects. These projects would also not be possible without the funding agencies I have worked on projects for including the US Army TARDEC, FPInnovations, Transport Canada, and FHWA among others. This work has carried me to places I never thought I may go such as Detroit test tracks, NCAT at any or all hours of the day, and the depths of the Canadian forest. I appreciate the vote of confidence in the GAVLAB and enjoyed the folks I met along the way.

I have to acknowledgment my colleagues who I hold in high esteem for mentoring me. In particular, I thank Grant Apperson and Dan Pierce for their countless time and help when working on the truck projects. They also made work enjoyable and aren't afraid to drink coffee any time of day. I also must mention the other lab compadres who made graduate school and Auburn more enjoyable. This includes the Siberia office with Tanner, Troupe, Kamraths x3, and Jake among others like Robert, Houston, Tanner W, and many more.

This thesis would not be possible without the countless hours of testing and evaluation. I had the pleasure of working with a fellow Auburn engineer, James Johnson, as our professional driver. James made every bit of testing fun and/or interesting and I thank him for that. I also thank the NCAT test track and drivers for their help as well.

"I have learned a lot of things in life, but not all those things were written down in a book." -James Johnson, 2019. I resonate with this statement and look forward to continue learning from others as I turn this proverbial page and start a new chapter of my life.

Table of Contents

List of Figures

List of Tables

List of Abbreviations

β	Bearing angle
$\dot{v_f}$	Fuel rate
ϕ	Grade angle
ψ	Yaw angle, relative wind direction
ρ	Air density
τ_i	Controller time constants
A	Frontal area
a	Acceleration
b_{eff}	Effective damping
b_i	Damping
C_D	Drag coefficient
$C_D A$	Drag Area
C_f	Fuel rate calibration constant
C_{RR}	Coefficient of Rolling Resistance
e	Error
F_i	Force

F_{aero} Aerodynamic drag force

F_{grade} Road grade force

F_{mech} Mechanical resistance force

F_{RL} Road load force

F_{RR} Rolling resistance force

h Headway or range

I_i Inertia

k_P, k_I, k_D Proportional, Integral, Derivative Gains

m_f Mass of fuel

m_{eff} Effective mass

n Number of tires

n_i Gear ratio

Q Dynamic pressure of the wind

R_{eff} Effective radius

$R_{RR}(v)$ Velocity dependent component of rolling resistance

t Time

T_i Torque

U Relative wind speed

V Volume of fuel

v Vehicle speed

v_i Velocity

W Weight

x Range

ACC Adaptive Cruise Control

CACC Cooperative Adaptive Cruise Control

CAN Controller Area Network

CC Cruise Control

CCW Counter-Clockwise

CFD Computational Fluid Dynamics

CI Confidence Interval

CW Clockwise

DRTK Dynamic-Base Real Time Kinematic

DSRC Dedicated Short Range Communication

ECM Electronic Control Module

ECU Electronic Control Unit

EOM Equation of Motion

EPA Environmental Protection Agency

FBD Free Body Diagram

FHWA Federal Highway Administration

FOV Field of View

FOV Field of View

GAVLAB GPS and Vehicle Dynamics Lab

GEM Greenhouse gas Emissions Model

GHG Greenhouse Gas

GPS Global Positioning System

GVWR Gross Vehicle Weight Rating

NCAT National Center for Asphalt Technology

NHTSA National Highway Traffic Safety Administration

NRC National Research Council Canada

PID Proportional Integral Derivative

RADAR Radio Detection and Ranging

ROS Robotic Operating System

RPV Relative Position Vector

RTK Real Time Kinematic

SAE Society of Automotive Engineers

V2V Vehicle 2 Vehicle

WB Wheelbase

Chapter 1

Introduction

1.1 Background and Motivation

The transportation sector is an important part of modern society and often is an indicator of economic strength. According to the U.S. Department of Commerce, the transportation sector "links producers and consumers" through several modes such as air delivery, logistics, railroad freight, maritime, and trucking [1]. In 2017, a total of 15.78 billion tons of freight was shipped in the United States, and a breakdown of the freight by industry is shown in Figure 1.1. The trucking industry accounts for the most freight with 10.7 billion tons, or 68.1% of the total weight of freight moved [2]. The trucks in this category belong to a vehicle class based on

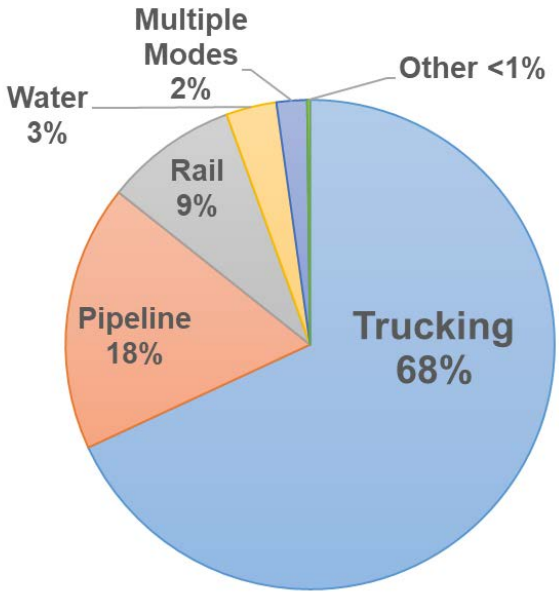

Figure 1.1: Percentage of freight shipped by industry in 2017 with data from [2].

their Gross Vehicle Weight Rating (GVWR) as defined by the Federal Highway Administration (FHWA). The majority of truck freight is hauled by Class 8, heavy duty trucks that have a GVWR rating of >33,001 lbs [3]. These vehicles are often called tractor-trailers or combination vehicles and typically have a large diesel engine to power them.

Heavy duty trucks travel a large distance to deliver freight to consumers. In 2017, tractor-trailers traveled over 184 billion miles, with an average of 62,751 miles per each vehicle. For comparison, the miles traveled per vehicle type are shown in Figure 1.2. Combination vehicles travel over 3.5 times more miles per vehicle than the next biggest type (buses) and nearly 5.5 times more than typical passenger vehicles (light duty with short wheelbase (WB)) [4]. As a result of the long distance traveled, heavy duty trucks consumed over 30 billion gallons of fuel in 2017. They are also the least fuel efficient vehicle type with an average consumption of 6.0 miles per gallon [4].

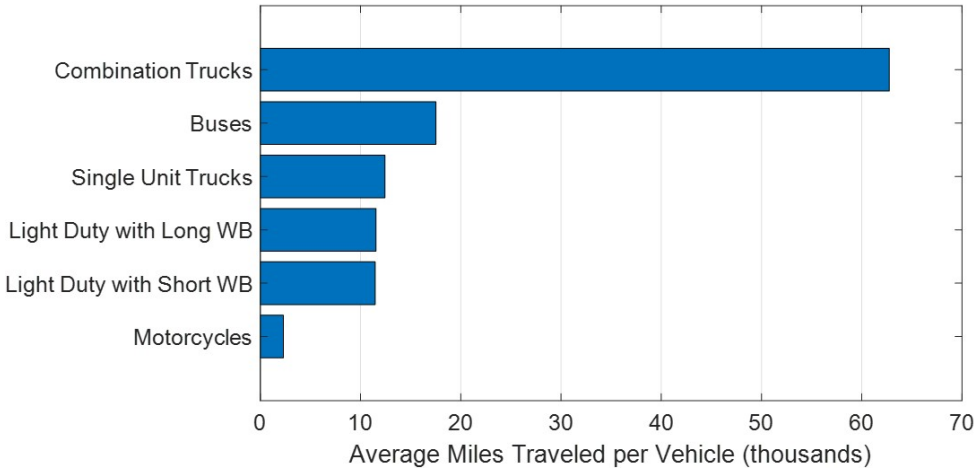

Figure 1.2: Average miles traveled per vehicle group in 2017 with data from [4].

Over the past decade, the trucking industry has received significant attention because of its importance, high utilization, and low fuel efficiency. In the United States, the President issued a memorandum in 2010 calling for vehicles to improve fuel efficiency and lessen their impact on the environment. As a result, the Environmental Protection Agency (EPA) and the National Highway Traffic Safety Administration (NHTSA) formed the rules and regulations called “Greenhouse Gas Emissions Standards and Fuel Efficiency Standards for Medium- and

Heavy-Duty Engines and Vehicles" to meet this goal [3]. This regulation, known as Greenhouse Gas (GHG) Phase I, described the procedures and metrics that truck manufacturers must follow to certify their vehicles. The Phase I rule also discusses the types of losses that a combination vehicle experiences. At 65 mph, a combination vehicle's losses are estimated as 53% aerodynamic, 32% rolling resistance, 6% driveline, and 9% auxiliary loads [3]. The regulations on tractor-trailers has spurred significant research and development into aerodynamic and fuel reduction technologies.

A number of truck technologies have been developed with the goal of increased efficiency, and many of these technologies are summarized in [5]. The main technologies can be categorized into three groups: device, vehicle, and driveline. The device technologies are changes to the external tractor-trailer vehicle. Aerodynamic drag reduction devices include tractor fairings and trailer side skirts and boat tails. Lower rolling resistance tires are another example of a device. Vehicle technologies are changes to the how the vehicle operates to improve efficiency. Typically, vehicle technology includes some form of automated control which replaces some function of the driver. For example, cruise control (CC) is a vehicle technology that replaces the throttle/speed control of the driver. Another example is a speed governor which limits the maximum speed of the vehicle. Lastly, driveline technology can improve vehicle efficiency. This group is often associated with fuel and lubrication, but a large change to the driveline is the automated manual transmission. Engine development is also included in this category, and engine related technology has been developed for air handling, combustion, and aftertreatment.

The previously described technologies were developed to reduce GHG emissions or fuel consumption of trucks. GHG Phase I introduced the methodology to evaluate these technologies and certify vehicles based on the Greenhouse gas Emissions Model (GEM). In 2016, GHG Phase II [6] was introduced, building off the original regulations and improving the GEM. In general, a user inputs the vehicle parameters (coefficient of drag, tire rolling resistance, weight reduction, and idle reduction) and the GEM outputs the fuel and GHG parameters for vehicle compliance. More specifically, the output values are used by the manufacturer for reporting their fleet-average GHG emissions, which in aggregate defines whether they comply with the regulation. The GEM necessitates the determination of vehicle parameters, namely the drag

coefficient and the coefficient of rolling resistance, to input into the model. Therefore, GHG Phase II describes a variety of evaluation methods to solve for these parameters by using experimental or simulated tests.

Beyond technologies for a single vehicle, two or more vehicles traveling in close proximity to each other can achieve aerodynamic drag reduction. This concept is known as drafting, or platooning, and has been used in sports for decades. In motor sports, such as NASCAR and Formula 1, this aerodynamic benefit is typically known as drafting and is a critical part of the fuel saving strategy [7]. Additionally, cycling uses the drafting technique when two or more cyclists travel in a group, or peloton [8]. In sports, these benefits are achieved by professional drivers, but the same benefits exist for on-road vehicles.

Advances in vehicle automation also have the potential to impact fuel consumption and GHG emissions. Specifically, a class of vehicle automation called Cooperative Adaptive Cruise Control (CACC) is designed for two or more vehicles to operate cooperatively together. One application of CACC is vehicle platooning, where two or more vehicles are "connected" to achieve close following distances. In recent years, heavy duty truck platooning has gained interest for its fuel saving potential. Fuel savings and other benefits, such as reduced traffic congestion and increased safety, have spurred a significant amount of research and development in vehicle automation like CACC.

1.2 Prior Research

As previously discussed, tractor-trailers are an important part of the transportation sector and have a need to improve their fuel consumption and GHG emissions. A number of vehicle technologies have been developed, but vehicle automation is another approach to help improve truck efficiency. Technology advances have developed the need to quantify their impact, e.g. reduced rolling resistance, air drag, or fuel savings, and have led to a number of evaluation methods. This section provides an overview of CACC systems and methods for evaluating vehicle platoon benefits.

Adaptive Cruise Control (ACC) is a commercially available driver assistance technology that builds on the functionality of standard CC. ACC uses a ranging sensor, such as RADAR,

to detect forward vehicles and adjust the vehicle's speed relative to the forward vehicle. A vehicle with ACC can follow, or "platoon", with another vehicle, but prior research shows that three or more vehicles with ACC following can be unstable [9]. Cooperative Adaptive Cruise Control is an extension of ACC that uses a Vehicle 2 Vehicle (V2V) network to share information between vehicles. CACC combines sensor data, communicated information, and automated vehicle control for a variety of applications. The idea of CACC has been around for decades [10], but Naus et al. in 2010 was one of the first practical implementations with several passenger vehicles [11]. Overall, CACC systems can be classified by their functions or automation levels as defined by the Society of Automotive Engineers (SAE) [12]. For example, longitudinal control, i.e. vehicle throttle and braking, is SAE Level 1 and longitudinal plus lateral control, i.e. steering, is defined as SAE Level 2.

Many experimental implementations of CACC systems exist for heavy duty trucks. Tsugawa et al. cover several examples of CACC systems including the Energy ITS project in Japan, the KONVOI project in Germany, and PATH in the United States [13]. Additionally, Auburn University has developed a CACC system for the heavy duty trucks shown in Figure 1.3 [14], [15], [16]. Overall, these CACC systems have differing capabilities and applications but most have common features like automated longitudinal control. The goal of the longitudinal

Figure 1.3: Auburn University Peterbilt 579 trucks with CACC platooning system. Reprinted with permission from [14]. ©SAE International.

control system is to maintain the set speed and follow a preceding vehicle at a specific headway, defined in terms of length or time gap. In the context of this thesis, platooning occurs when the controlled headway between two vehicles decreases such that the vehicles experience aerodynamic effects from each other. Specifically, platooning results in two aerodynamic drag reduction effects described by McAuliffe et al. [17]. The platoon following vehicle experiences a relatively lower airspeed due to the wake of the lead vehicle, and the platoon lead vehicle experiences a "push" from the high pressure region created in front of the following vehicle [17]. These two effects are influenced by a number of factors, specifically the inter-vehicle separation distance.

The development of truck platooning, drag reduction, and fuel saving technologies has necessitated evaluation methods to quantify the performance improvements. There are two types of evaluation methods: simulation or experimental. Simulation methods are a representation of the physical system or vehicle, and two of the most common types are wind tunnel testing and Computational Fluid Dynamics (CFD) . Wind tunnel testing is an aerodynamic evaluation where a vehicle, or scaled model, is placed in a wind tunnel which simulates the environment a vehicle experiences on the road. Wind tunnel testing has previously been used to study trailer side-skirts and boat-tails designs [18], two and three truck platoons [19] - [20], and truck platooning with mixed traffic around the platoon [21]. Wind tunnel testing allows for greater flexibility in the type of orientation and setup of a test but is challenging to properly recreate all the conditions experienced by a single vehicle or platoon.

CFD is another simulation-based evaluation method that uses modeling and computer software to simulate the flow characteristics around vehicles. A CFD study can be very diverse and prior research has studied many characteristics of the simulation: steady state vs. transient analyis, vehicle model fidelity, and different computational solvers. This simulation method has also been used to study two truck [22], three truck [23] - [24], and four truck platoons [25]. A visualization of the CFD pressure fields, shown in Figure 1.4, illustrates the reduction in pressure for each platooning truck [25]. CFD is a powerful analysis tool but requires expertise to setup the simulation and resources for the computations to be solved in an efficient amount of time.

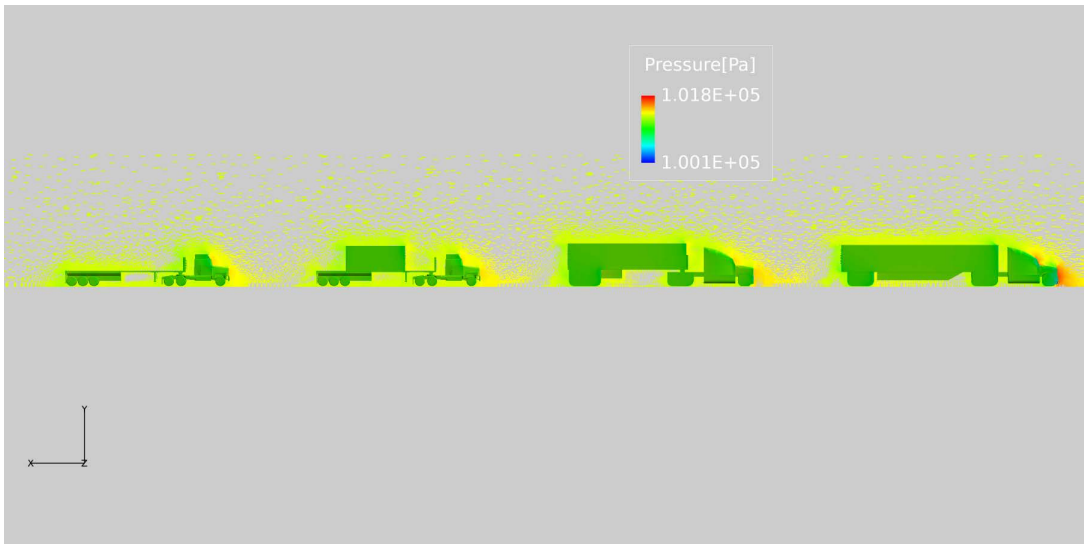

Figure 1.4: CFD visualization of pressure field of four truck platoon. Reprinted with permission from [25]. ©SAE International.

In addition to simulation testing, there are a number of experimental evaluation methods. For truck platooning, one of the main benefits is the fuel savings, and a number of studies have experimentally quantified these savings through extensive fuel tests [17], [26], [27]. These tests used a modified SAE J1321 fuel testing procedure [28] and each studied a variety of parameters as a function of platoon gap distance. This SAE standard is typically used to evaluate a single vehicle but was modified to study the effect of platooning from two or more vehicles. Overall, the results show platoon fuel savings across all gap distances, with the following vehicle having a much higher magnitude of savings. Additionally, an unexpected trend occurred in the tests: the following vehicle's savings dips as the following distance decreased. For example, Bevly et al. shows the following vehicle's fuel savings of $10.2 \pm 0.5\%$ at 50 ft, $9.8 \pm 0.7\%$ at 40 ft, and $8.7 \pm 0.8\%$ at 30 ft [26]. This discrepancy has motivated the use of alternative evaluation methods, including the previously mentioned simulation-based techniques, to further study platooning. One goal of alternative methods is to understand the physical mechanism causing the decrease in savings for the platoon following vehicle.

Fuel testing is a direct measurement of the fuel-saving potential of a technology, like truck platooning. Other experimental test procedures can quantify aerodynamic parameters, providing more insight into the complex effects of truck platoons. Two of the most common

tests are the coastdown and constant-speed tests. Coastdown testing includes modeling the forces on a vehicle, coasting un-powered (neutral gear) through a speed range, and inferring the resulting road load forces. Constant-speed testing is completed by driving a vehicle at constant speed and measuring the torque exerted to keep the speed constant. Both these methods can be used to solve for the drag area ($C_D A$) and the coefficient of rolling resistance (C_{RR}) . The drag area is simply the coefficient of drag multiplied by the frontal area, and this value is comparable to the simulation-based test results. More specifically, the drag area is the drag force divided by the dynamic pressure of the air, which does not require any geometric information about the vehicle.

In prior research, coastdown and constant speed testing typically have been used to study single vehicles only [29], [30], [31]. Specifically, Gururaja tested five different tractor-trailer combinations using constant-speed testing to help evaluate test procedures for GHG Phase 2 [6], [29]. Ragatz and Thornton also completed coastdown testing of heavy duty trucks and smaller vocational vehicles [30], and Moomen et al. compared coastdown tests of a single vehicle with those determined using a simulation software, TruckSim [31]. In addition, several other researchers have used both types of testing to compare results. Hausberger et al. claim to be the first to compare these two test methodologies when they tested a variety of modifications: tires, trailer technology, and vehicle loading [32]. McAuliffe and Chuang used coastdown and constant-speed testing to compare results and evaluate changes for GHG Phase 2 as well [6]. Specifically, McAuliffe and Chuang evaluated a new method, the "High Low Iteration", to complete coastdown testing rather than the typical regression approach. The results from the two coastdown analysis techniques were found to differ by only 0.2%, and the constant-speed tests were also within 1% compared to the coastdown tests [33].

Although experimental testing is common for single vehicles, very little literature exists for these evaluation methods on platoons of vehicles. Hong et al. were one of the first to document the drag reduction of two platooning passenger vehicles [34]. In Hong's testing, two vehicles were physically attached using a special "tow bar" mechanism and the drag reduction was calculated using a modified coastdown procedure. More recently, Duoba and Fernandez

Canosa completed constant-speed testing for a two vehicle platoon of sedans. During the testing, the lead vehicle was manually operated to modulate the gap distance measured from a LIDAR sensor [35]. The lead vehicle must adjust its relative distance because the following vehicle experiences drag reduction and approaches the lead vehicle as a result [19]. Therefore, the drag reduction measurements are only for the following vehicle from this testing. In this literature review, McAuliffe was the only person to document drag reduction from platooning heavy duty trucks [36]. McAuliffe applied constant-speed analysis to three trucks from a CACC platooning fuel test [17]. In this case, the platoon operated at a constant-speed and the inter-vehicle gap distance was controlled by the CACC system. To the author's knowledge, there has never been a platooning coastdown test completed, especially with heavy duty trucks. Again, Duoba and Fernandez Canosa [35] and McAuliffe [36] demonstrate the need for a control system to allow for coastdown analysis of platooning vehicles. The controlled coastdown of platooning trucks could provide additional insight into the aerodynamic behavior from platooning. Additionally, the controlled coastdown is a novel aerodynamic evaluation of platooning technology.

1.3 Contributions

There have been many prior examples of Cooperative Adaptive Cruise Control and truck platooning. Similarly, there are several evaluations of truck platooning through fuel tests and aerodynamic evaluations. The main goal of this thesis is to describe a CACC system and evaluate the fuel saving and aerodynamic performance of truck platooning. Specific contributions are listed below:

- Provided background and motivation for the efficiency of heavy duty trucks and the need for evaluation methods for these vehicles and associated technologies
- Provided a thorough description of the Auburn University CACC system used for truck platooning
- Described and analyzed results from test track and on-road fuel testing to evaluate the fuel saving potential of platooning

- Implemented a novel method to achieve a platooning controlled coastdown for aerodynamic evaluation
- Described and analyzed results from platooning controlled coastdown for heavy duty trucks

1.4 Thesis Outline

This thesis has five remaining chapters and three appendices. Chapter 2 discusses the components, development, and implementation of the CACC truck platooning system. This chapter also describes the system capabilities. Chapter 3 then documents the test campaign completed to study the fuel saving potential of truck platooning. This extensive fuel test studied a number of factors such as inter-vehicle gap distance and the effect of mixed traffic on truck platoons. Chapter 4 describes an alternative evaluation of platooning through the controlled coastdown test. This chapter describes the CACC system modifications and test procedures used to accomplish the platoon coastdown test. Chapter 5 introduces and discusses an on-road fuel test to provide initial insight for real-world effects of platooning. The basic gravimetric results are provided, and the results are given context with the amount of traffic and platoon interactions during testing. Finally, Chapter 6 summarizes the conclusions of this work and discusses future work. Appendix A gives additional details about the CACC control system. Appendix B provides supplementary information related to the fuel test, including the test procedure and analysis techniques. Appendix C describes relevant information for the coastdown test methodology.

Chapter 2

CACC System Overview

Auburn University's GPS and Vehicle Dynamics Lab (GAVLAB) has developed a CACC system that enables platooning for heavy duty trucks. The system has been designed and implemented on two Peterbilt 579 commercial trucks shown in Figure 2.1. The system capabilities include automated longitudinal control and cut-in detection. The system is defined as SAE Level 1 [12], meaning the system acts as driver assistance, and the throttle and braking are automated while steering and safety checks are completed manually by the driver.

Figure 2.1: Auburn University's Peterbilt 579 heavy duty trucks.

This CACC system has been actively developed over the past four years at Auburn University. The foundation of the system was largely designed and implemented by Apperson [15]. This CACC system implementation is described in Apperson's work and many of the large components are currently the same. This base system was then improved with the design and implementation of an updated longitudinal control system [16]. The updated control system was experimentally tested on highways and off-road environments. Then, an on-road

test campaign was completed on highways surrounding Montreal, Quebec and demonstrated the on-road capability of this system [14]. This paper shows the expected performance of the overall control architecture and also motivates formal fuel testing of this CACC system. This chapter describes the current CACC system used for the duration of this thesis. In the next sections, the system components, hardware and software setup, longitudinal estimation and control, and cut-in detection are described.

2.1 System Components

The CACC system is comprised of three main components: the Dedicated Short Range Communication (DSRC) network, the Upper Level Control, and the By-Wire kit, as shown in Figure 2.2. A description of each component follows.

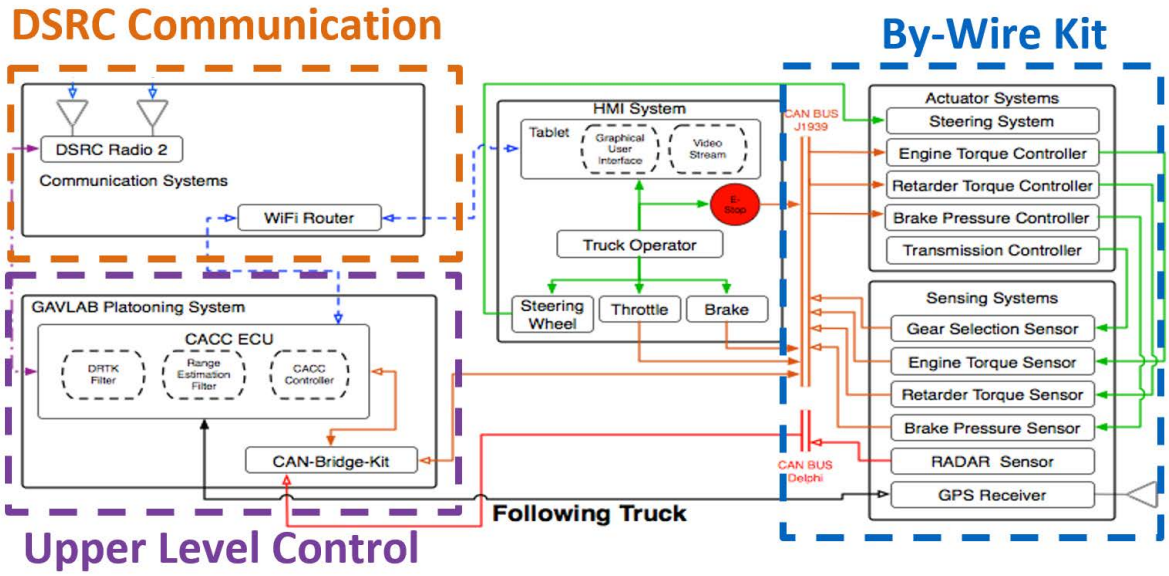

Figure 2.2: CACC system architecture.

2.1.1 DSRC Communication

DSRC radios are used for Vehicle 2 Vehicle (V2V) communication. The 5.9 GHz radios have been used in the automotive/transportation industry as a viable option for wireless communication [37]. A custom UDP packet was defined to share information across the radio network. Vehicle state information, such as vehicle speed, acceleration, and brake status, is

shared across this network for cooperative control. Additionally, GPS observables (pseudorange and carrier phase) are shared and used for relative positioning of the platooning vehicles, as described in the "Range Estimation" section. The vehicle state and GPS information are communicated at 20 Hz and 2 Hz, respectively. Each UDP packet is tagged with a vehicle ID in order to identify to which vehicle the information belongs. All vehicles on this DSRC network have the ability to receive all vehicles' information, but in this thesis, only the preceding vehicle's data is used for Upper Level Control. Additionally, the DSRC software is flexible in order to test new control architectures. For example, new data can be added and existing data can be edited in the UDP packet. This flexible architecture allows for quick development and testing of new components using different data.

2.1.2 Upper Level Control

The Upper Level Control system includes the necessary algorithms and software library for CACC platooning. This system uses the information from the V2V network for estimation and control. The primary objective of the Upper Level Control is to follow the lead vehicle at the specified distance (i.e. longitudinal control). The outputs of the Upper Level Control system are the commands sent to the vehicle for actuation. These commands are the desired engine torque, engine retarder torque, and brake rate. The longitudinal estimation and control systems are detailed further in following sections.

2.1.3 By-Wire Kit

The By-Wire kit is the vehicle software interface needed for automated control. This interface uses a physical Controller Area Network (CAN) connection, which follows the SAE J1939 standard for heavy duty trucks [38]. The software interface includes the ability to read and write data to the vehicle CAN bus. Through this interface, sensor data, such as vehicle speed, current gear, brake status, is read from the various Electronic Control Units (ECUs) . Automated vehicle control is achieved by taking the Upper Level Control output, generating the appropriate CAN message, and sending it to the respective vehicle ECU. For example, the longitudinal controller outputs a desired engine torque command, the by-wire kit creates a

CAN message with this information, and the by-wire kit sends the CAN message to the engine ECU over the physical J1939 CAN connection. As a result, this interface is vehicle specific based off the combination of engine, transmission, and brake system manufacturers. Overall, the CACC system operates similar to the stock Adaptive Cruise Control (ACC) system on the vehicle. The ACC possesses the same functionality needed for automated vehicle control: generating control commands and sending them to the vehicle for actuation. Some parts of the ACC system, e.g. CAN message content and locations, were reverse engineered in order to implement the CACC system [15]. The resulting system does not require external actuators, i.e. to press the throttle, and uses the stock buttons (cruise control on, cruise control set) in the vehicle to engage platooning.

2.2 Hardware and Software Setup

The CACC system has a number of hardware components including a computer, DSRC radio/antennas, GPS receiver/antennas, RADAR , and CAN gateway, as shown in Figure 2.3. A summary of each hardware component is summarized here from [39], and a complete list of the hardware manufacturers and models is given in Table 2.1.

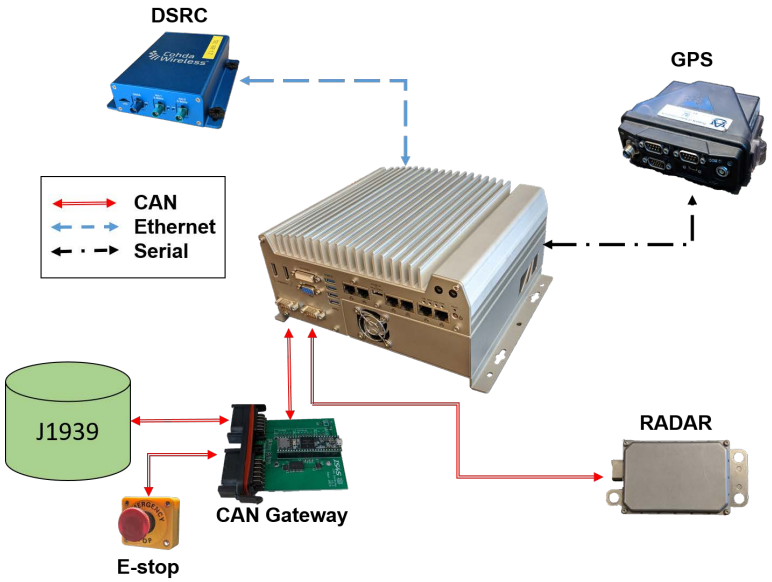

Figure 2.3: Hardware components for CACC system. Reprinted with permission from [39]. ©SAE International; National Renewable Energy Laboratory; National Research Council Canada.

- The central component is a rugged, industrial computer running the Ubuntu 16.04 Linux operating system. The computer is the main processing unit and receives all the sensor and CAN bus data. The system software is also compiled and executed on this computer.
- DSRC radios are used for V2V communication. It is assumed that platooning vehicles have DSRC communication and all other vehicles have no communication to the platoon.
- A dual frequency (L1/L2) GPS receiver is used for position information. Raw GPS observables are also used for GPS relative positioning.
- A forward facing RADAR is used to provide higher frequency range, range rate, and bearing (angular offset) measurements. The RADAR is also used to track neighboring vehicles for cut-in detection between platooning vehicles.
- A device, called the CAN Gateway (custom built by IS4S), is connected between the computer's CAN bus to the rest of the vehicle. The CAN Gateway is used as a physical disconnect of the CACC system from the vehicle. An emergency stop button is also connected to this device to disconnect the CAN bus from the CACC computer. Pressing this button gives full manual control to the driver.

Table 2.1: CACC system hardware manufacturers. Reprinted with permission from [14]. ©SAE International.

Hardware	**Make**	**Model**
Computer	Neousys	Nuvo-5095GC
GPS Receiver	Novatel	FlexPak6
GPS Antenna	Novatel	Pinwheel
RADAR	Delphi	Delphi ESR
DSRC Radio	Cohda Wireless	MK5 OBU
DSRC Antenna	MobileMark	ECOS6-5900DN

The system software is implemented using the Robotic Operating System (ROS) middleware [40]. ROS is used for its ease and flexibility in developing robotic applications. In ROS, software components are written for a specific task, and each task is known as a ROS *node*. The underlying software can be written in a supported programming language (e.g. C++ or

Python) and then implemented in this system using the ROS software library. The main features of ROS include message handling, package structure, and a variety of other features such as visualization, plotting, and data recording.

The CACC system implemented in ROS is shown in Figure 2.4 for a lead and following vehicle. The ROS nodes include sensor drivers, estimation/control algorithms, and the J1939 vehicle interface. The main ROS nodes are shown for each vehicle, with many more nodes on the follower than the leader. On the lead vehicle, the CACC system only needs to collect the relevant data and transmit the V2V data. The following vehicle, however, must collect the same information, process the data for the Upper Level Control algorithms, and generate commands for the By-Wire Kit.

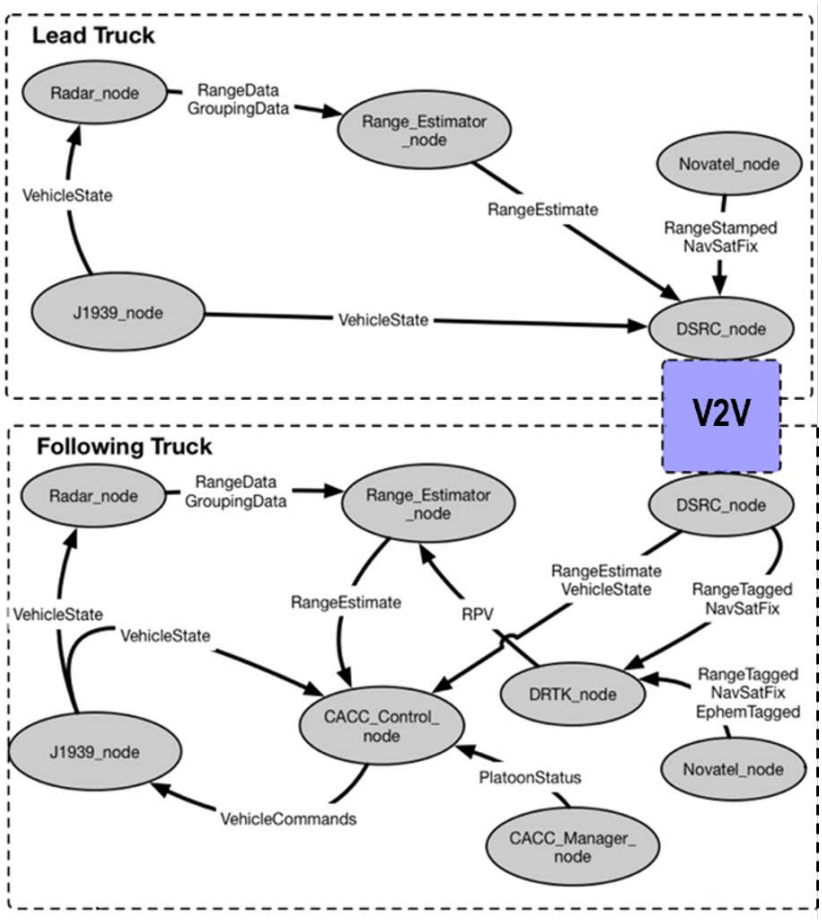

Figure 2.4: CACC software architecture.

2.3 Longitudinal Modeling

The goal of the longitudinal control system is to follow the preceding vehicle at a specified gap distance. The longitudinal system is comprised of the estimation and control algorithms for operation, which have been previously described in [16]. The range, or headway, estimation combines measurements to produce high quality state estimates for feedback control. The control system uses the range estimate, a simple vehicle model, and a classical controller to track the reference, or desired, following distance. The vehicle model used for the controller design is derived from the Free Body Diagram (FBD) and driveline shown in Figure 2.5.

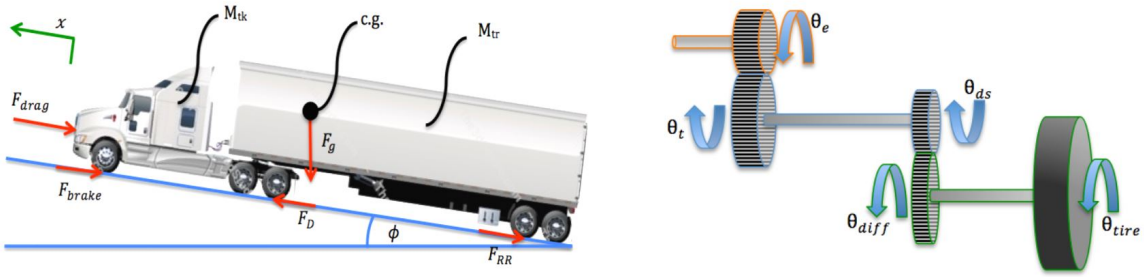

Figure 2.5: Longitudinal vehicle modeling diagrams [15].

The longitudinal dynamics can be solved for by using Newton's 2nd law with the FBD and incorporating the driveline dynamics. The driveline dynamics describe how torque is transmitted from the engine, through the transmission and differential, and to the tire. A full derivation of this model is shown in the Appendix of [15]. The resulting differential equation assuming no wheel slip or driveline compliance is shown as

$$m_{eff}\ddot{x} + b_{eff}\dot{x} = m_{eff}a_{lead} + b_{eff}v_{lead} - \frac{n_{diff}n_{trans}}{R_{eff}}T_{engine} + F_{brake} + F_{RR} + F_{drag} + F_{grade} \tag{2.1}$$

where x is the range, or forward distance. The resistive forces, such as the force of rolling resistance, air drag, and road grade, can also be seen in Equation (2.1). This equation is specific for a following vehicle of the platoon. Thus, the lead vehicle's dynamics are incorporated into this model with the velocity and acceleration terms. The effective mass and damping terms are

defined as

$$m_{eff} = m + \frac{(I_{trans} + I_{ds} + I_{engine} n_{trans}^2) n_{diff}^2 + I_{diff} + I_w}{R_{eff}^2} \tag{2.2}$$

$$b_{eff} = \frac{(b_{trans} + b_{engine} n_{trans}^2) n_{diff}^2 + b_{diff}}{R_{eff}^2} \tag{2.3}$$

where m is the total vehicle mass, I_i are the various intertia components, b_i are the driveline damping components n_i are gear ratios, and R_{eff} is the effective wheel radius. The components include the transmission ($trans$), driveshaft (ds), engine, differential ($diff$), and wheel (w). A summary of the vehicle parameter values used throughout this thesis are shown in Table 2.2. It is important to note that the trailer mass is a variable parameter and is updated when the truck pulls a new trailer. The table shows the trailer mass used for the testing in Chapter 3.

Table 2.2: Vehicle model parameters.

Parameter	**Value**	**Units**
Tractor Mass	8,892	kg
Trailer Mass	20,900	kg
Engine Inertia	2.75	$kg \cdot m^2$
Transmission Inertia	0.13	$kg \cdot m^2$
Drive Shaft Inertia	0.012	$kg \cdot m^2$
Differential Inertia	0.028	$kg \cdot m^2$
Wheel Inertia	1700	$kg \cdot m^2$
Engine Damping	2.21	$\frac{N \cdot m}{s}$
Transmission Damping	1.40	$\frac{N \cdot m}{s}$
Differential Damping	9.7	$\frac{N \cdot m}{s}$
Drag Coefficient	0.79	$-$
Frontal Area	8.01	m^2
Coefficient of Rolling Resistance	0.0045	$-$
Differential Gear Ratio	4.4	$-$
Effective Wheel Radius	0.527	m

2.4 Range Estimation

A high quality range estimate is needed for longitudinal control, and Kalman Filtering is one method to produce the state estimates. The Kalman Filter is known as the "optimal"

estimator and provides a way to combine measurements from differing sources. In this implementation, measurements from relative GPS positioning, a forward facing RADAR, and wheel speed are used.

2.4.1 DRTK

The differential GPS relative positioning technique is known as Dynamic Base Real Time Kinematic (DRTK) . The DRTK algorithm leverages the accuracy of the GPS carrier phase measurements to calculate an inter-vehicle Relative Position Vector (RPV) [41]. This process is similar to Real Time Kinematic (RTK), which exchanges information with a fixed base-station for accurate global positions. In DRTK, two receivers are still used but the "base-station" is mobile, i.e. located on another vehicle. The raw observables of the lead vehicle's GPS receiver are communicated to the following vehicle via DSRC. The observables are differenced across receivers to cancel out atmospheric and other common modes of error. The single differenced observables are used in the measurement update of a Kalman filter for estimating the integer ambiguity in the single differenced carrier phase measurements. After resolving the integer ambiguity, the carrier phase measurements are combined using weighted least-squares to estimate the inter-vehicle RPV [16]. The resulting RPV is an antenna to antenna measurement as shown in Figure 2.6. After taking the antenna offsets, the 3-D RPV can be resolved into a longitudinal component and lateral component. An angular offset, or bearing angle, measurement can also be derived from these components by using the following vehicle's attitude to rotate the RPV into a local vehicle frame.

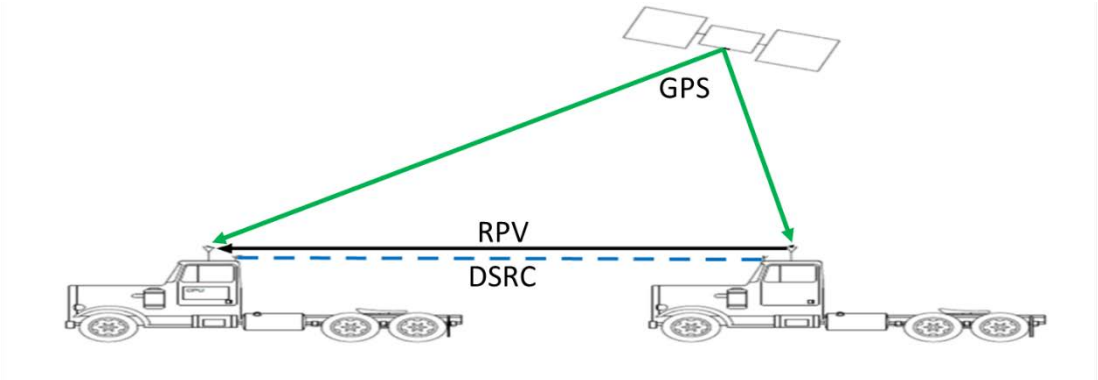

Figure 2.6: DRTK algorithm output RPV measurement.

2.4.2 RADAR

A forward facing RADAR is used for redundant, higher frequency range measurements. In particular, an automotive grade 64 channel RADAR is used, and each channel produces a single data point at each measurement epoch. The RADAR has a mid-range capability of 60 m with a $\pm$ 45 $^\circ$ Field of View (FOV) and a long-range capability of 174 m with $\pm$ 10 $^\circ$ FOV. The RADAR produces range, range rate (i.e. relative speed), and bearing measurements for each channel. A visualization of the RADAR range data is shown in Figure 2.7 for a highway test. The figure shows the following vehicle and RADAR points on the left and a camera image that is taken from the following vehicles perspective at the same time.

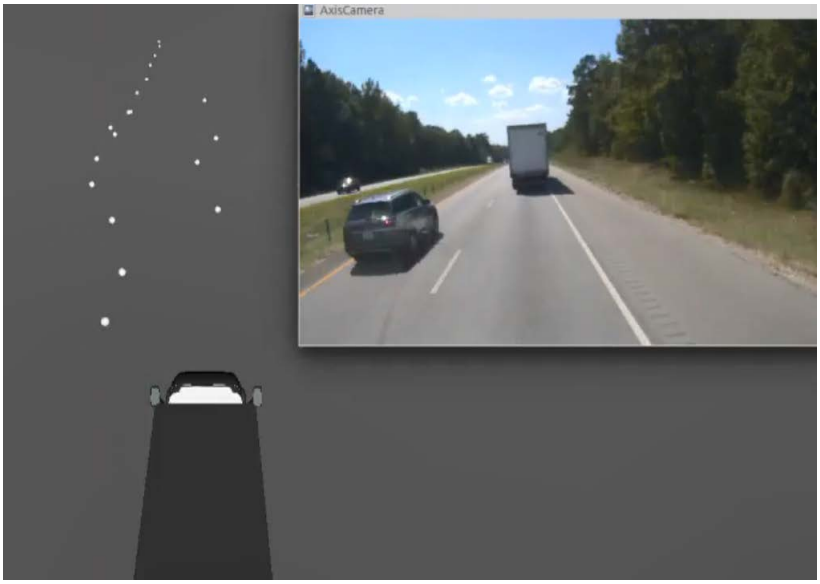

Figure 2.7: Visualization of raw RADAR data and camera image from highway testing.

As shown in Figure 2.7, a number of RADAR points are returned for the lead truck, but there are also a number of points for the neighboring vehicle and guard rail (along the left side of the road). Although the RADAR provides higher frequency measurements, the raw RADAR returns must be filtered and classified in order to use in the estimator. First, all returns that are static objects are removed. Next, the data points of the lead vehicle must be extracted and classified. For example, in Figure 2.7 there are several returns along the length of the lead truck/trailer combination. These points could be returned from the underside of the trailer, trailer axles, tractor, or the desired location, the back of the trailer. In order to classify which

points are valid, a Chi Squared test is used. The Chi Squared test uses the current estimate and measurement covariance to determine if a selected measurement is valid and should be used as a measurement update in the estimator. Figure 2.8 shows how the current state estimate (described in the next section) is used with the measurements of range and range rate to find valid measurements [15]. If measurements are outside of the bounds of the measurement covariance, they are not used. The Chi Squared test is used to eliminate returns and range measurements that do not correspond to the back of the lead vehicle.

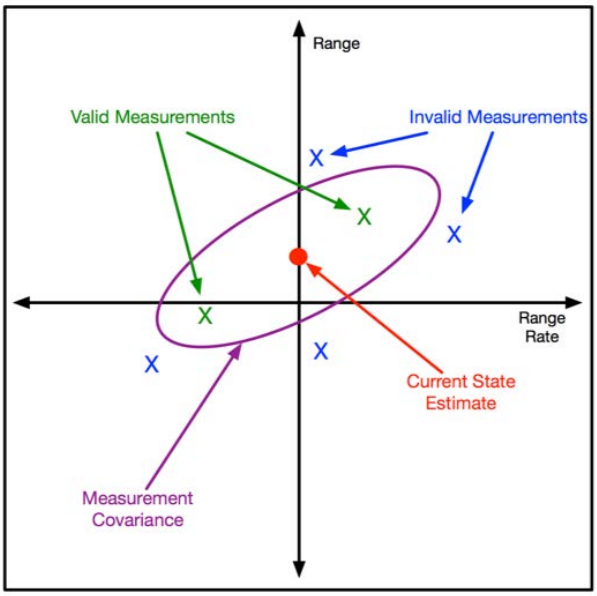

Figure 2.8: Chi Squared test [15].

2.4.3 Wheel Speed

Both the lead and following vehicles' wheel speeds are read from the CAN bus. The leader's speed is read locally and transmitted to the following vehicle over the DSRC network. The pair of wheel speeds (leader/follower) are then differenced to produce another measurement of range rate. The range rate convention used is the leader's speed minus the follower's speed. The wheel speeds provide a non line of sight range rate measurement as long as the vehicles are within range of DSRC communication.

2.4.4 Kalman Filter

The measurements from DRTK, RADAR, and wheel speed, shown in Figure 2.9, are combined in a Kalman Filter. In particular, this filter is used to estimate the inter-vehicle range/headway, range rate, and bearing (state vector $x = [h, \dot{h}, \beta]^T$). The filter assumes constant range rate and bearing angle between measurement epochs. The time update is performed at 20 Hz and predicts a state estimate and estimate covariance. When a measurement is available, the measurement update is applied depending on the measurement source. For a DRTK measurement, the measurement update includes range and bearing information only. For a RADAR measurement, there are two forms of the update. If a RADAR return passes the Chi Squared test, the RADAR point produces a full state update (range, range rate, and bearing). As previously mentioned, there are likely returns from the lead vehicle that do not correspond to the rear-most point of the vehicle. In this case, the range rate is still valid and can be used alone in the measurement update. This technique allows for more data from the RADAR to be used for a better estimate of range rate [16]. Lastly, the wheel speed update produces only a range rate update as previously described. The wheel speeds help the filter if the RADAR loses line of sight to the lead vehicle.

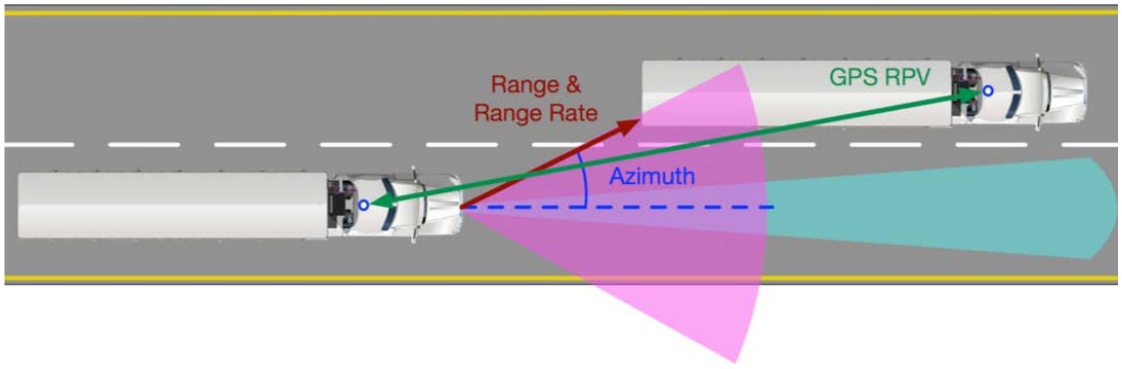

Figure 2.9: Measurement update sources for Kalman Filter [15].

2.5 Longitudinal Control

The goal of the longitudinal control system is to regulate the following vehicle to a set following distance, shown in Figure 2.10. A simple controller was designed in order for quick implementation and ease of tuning.

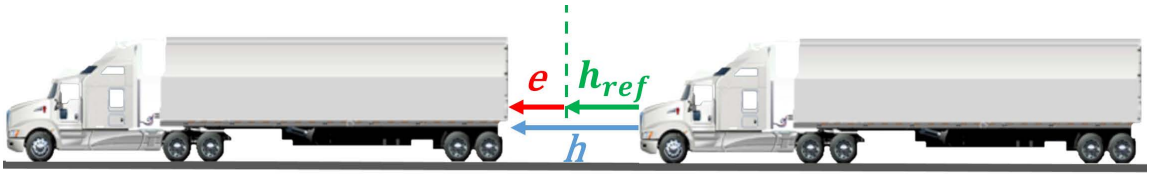

Figure 2.10: Longitudinal control system reference, range estimation feedback, and controller error [16].

The longitudinal system uses a classical Proportional Integral Derivative (PID) controller with feedforward control. The control block diagram is shown in Figure 2.11, where h is the range estimation range, h_{ref} is the input set reference distance, and e is the controller error.

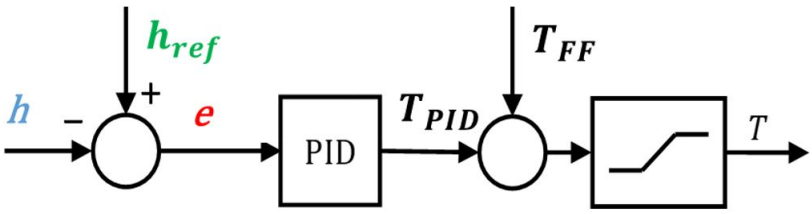

Figure 2.11: Longitudinal control block diagram [16].

In Figure 2.11, there are two torque components: the controller torque and the feedforward torque. The controller torque is shown from [16] as

$$T_{PID} = k_P(h_{ref} - h) + k_I \int (h_{ref} - h)dt + k_D(v - v_{lead}) \tag{2.4}$$

where $(h_{ref} - h)$, $\int (h_{ref} - h)$, and $(v - v_{lead})$ are the error, integral of error, and derivative of error. The controller gains (k_i) are calculated by combining and solving Equations (2.1) and (2.4) and are shown as

$$k_P = -\frac{m_{eff}R_{eff}}{n_{diff}n_{trans}}\left(\frac{1}{\tau_1\tau_2}+\frac{1}{\tau_1\tau_3}+\frac{1}{\tau_2\tau_3}\right) \tag{2.5}$$

$$k_I = -\frac{m_{eff}R_{eff}}{n_{diff}n_{trans}}\frac{1}{\tau_1\tau_2\tau_3} \tag{2.6}$$

$$k_D = -\frac{m_{eff}R_{eff}}{n_{diff}n_{trans}}\left(\frac{1}{\tau_1}+\frac{1}{\tau_2}+\frac{1}{\tau_3}-\frac{b_{eff}}{m_{eff}}\right) \tag{2.7}$$

where τ_i are the desired closed loop time constants. It is important to note that the controller gains are in terms of the model parameters. For example, the current gear ratio, n_{trans}, is present in the controller gain calculation. As a result, the PID controller is gain scheduled based of the current gear, which is read from the CAN bus, and allows for an improved control response. This formulation allows for ease of changing the control response with selection of the time constants. Additionally, vehicle parameters that change, such as the vehicle mass (i.e. when a tractor connects to a different trailer), can easily be accounted for. The controller time constants used throughout this thesis are shown in Table 2.3.

Table 2.3: Controller time constants.

Time Constant	**Value [seconds]**
τ_1	12.5
τ_2	6.25
τ_3	2.5

An example set of controller gains is given in Appendix A. The gain values are negative based on the definition of the controller error. A negative error means the following vehicle is further away than the current reference and a positive value means the vehicle is closer than desired. Therefore, a negative error (multiplied by a negative controller gain) results in a positive torque value for forward motion.

The feedforward torque is used to account for known disturbances to the longitudinal model. The feedforward torque accounts for the lead vehicle dynamics and the resistive forces and is calculated from [16] as

$$T_{FF} = \frac{R_{eff}}{n_{diff} n_{trans}} \left(m_{eff} a_{lead} + b_{eff} v_{lead} + F_{RR} + F_{drag} + F_{grade} \right) \tag{2.8}$$

where the scaling factor outside the parentheses converts the value from a force to a torque value. Measurements of the lead vehicle's dynamics are communicated over DSRC and used in the feedforward calculation. The force of rolling resistance and air drag are calculated from constant parameters (C_{RR} = 0.0050, C_D = 0.79, A = 8.52 m^2) taken from [15] . The force due to road grade can have a significant impact on heavy duty trucks. As a result, an estimate of the grade angle is calculated on-line using GPS velocity [16]:

$$\phi = \tan^{-1} \left(\frac{v_U}{\sqrt{{v_E}^2 + {v_N}^2}} \right) \tag{2.9}$$

where v_E, v_N, v_U represent the East, North, and Up GPS velocities, respectively. The grade estimate is shown in Figure 2.12 and is used in the feedforward torque. In the figure, the estimate is compared to a profilometer that is considered the true value. The GPS estimate produces a reliable value for the current grade angle to be used in the feedforward torque.

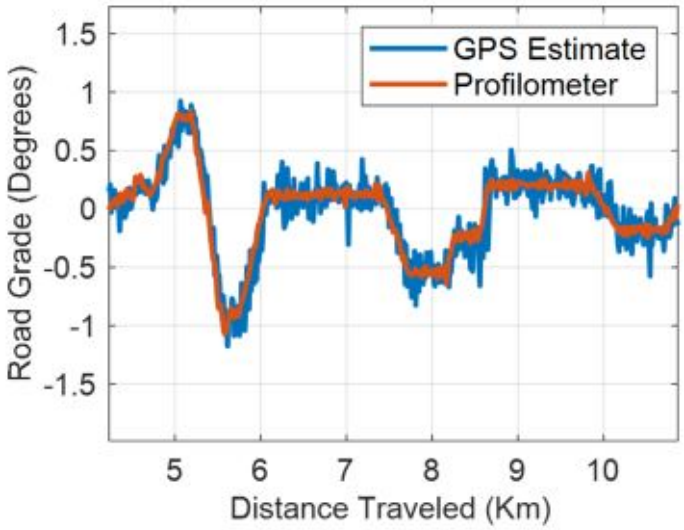

Figure 2.12: Grade angle estimation using GPS velocity [16].

The controller output, T in Figure 2.11, is the sum of the controller and feedforward torques. This torque is then split into desired vehicle commands (engine torque, retarder torque, and brake rate) based on the magnitude and sign. The commands are generated from the logic

shown in Figure 2.13 along with torque threshold parameters, T_i. The amount of a given actuation is changed by the selection of the torque thresholds. In general, a positive controller torque results in a desired engine torque, while the magnitude of a negative torque determines if the retarder only is used or the retarder plus foundation brakes. These desired vehicle commands are the values sent to the By-Wire kit for automated control.

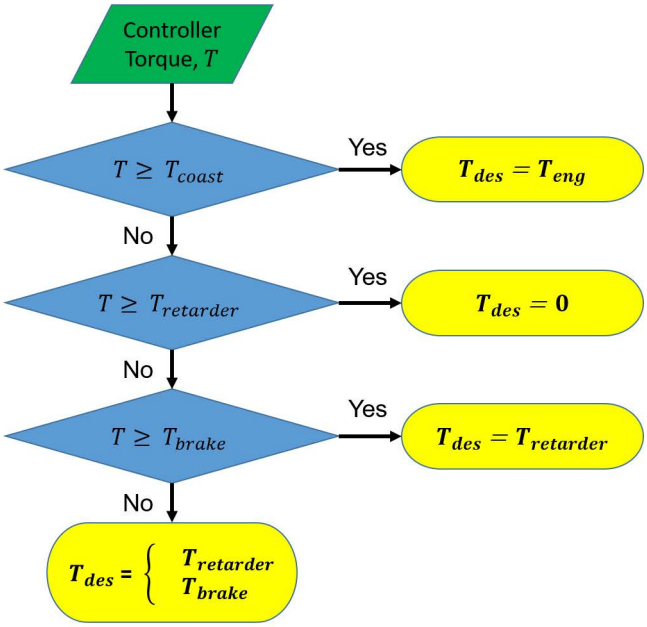

Figure 2.13: Control commands logic.

2.6 Cut-in Detection

In addition to longitudinal control, the CACC system has a cut-in detection feature that was developed for interaction with mixed traffic on a roadway. The cut-in detection is similar to [42] and a brief description is given here. Neighboring vehicles on the roadway can insert themselves in-between two platooning vehicles, i.e. a cut-in. The CACC system tracks and estimates the positions of these neighboring vehicles using the forward facing RADAR. The vehicles' position is estimated using the same range estimation technique previously described, but only using RADAR updates. The following vehicle then projects its predicted forward path using the lead/follow vehicles positions, a nominal lane width, and a pure pursuit model

described in [43]. The cut-in detection then operates by checking if any of the estimated neighboring vehicles' positions are within this predicted forward path, and if so, a cut-in is detected.

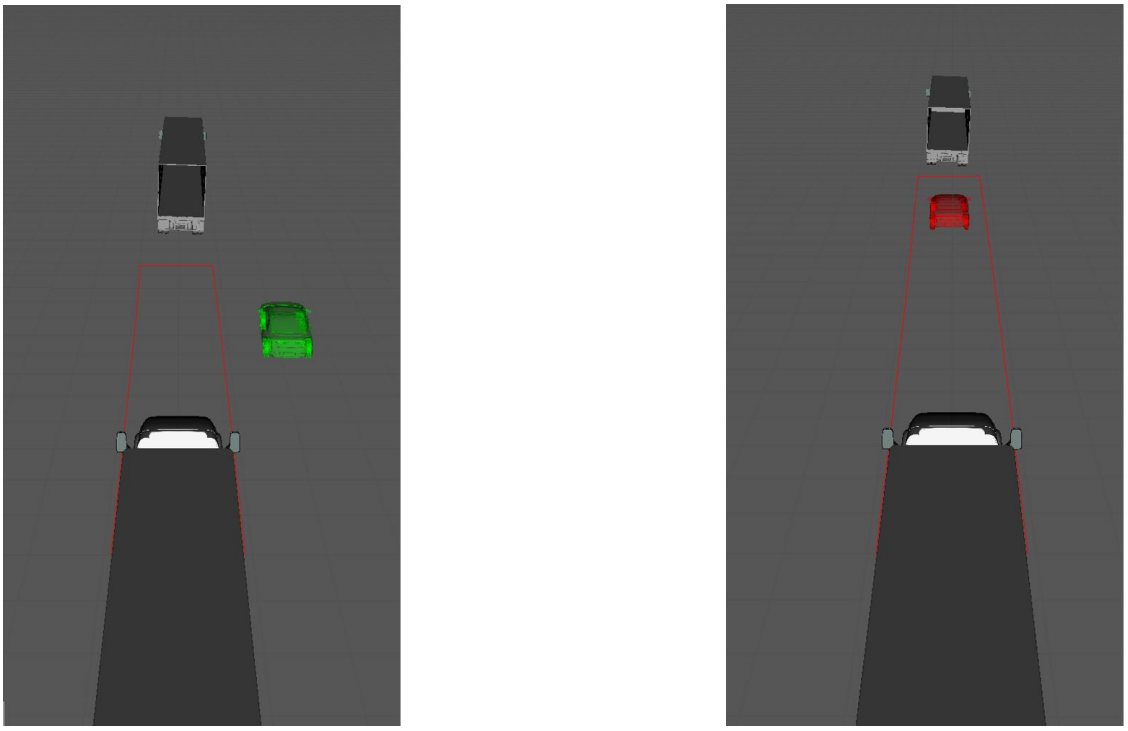

(a) Neighboring vehicle tracking.

(b) Cut-in detected.

Figure 2.14: Predicted forward path and neighboring vehicle estimate and cut-in detection.

An example of the predicted forward path and cut-in detection is shown in Figure 2.14. Figure 2.14a shows the estimated neighboring vehicle's position that is traveling alongside the platoon. Once a cut-in is detected, the following vehicle switches to ACC, measures its range to the vehicle, and falls back to a safe distance relative to it, as shown on the right of Figure 2.14b. In this thesis, the "safe distance" was selected to be the platoon following distance which likely would not be used in a commercial system (i.e. 250 ft). The following vehicle follows in ACC mode until the cut-in vehicle is no longer detected, and CACC mode resumes.

2.7 Conclusions

A Cooperative Adaptive Cruise Control system was developed for truck platooning and an overview of the system was given in this chapter. The system components, including the DSRC communication, upper level control, and by-wire kit were described. In particular, prior research detailed the design and implementation of the estimation and control algorithms used

for this thesis. This CACC system has been previously tested and demonstrates a number of system capabilities, such as longitudinal control and cut-in detection. This chapter summarized the CACC system, and the subsequent chapters provide evaluations of a truck platoon using this system.

Chapter 3

Canada Fuel Test

One of the primary benefits of truck platooning is the fuel savings from two or more vehicles traveling in close proximity. This chapter describes a test campaign to study the fuel saving potential of CACC truck platooning. The vehicles, test site, instrumentation, and test procedures are introduced first. Then, the individual test setups are described, and the results are presented. The aligned platoon results represent the nominal savings of truck platooning. New results are then presented to show the effectiveness of platooning in mixed traffic scenarios. Overall, this chapter is a summary of two published technical papers from the fuel tests [39], [44]. These two papers [39], [44] also document other tests completed, such as the effect of lateral offset and dynamic traffic events, but these are not the focus of this study.

3.1 Background

The test campaign took place in Blainville, Quebec in June of 2019. The testing was completed to study a number of factors including the impact of mixed traffic on truck platoons. In this context, mixed traffic is used to describe a more realistic environment experienced by trucks on-road, rather than an isolated test track. To evaluate the fuel savings, the SAE J1321 Type II procedure was used with gravimetric and fuel rate measurements [28].

3.1.1 Vehicles

Three Class 8 heavy duty trucks were used for the duration of testing. Auburn University's two Peterbilt 579 trucks were used along with a Freightliner Cascadia. All testing was

completed using the Peterbilt trucks as the "test" vehicles and the Freightliner as the "control" vehicle. The test and control vehicles are shown in Figure 3.1, and a summary of the vehicle specifications are shown in Table 3.1. The vehicles were prepared such that they were in top working condition prior to the tests.

(a) Test vehicles A1 and A2.

(b) Control truck.

Figure 3.1: Test vehicles (left) and control (right) vehicle during fuel test. Reprinted with permission from [39]. ©SAE International; National Renewable Energy Laboratory; National Research Council Canada.

Table 3.1: Canada fuel test vehicles specifications.

Specification	**Lead Truck**	**Following Truck**	**Control Truck**
Name	A1	A2	T3
Manufacturer	Peterbilt	Peterbilt	Freightliner
Model	579	579	Cascadia
Year	2015	2015	2016
Engine	Paccar MX-13	Cummins ISX15	Detroit DD15
Brake System	Bendix	Meritor WABCO	WABCO 4s/4m
Transmission	Eaton Fuller Automated 10 speed	Eaton Fuller Automated 10 speed	Detroit DT12-DA-1750
Trailer	Manac 53' Dry-van Trailer + Skirts and Tail	Manac 53' Dry-van Trailer + Skirts and Tail	Manac 53' Dry-van Trailer + Skirts and Tail

Standard 53 ft box trailers were used for the scope of testing described here. The trailers were loaded to represent a typical trailer load with a gross vehicle weight of 29,500 kg (65,000 lbs). Concrete ballasts were evenly placed in the trailer to meet the weight requirement and ensure an even weight distribution. All trailers were equipped with the same aerodynamic reduction features: side skirts and boat tails.

3.1.2 Test Site

Testing was completed on the *BRAVO* test track at the PMG Technologies facility in Blainville, Quebec [45]. This track is 6.5 km (4.0 miles) in length and has a concrete surface. The track is oval shaped with equidistant straight and curved segments. The curved sections are banked such that the driver "rides" the bank by finding the neutral position of the bank and removing their hands from the steering wheel. A top down view of the test facility and track are shown in Figure 3.2 (created using [46]).

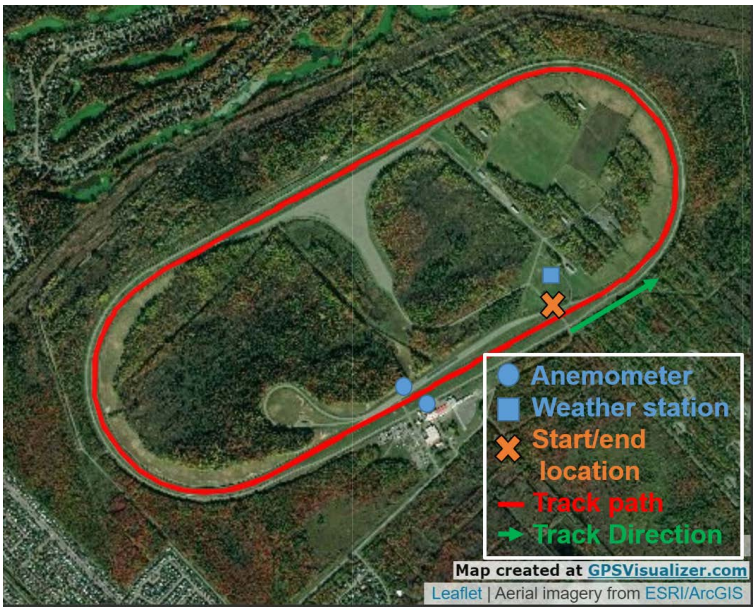

Figure 3.2: Top down view of site for Canada fuel testing.

3.1.3 Instrumentation

Gravimetric fuel measurements were taken for this testing. External fuel tanks were installed on the railing behind the cab and in front of the truck's fifth wheel, as shown in Figure 3.3. The external tank weight was recorded before and after each run such that the weight was a direct measure of the fuel used in the test. A precision scale was used to measure the weights to an accuracy of 0.02 kg [39]. In addition, extra fuel lines were installed directly to the fuel filter, such that all fuel was pulled from the external fuel tank. Quick connect fittings were used to easily remove the fuel lines.

Figure 3.3: External fuel tank installed for Canada fuel testing. Reprinted with permission from [39]. ©SAE International; National Renewable Energy Laboratory; National Research Council Canada.

A number of additional key parameters were collected throughout the testing. Each vehicle was instrumented with an independent data collection system by research partner National Research Council Canada (NRC). The Peterbilt trucks also recorded data using their own CACC systems. Parameters including GPS position, gap spacing, fuel rate, and control status were recorded to use in post-process analysis of the data. During testing, vehicle speeds were independently checked by track-side RADARs to ensure the vehicles maintained the test speed.

In addition, local weather and wind conditions were collected during the test campaign. The weather station was located at the test facility, and weather data included ambient pressure, temperature, and wind direction/speed. Two track side anemometers were also used to monitor local wind conditions. The weather station and anemometer locations are shown in Figure 3.2.

3.1.4 Test Procedures and Analysis

Each individual test run consisted of 13 laps for a total distance traveled of 84 km (52 miles). The vehicles were operated at highway speeds of 105 km/hr (65 mph) with gross vehicle weight of 29,500 kg (65,000 lbs). The duration of each test was completed with a given

configuration, such as platooning at a specified following distance, and are described in the following section. Each day, the vehicles were inspected and warmed up to ensure that each vehicle was prepared for testing. All tests began with a specific starting procedure to ensure all the tests were completed in the same manner. The full testing procedure is described in the Appendix Table B.1.

The modified SAE J1321 Type II test procedure was used for this test campaign [28]. Typically, this procedure is used to document the change in fuel consumption for a modification to a single vehicle. The standard procedure is applied such that truck platooning is the vehicle modification tested. As previously mentioned, gravimetric fuel measurements were taken to perform the analysis. A minimum of three runs were conducted for each test configuration. All tests were executed with the appropriate test and control vehicles operating simultaneously, with the control vehicle adequately spaced (1/3 track length or approximately 2.2 km apart) from the test vehicles to ensure it had no effect on the test. Overall, there were only two exceptions to the SAE 1321 procedure: the control vehicle make and the wind speeds. The test procedure requires that the control vehicle be of the same make and model as the test vehicles. This was not the case for this testing, but the control vehicle had a similar aerodynamic package and profile as the test vehicles. This is important because it is assumed that environmental conditions, e.g. the wind, affect all vehicles the same and differing vehicle shapes could influence this. Also, some of the testing was completed with wind conditions exceeding the limit of 20 km/hr. The test results were analyzed with respect to the wind conditions, and the results presented here were not identified to be effected by high winds [39], [44].

The Type II analysis uses fuel ratios to quantify fuel consumption. These ratios are the fuel mass of the test vehicle to control vehicle, for a given configuration. To calculate the fuel savings, the test fuel ratios, i.e. from platooning, are then compared to the baseline fuel ratios. The amount of fuel saved is the percent change of fuel use between baseline and test cases. The gravimetric analysis used for this study is summarized in Appendix B.2. An alternative analysis is also completed by using the gravimetric measurements to calibrate the CAN bus fuel rate. The fuel rate calibration process is described in Appendix B.3. Overall, the gravimetric

analysis is used to calculate the total fuel saving results, and the calibrated fuel rate is used for detailed analysis, such as track-segmented results.

The SAE J1321 standard provides a helpful spreadsheet to calculate the fuel savings and was used for the data analysis [28]. Given the fuel masses, the spreadsheet calculates the fuel ratios, percent fuel saving, and a confidence interval (CI) for the result. The uncertainty in the result is derived using a 95% CI. An example calculation using the spreadsheet is provided in the Appendix Figure B.4.

3.2 Test Configurations

A number of different test configurations were used to study various aspects of truck platooning. This section describes each test configuration and how it was accomplished. Note, all tests labeled 'platoon' were accomplished using the CACC controller on the platoon following vehicle.

3.2.1 Baseline

The baseline tests represent the reference fuel consumption to compare to the platooning tests. These tests were accomplished by operating each vehicle isolated from each other, approximately a third of the track length apart. The lead and control vehicles operated their stock Cruise Control (CC) systems. Truck A2, usually the platoon following vehicle, operated a CC system implemented using the CACC system. This was done because the CACC and stock system use different RADAR devices and were not easy to change out. Functionally, the CACC implemented CC and stock CC are the same.

3.2.2 Aligned Platoon

The aligned platoon case refers to the nominal platooning scenario. The platooning vehicles were operated such that they were in the best alignment with each other, i.e. no lateral deviation. The lead and control vehicles operated their stock CC, and the following vehicle

used the CACC controller described in Chapter 2. In previously published fuel tests, it is assumed the results are for the "aligned" platoon case. The aligned platoon results were also used as a comparison to the more advanced mixed traffic configurations tested.

3.2.3 Fixed Traffic

The fixed traffic category was designed to test truck platooning in more realistic conditions likely seen on a real roadway. In the controlled test track environment, a fixed traffic pattern was placed ahead of the platoon to emulate traffic conditions and to study the traffic's effect on truck platoons. The goal of this testing was to answer the following question: are truck platoon savings still beneficial with the presence of other vehicles on the roadway? During this campaign, two fixed traffic patterns were tested: a single heavy duty truck and a group of passenger vehicles.

The first traffic pattern, the "3-truck" platoon, represented a two truck platoon following a forward heavy truck. This was accomplished by operating the control truck as the truck ahead of the platoon. In this case, the control truck used stock CC, Truck A1 operated ACC at 78 m relative to the control truck, and Truck A2 platooned using the CACC system. The results from this configuration were then compared to the single, isolated vehicle baseline tests. While ahead of the platoon at 78 m, the control vehicle does not experience conditions different than if isolated and can still be used as the control for the J1321 calculations [44].

The second traffic pattern included a group of passenger vehicles to study the effect of upstream traffic on truck platoons. This "surrounding vehicle traffic" case used three vehicles, a Toyota Highlander SUV, a GMC Sierra pickup truck, and a Subaru Impreza sedan, driving in a fixed pattern as shown in Figures 3.4 and 3.5. The truck platoon followed behind the SUV at 78 m in the outside lane of the track, while the pickup truck was approximately 57 m from the platoon with the sedan 30 m behind it in the inside lane. In order to keep the traffic pattern fixed, the SUV and the pickup truck operated their stock CC, and the sedan followed the pickup truck with an ACC system.

New baseline tests were conducted in order to quantify the surrounding-vehicle traffic savings. This "zeros out" the savings a single vehicle achieves from traveling behind this traffic

Figure 3.4: Side view of surrounding vehicle traffic with truck platoon. Reprinted with permission from [44]. ©SAE International; National Renewable Energy Laboratory; National Research Council Canada.

pattern. The new fixed traffic baselines were conducted by a single truck traveling behind this traffic pattern and using those results as the reference for the platooning tests. A1 followed the SUV with its stock ACC system at a following distance of 78 m. In order for A2 to follow the traffic pattern, an additional hardware system, called the "mergebox", was placed in the SUV, allowing A2 to "platoon" with the SUV. The mergebox hardware includes a GPS, DSRC radio, and computer. This setup generates the necessary measurements needed for the following vehicle's CACC system to operate. An example of the surrounding vehicle traffic reference case is shown in Figure 3.5.

Figure 3.5: Surrounding vehicle traffic single truck reference case. Reprinted with permission from [44]. ©SAE International; National Renewable Energy Laboratory; National Research Council Canada.

3.2.4 Control Performance

The previously described test configurations were evaluated across a number of platoon gap distances. Since the results are represented as a function of the platoon gap distance, it

is important to understand how well the control system maintained this desired distance. An example of the controller performance is shown in Figure 3.6 for the aligned platoon configuration at 9.1 m gap distance. The figure shows the CACC system's range estimate and the desired gap distance, the controller error, and the engine torque command. The controller performs well in this benign environment, the test track, with $\pm$ 1 m of error during the hour test. Overall, the average and standard deviation of the error were 0.00 m and 0.34 m respectively, and it is assumed that other tests displayed a similar level of performance was achieved with all other test configurations.

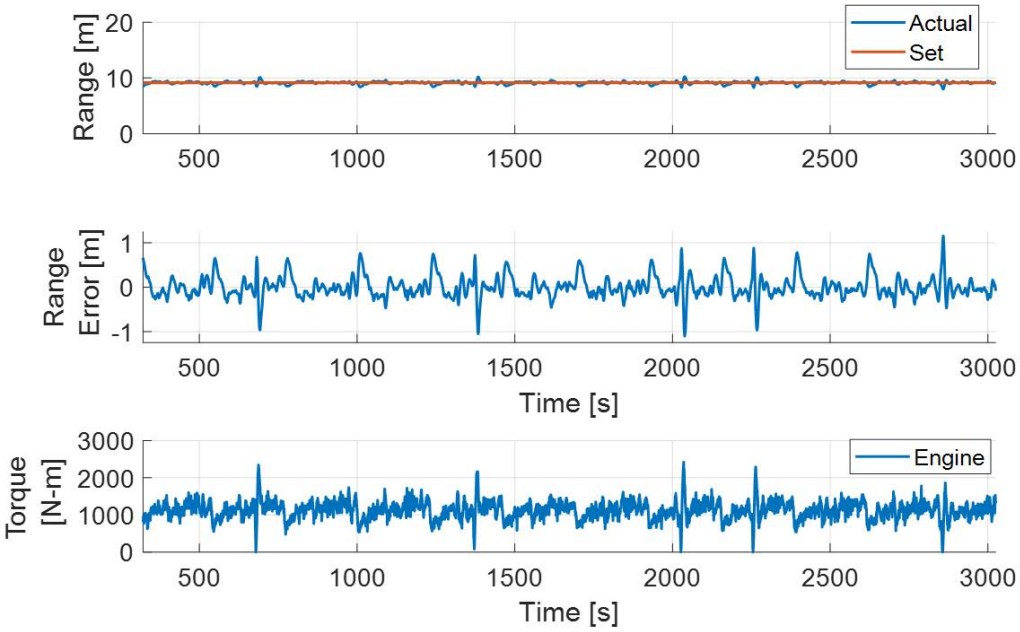

Figure 3.6: CACC control system performance during fuel test.

3.3 Results

The results from this fuel test represent the benefits of a two truck platoon across a number of inter-vehicular gap distances and configurations. The fuel saving results are relative to the appropriate baseline test and are represented by an average and *95%* CI error bars. These results were independently calculated using the same gravimetric data used in [39] and [44]. This was done to validate those calculations, and the results may differ depending on the baseline runs or analysis technique used. The gravimetric fuel saving results are provided in the Appendix B.5.

3.3.1 Aligned Platoon

The aligned platoon results are the nominal fuel saving results for the platoon. The platoon is isolated from other vehicle interactions, and these results are used to compare to the other traffic scenarios. The aligned platoon results, as a function of gap distance, are shown in Figure 3.7. These results are similar in magnitude and trends to previous truck platoon fuel tests [17], [26], [27]. The lead vehicle only has savings at closer following distances of less than 15 m (50 ft). As following distance decreases, the lead vehicle's savings increase to a maximum of 6.0% at 9.1 m. The following vehicle has much higher savings, from 6.1% at 78.6 m to 10.7% at 9.1 m, across all gap distances. These results, however, do not monotonically increase, and the maximum benefit of 12.1% occurs at 12.2 m. This trend is consistent with prior research where the follower vehicle has a dip in savings below the 12 to 15 m range. The physical mechanism causing the dip in fuel savings is not identified in this study and is part of on-going research. These results also show significant fuel savings of 6.1% for the trailing vehicle at the longest following distance of 78 m. This is important because that gap distance is a typical ACC following distance, i.e. a realistic following distance of trucks using ACC today. Therefore, trucks on road are likely already achieving fuel savings and further investigation into the fixed traffic cases is important.

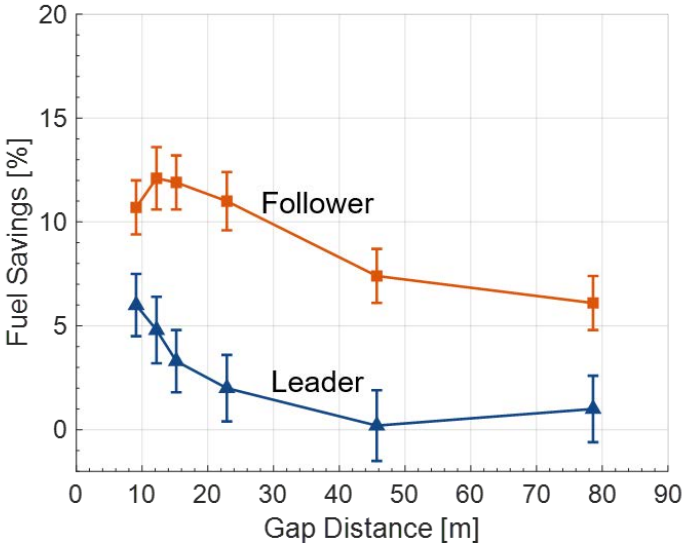

Figure 3.7: Gravimetric fuel saving results for the aligned platoon.

In addition to the fuel saving results, alternative analyses can be completed using the CAN bus fuel rate. In particular, Lammert et al. shows the contrasting fuel rate behavior of the baseline and platoon test runs [39]. In this analysis, the CAN fuel rate measurement was plotted as a function of track segment and compared between baseline and platooning scenarios, as shown in Figure 3.8. In each plot, the black lines represent the fuel rate for each lap, and the red line is the total run average. In Figure 3.8a, there are significant differences between all the vehicles' fuel rate behavior as a function of track segment, which is attributed to the CC/ACC control system implementation. It is important to note the difference in fuel rate behavior for Truck 2 (A2) during CC and platooning. The following vehicle's behavior changes from a fairly constant but noisy signal during CC, to the same profile as the lead vehicle during platooning, shown in Figure 3.8b. The specific impact of this behavior is not identified in this text but may have an impact on the overall fuel savings results.

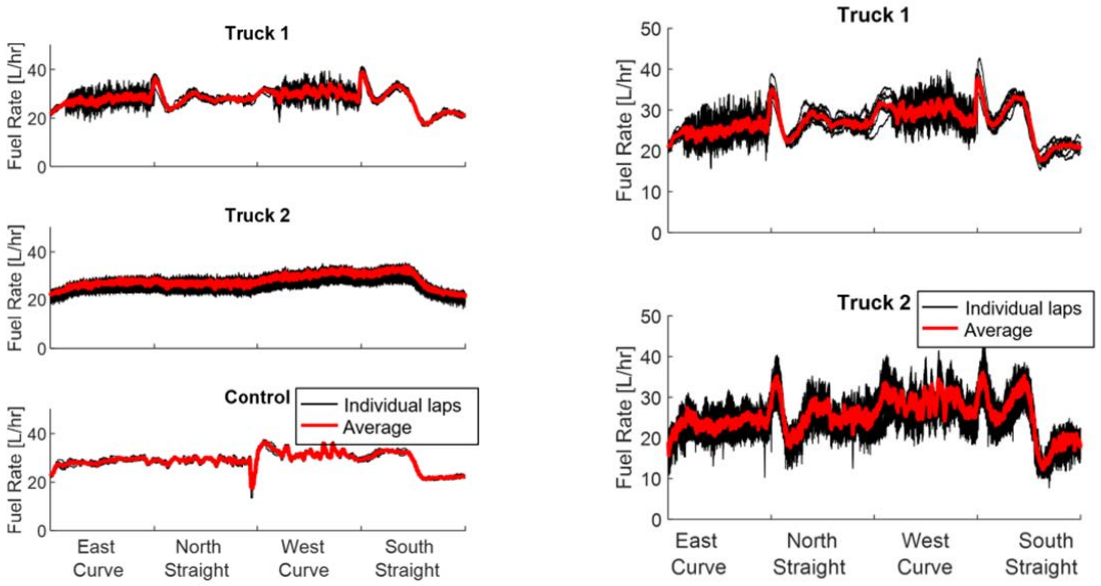

(a) Individual vehicle CC behavior.

(b) Platooning behavior.

Figure 3.8: Comparison of fuel rate behavior between CC and CACC platooning. Reprinted with permission from [39]. ©SAE International; National Renewable Energy Laboratory; National Research Council Canada.

Another analysis is completed using the calibrated J1939 CAN fuel rate. Using this technique, the fuel savings can be separated as a function of track segment. Prior research at the same test facility identified fuel saving differences up to 5% between the straight and curved

segments of the track [17]. As a result, the data for this test campaign was studied in this manner as well. The track segmented, aligned platoon results are shown in Table 3.2. The following vehicle results show the same behavior described in [17] but with nearly double the difference of savings between the straights than curves, up to 9.4%. Additionally, the following vehicle always demonstrated higher fuel savings in the straight segments compared to the curves. It is hypothesized this effect is from the articulation of the tractor trailer combination and the high degree of bank in the curved segments of this track [39].

Table 3.2: Track segmented CAN bus fuel rate results for the aligned platoon with data from [39].

	Truck 1 [%]		Truck 2 [%]	
Gap Distance [m]	Straights	Curves	Straights	Curves
9.1	6.5 ± 0.8	6.3 ± 0.7	14.4 ± 1.1	9.1 ± 1.2
12.2	4.5 ± 0.7	4.4 ± 0.6	14.7 ± 1.1	9.4 ± 1.1
15.2	3.0 ± 0.8	3.2 ± 0.7	14.8 ± 1.2	9.2 ± 1.1
22.9	1.9 ± 0.8	1.6 ± 0.7	14.2 ± 1.2	7.7 ± 1.2
45.7	0.3 ± 1.0	-1.3 ± 0.8	11.4 ± 1.3	4.7 ± 1.2
78.6	1.1 ± 0.8	1.4 ± 0.7	9.6 ± 1.1	0.2 ± 1.2

3.3.2 Three-Truck Platoon

This test included a two truck platoon following the control truck at 78 m. The name "3-Truck" platoon is not technically accurate because the control truck is not connected to the other two trucks, but the control truck acts as an aerodynamic leader to A1. This test was completed for two different platoon gap distances, 15 m and 78 m, and the results are shown in Table 3.3 compared to the isolated aligned platoon. Both the lead and following vehicles show increased savings in this traffic pattern, but the lead vehicle experiences a higher benefit. This result is expected because of the additional forward heavy duty truck that helps break the upstream wake, like the platoon leader does for the follower. The additional savings from the upstream heavy duty truck are shown as the difference in savings from the 3-Truck and aligned platoons. The results show 3.5 - 4.2% and 1.0 - 2.5% additional savings over the isolated platoon case. These results suggest that the addition of "other traffic" adds to the benefit of platooning alone [44].

Table 3.3: Gravimetric fuel savings for the 3-Truck Platoon. Reprinted with permission from [44]. ©SAE International; National Renewable Energy Laboratory; National Research Council Canada.

Test	**Truck 1 [%]**	**Truck 2 [%]**
Isolated Platoon - 15 m gap	3.6 ± 1.3	11.6 ± 1.1
Platoon follow Control - 15 m gap	7.1 ± 1.6	12.6 ± 1.3
Added savings from "Other Traffic"	3.5	1.0
Isolated Platoon - 78 m gap	1.2 ± 1.4	4.6 ± 0.8
Platoon follow Control - 78 m gap	5.4 ± 1.3	7.1 ± 1.0
Added savings from "Other Traffic"	4.2	2.5

The 3-Truck platoon testing also allows for a comparison of the ACC and CACC control systems at the same following distance. This was completed by taking A1's results of the 3-Truck platoon at 78 m (ACC) and comparing them to A2's results of the aligned platoon at 78 m (CACC). Table 3.4 shows the results for this comparison. From the table, the gravimetric (J1321) results for A1 and A2 are 5.4% and 4.6% respectively. Although these results are different, the uncertainty in the results overlap each other, suggesting a common value for both. These results show that the CACC system, which is an extension of an ACC system, is not detrimental to the fuel savings. The advantage of CACC over ACC is the ability to decrease the following distance with the additional hardware and software. Lastly, Table 3.4 shows the track segmented results for the same test configuration. The track segmented results for A1, now as a following vehicle to the control truck, also exhibit the same trend as the following vehicle of the aligned platoon: higher savings in the straight than curved segments. A2 also retains this same trend as well.

Table 3.4: Fuel saving results at 78 m for ACC/CACC comparison. Reprinted with permission from [44]. ©SAE International; National Renewable Energy Laboratory; National Research Council Canada.

Calculation Method	**Truck 1 [%] (ACC)**	**Truck 2 [%] (CACC)**
J1321	5.4 ± 1.3	4.6 ± 0.8
Full Track CAN bus	5.3 ± 0.6	4.5 ± 1.1
Straight Segment CAN bus	7.1 ± 1.0	9.6 ± 1.1
Curved Segment CAN bus	3.8 ± 0.8	0.2 ± 1.1

3.3.3 Surrounding Vehicle Traffic Platoon

The surrounding vehicle fixed traffic case includes the effect of upstream vehicles on a truck platoon. In this situation, new "traffic" baselines were conducted to evaluate only the benefit of platooning behind this traffic pattern. Table 3.5 shows the single vehicle, fixed traffic results using the isolated baselines for the reference. The fuel savings were 7.4% and 4.6% for the lead and following vehicles, respectively. These results were expected to be closer, and the differences could be caused by the ambient conditions or different control systems [44]. The full track CAN bus results, however, suggest a common answer (6.7%) when the result and uncertainty are considered. The track segmented results, the last two rows of Table 3.5, also demonstrate a different behavior than expected: Truck 1 (A1) has higher fuel savings in the curved segments than the straight segments. This trend is the opposite when compared to A1 following another truck, as in Table 3.4.

Table 3.5: Fuel saving results for surrounding vehicle traffic baselines. Reprinted with permission from [44]. ©SAE International; National Renewable Energy Laboratory; National Research Council Canada.

Calculation Method	**Truck 1 [%] (ACC)**	**Truck 2 [%] (CACC)**
J1321	7.4 ± 1.2	4.6 ± 1.2
Full Track CAN bus	7.3 ± 0.6	5.6 ± 1.1
Straight Segment CAN bus	4.4 ± 0.8	7.9 ± 1.1
Curved Segment CAN bus	9.7 ± 0.7	3.7 ± 1.1

With the new traffic baselines for comparison, the two truck results show only the "platooning" effect from the traffic pattern. The surrounding vehicle traffic platoon results, compared to the aligned platoon, are shown in Figure 3.9. The results generally follow the same trends from the aligned platoon, with a noticeable decreased "improvement" in fuel savings for the following vehicle. The lead vehicle does not have any statistically significant savings beyond 15.2 m because the error bar straddles zero. This result differs from the aligned platoon case that showed a fuel savings of 2% for the leader at 22.9 m. For the close following distances, the leader's savings dropped by 0.3 - 0.6%. The trailing vehicle also follows the aligned platoon trends but with a greater decrease in savings from 1.0 - 2.7%. Interestingly,

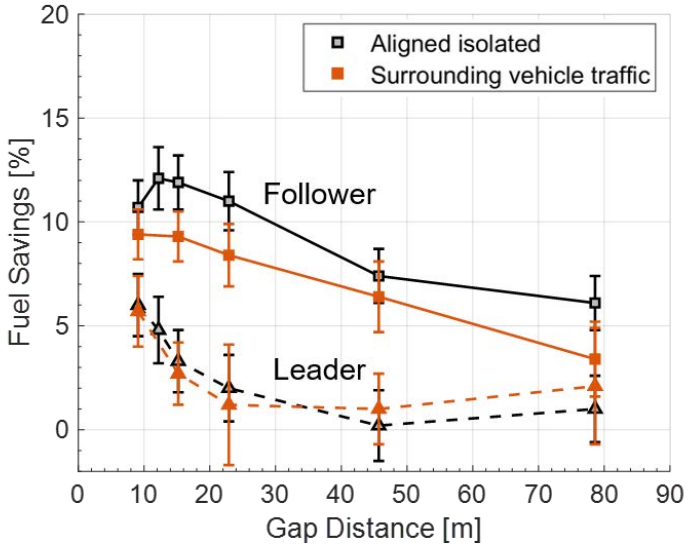

Figure 3.9: Gravimetric fuel saving results for the surrounding vehicle traffic platoon.

the following vehicle did not see a dip in savings as the following distance decreased, as the aligned platoon did. The results from 9.1 m and 15.2 m were nearly identical (9.4% and 9.3%), and this may suggest that the following vehicle's savings are less sensitive with the presence of upstream traffic at close following distances. More testing, such as the 12.2 m case, would be needed to validate this conclusion however. Overall, these results show that platooning is still effective with the fixed upstream traffic pattern. Although the magnitude decreases, the platoon fuel savings are still significant at all distance less than 78 m, with savings of 3.0 to 6.9% [44].

The track segmented fuel savings were also investigated because of the lead vehicle's anomaly during the traffic baselines. The track segmented results are shown in Table 3.6. These results show that the lead vehicle has the same behavior for the statistically significant data points of 9.1 m and 15.2 m: higher savings in the curves than straights. In addition, the

Table 3.6: Track segmented CAN bus fuel rate results for the surrounding vehicle traffic platoon with data from [44].

	Truck 1 [%]		Truck 2 [%]	
Gap Distance [m]	Straights	Curves	Straights	Curves
9.1	3.9 ± 1.0	4.9 ± 0.9	7.6 ± 1.2	11.8 ± 1.2
15.2	1.7 ± 1.0	1.3 ± 0.8	8.4 ± 1.2	10.4 ± 1.2
22.9	1.0 ± 1.1	-1.9 ± 1.0	8.0 ± 1.3	9.4 ± 1.3
45.7	0.0 ± 1.0	-0.2 ± 1.0	4.8 ± 1.3	6.8 ± 1.4
78.6	0.0 ± 1.1	0.3 ± 1.0	3.9 ± 1.3	3.2 ± 1.2

following vehicle's trends flipped from the expected savings per segment, to the same trend as the lead vehicle.

To further investigate the cause of this behavior, the fuel rate per lap were compared for these test cases. In Figure 3.10a, the lead vehicle's fuel rates are compared for the isolated baseline (top) and the traffic baseline (bottom). This figure shows the fuel rate behavior changes significantly, especially in the straight segments of the track. In the isolated case, A1's fuel rate was smooth in the straights and variable/noisy in the curves. In the traffic baseline case, however, A1's fuel rate is noisy the entire length of the track. Figure 3.10b shows how the lead vehicle affects the following vehicle's fuel rate behavior. Like the aligned platoon fuel rate shown in Figure 3.8, the following vehicle fuel rate follows the lead vehicle. This result helps explain why the following vehicle's behavior changes from the traffic baseline (as expected) to the opposite (unexpected) trend during the surrounding traffic platoon.

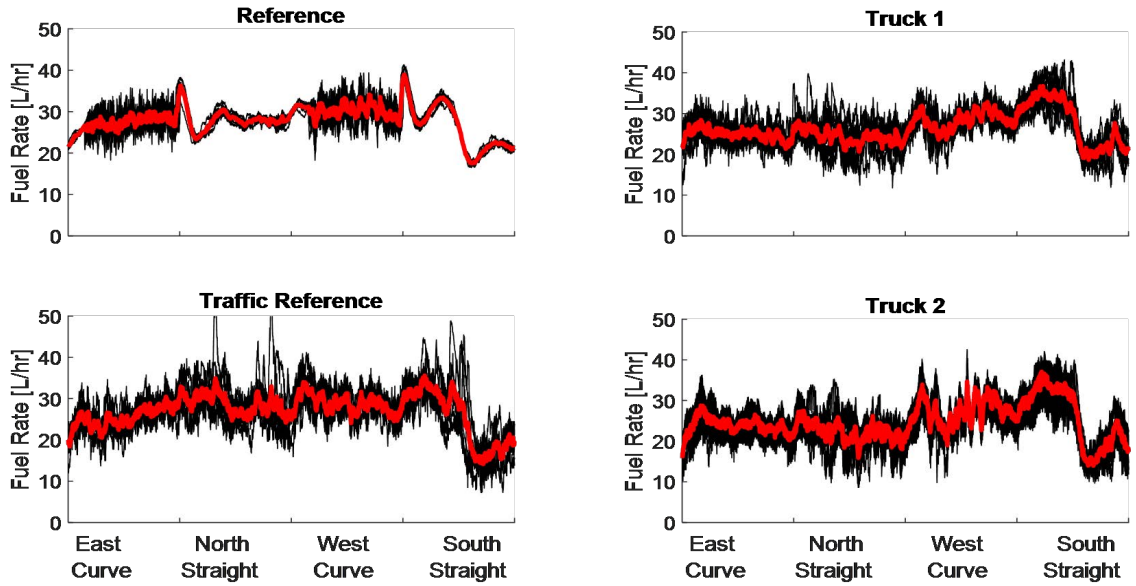

(a) Lead vehicle fuel rate for isolated and traffic baselines.

(b) Surrounding vehicle traffic platoon fuel rate for example run.

Figure 3.10: Comparison of fuel rate behavior between isolated/traffic baselines (left) and the effect on the surrounding vehicle traffic platoon (right). Reprinted with permission from [44]. ©SAE International; National Renewable Energy Laboratory; National Research Council Canada.

The test runs were analyzed further to understand the cause of the noisy fuel rate for A1. In particular, the interactions of the vehicle's ACC control system was studied between the two

traffic patterns. The vehicle interactions were compared for the 3-Truck case (forward heavy truck) and the surrounding traffic case (forward SUV), as shown in Figure 3.11. In Figure 3.11a, the fuel rate is steady throughout the lap. It is important to note the ACC "Target Detected" subplot for the forward heavy truck; the ACC system switches between distinct 'on' and 'off', meaning that the ACC system has detected the forward truck. When the detection occurs, the ACC system begins to slow its vehicle speed, as shown in the East Curve to North Straight transition in Figure 3.11a. In contrast, the ACC system performs differently with the forward SUV. The system detects the forward SUV almost the entire duration of the track, with an exception in the straights. In Figure 3.11b, the ACC system quickly loses and regains detection of the SUV in the straight segments. Each time this occurs, the vehicle speed deviates from the set speed and there is a spike in the fuel rate. This occurs because the ACC keeps the vehicle speed slightly below the set speed when a target is detected. When the detection switches off, the system thinks it can follow the set speed again, causing the spike in fuel rate to accelerate. This effect is hypothesized to be the main cause for the increased variability in the fuel rate. As a result, the track segmented fuel savings would reflect the decrease in savings for the straight segments, where this ACC behavior occurs.

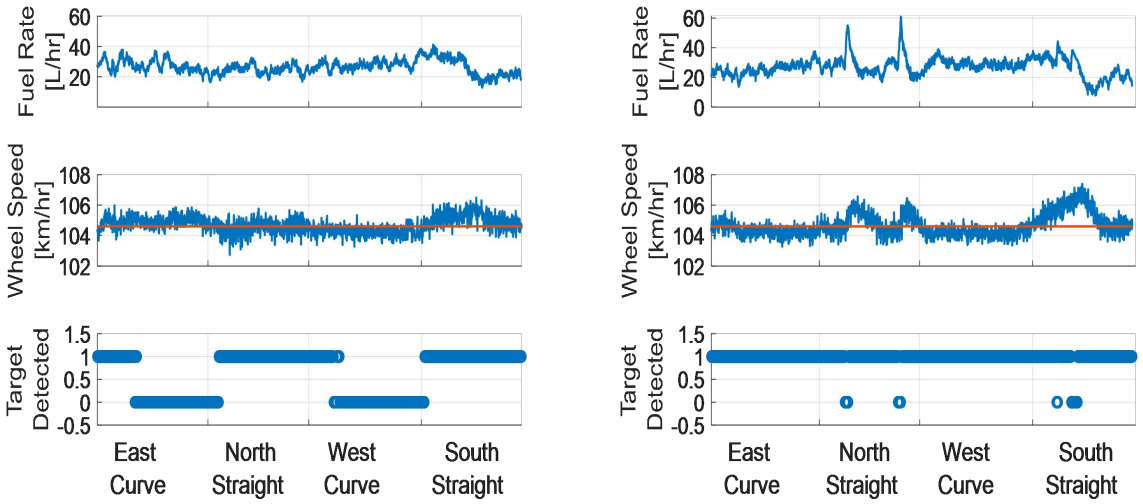

(a) Interaction with forward heavy truck.

(b) Interaction with forward SUV.

Figure 3.11: Comparison of vehicle interactions for 3-Truck (left) and surrounding vehicle traffic platoons (right). Reprinted with permission from [44]. ©SAE International; National Renewable Energy Laboratory; National Research Council Canada.

The surrounding-vehicle traffic platoon can also be compared to the isolated vehicle baselines. These results include the total benefit the upstream traffic pattern has on the two truck platoon. The results of this analysis are shown in Figure 3.12. These results are similar in trends to the surrounding traffic with the traffic baselines but with a much larger magnitude increase in fuel savings. It is important to remember that the nominal savings of the single vehicles behind the traffic pattern were 7.4% and 4.6% for the leader and follower. In this comparison, the lead vehicle has a much larger increase in fuel savings (4.9 - 6.7%), since it did not have a forward vehicle in the aligned platoon. The following vehicle's savings also increased by 1.8 - 3.5%, depending on the gap distance. These results show that the presence of upstream traffic has a positive, or additive, effect on the platoon fuel savings.

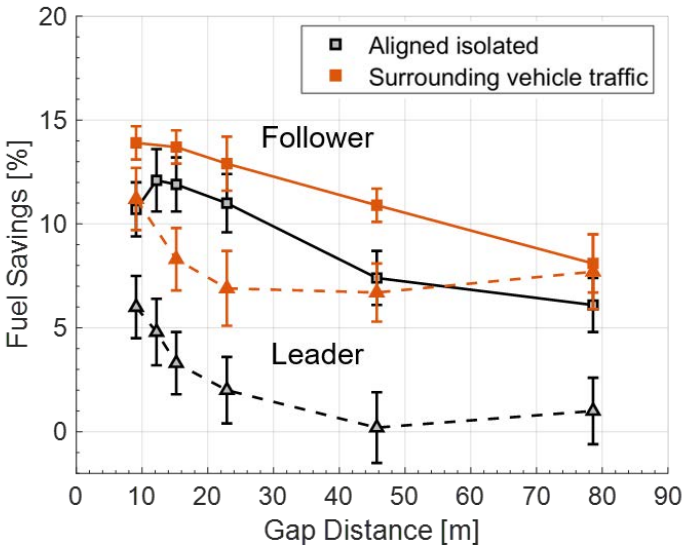

Figure 3.12: Gravimetric fuel saving results for the surrounding vehicle traffic platoon with isolated vehicle baselines.

3.4 Conclusions

This chapter presented a test campaign using an extensive SAE Type II fuel test to quantify the fuel saving potential of truck platooning. A variety of gap distances and two fixed traffic patterns were tested. The standard gravimetric analysis provided the foundation for the results presented, and further analyses were provided using the calibrated CAN bus fuel rate. The aligned platoon results were similar in magnitude and trends to prior research and add to the

current body of literature. Furthermore, the fixed traffic tests showed that platooning is still effective and significant savings can be achieved in the presence of other traffic. Using the fuel rate analysis, these tests showed unexpected trends in the fuel savings for the straight and curved segments. The stock control system on the lead vehicle was identified as the source of this discrepancy. These results suggest that the lead vehicle's control system is important and can have an influence on the following vehicle's behavior.

Chapter 4

Coastdown Test

Prior research has studied the fuel saving benefit of truck platooning, which is largely due to the aerodynamic drag reduction of these heavy duty vehicles. As an alternative approach, an aerodynamic evaluation of truck platooning can provide insight into the complex behavior from interacting vehicles. This chapter describes the coastdown test procedure to experimentally quantify parameters, the drag area ($C_D A$) and the coefficient of rolling resistance (C_{RR}), associated with the two dominant resistive force of vehicles. The coastdown test was completed for two platooning trucks by using a CACC system to maintain the gap distance from the coastdown vehicle. The "controlled" coastdown results are a novel aerodynamic evaluation of truck platooning. This chapter also discusses the background and test setup, the analysis method, the test configurations, and results.

4.1 Background

The coastdown test is used to infer the aerodynamic and rolling resistance components from the measured road load. This method has been applied previously to single heavy duty trucks [31], [32], [33] and is currently the reference aerodynamic method for heavy duty vehicle evaluation in the United States [6]. The basic idea of a coastdown test is simple: accelerate a vehicle to a high speed, shift into neutral, and allow the vehicle to coast un-powered to a lower speed. The deceleration rate and models of resistive forces are then used to calculate the vehicle's drag area and coefficient of rolling resistance. These two vehicle parameters are often performance indicators for a vehicle and are used in the Greenhouse-gas Emission Model (GEM) for certification with the EPA [6].

The aerodynamic evaluation of platooning vehicles is also of interest for quantifying the same vehicle parameters. However, prior research has described that coastdown testing cannot be applied to platooning vehicles because the vehicles' aerodynamic loads differ. In platooning, the differing aerodynamic loads result in different deceleration rates and a constant gap distance cannot be maintained [19], [36]. In a similar aerodynamic evaluation, constant-speed testing has been applied to platooning passenger vehicles in [35] where the gap distance was maintained manually and to platooning heavy trucks in [36] where the gap was maintained by a CACC system. This thesis presents the first known coastdown evaluation of platooning heavy duty trucks with a CACC system to maintain the gap distance during the coastdown.

The coastdown testing took place near Auburn, Alabama in March of 2020. The testing was completed as an alternative study of truck platooning benefits. The remainder of this section provides the foundation for coastdown testing and a method to study the effect on platooning vehicles.

4.1.1 Vehicles

The duration of testing was completed with the two Auburn University Peterbilt 579 trucks previously described in Chapter 3. All of the tests were completed by using vehicle "A1", which is typically the platoon lead vehicle, as the coastdown vehicle. As a result, the order of the platoon was changed to evaluate the aerodynamic benefit in the lead and following positions. A1 was the same vehicle used during the Canada fuel test but several modifications were made (for another test occuring at the same time) to the vehicle prior to coastdown testing, as shown in Figure 4.1. New DSRC antenna mounts were installed above the existing DSRC antennas, and the fifth wheel position was moved back to its furthest back position. The gap between the tractor and trailer was measured at 1.52 m, an increase of approximately 0.2 m from the fuel testing. A2, the other platoon vehicle under CACC control, also had the same physical modifications as A1.

The platooning vehicles both pulled unloaded, standard 53' box trailers with side skirts, shown previously in Figure 2.1. A summary of the coastdown vehicle specifications is shown in Table 4.1 with relevant information such as vehicle dimensions, weights, and tires. It is

Figure 4.1: Peterbilt 579 vehicle for coastdown testing.

Table 4.1: Coastdown vehicle specifications.

Tractor	2015 Peterbilt 579 Engine: Paccar MX-13 Transmission: Eaton Fuller Automated 10 speed Steer Tires: Michelin XZA3+ 275/80R22.5 Drive Tires: Michelin XDA Energy 275/80R22.5
Trailer	Hyundai Translead 53' dry van with side skirts Tires: Lancaster TL150 275/75R22.5
Weight and Dimensions	Tractor mass: 7,906 kg (17,430 lbs) Trailer mass: 6,146 kg (13,550 lbs) Tractor height: 4.0 m Tractor width: 2.6 m Tractor-trailer gap: 1.52 m (60.0 in) Trailer bogie position: 3.66 m from back of trailer to center Trailer wheelbase: 1.24 m (49.0 in)

important to note the trailers were different from those used during fuel testing. The fuel testing trailers were equipped with side skirts and boat-tail technology, which can change the overall performance. For example, the side skirts and boat-tails combination would produce lower absolute drag force than side skirts alone [18]. The absolute drag area results presented here are expected to be nominally higher than the drag experienced during the fuel test.

4.1.2 Test Site

Auburn University's National Center for Asphalt Technology (NCAT) test track was used for the coastdown testing. The test track is a 2.7 km (1.7 miles) oval and is shown in Figure 4.2 [47]. The NCAT facility is an asphalt testing facility, and the outer lane of the track has 200' sections paved with varying types of asphalt mix. The inside lane was used for the duration of testing. This lane also has sections that are paved with different asphalt, but the track surface is smooth throughout. Prior research at this test track demonstrated a change in the road load (for the same tractor-trailer) as a function of the track position [48]. These results suggest that the varying track sections could produce different rolling resistance values, but these effects are not considered in this thesis. In addition, there are several uneven transitions between track sections, but these locations are unavoidable so they are assumed to not influence the tests. The coastdown tests were performed on the straight segments of the track which are approximately 0.8 km (0.50 miles) long.

Figure 4.2: NCAT test track [47].

The straight segments of the test track are mainly flat while the curves have a change in grade, as shown in Figure 4.3. The elevation and grade data are calculated with RTK corrected GPS and have centimeter level accuracy. The South straight segment has the lowest road grade with small local changes, and the North straight is fairly constant but has noticeable changes. The maximum elevation difference on the North straight is approximately 0.6 m. The curved segments were excluded from the coastdown because of the large amount of road grade and degree of bank in the turns.

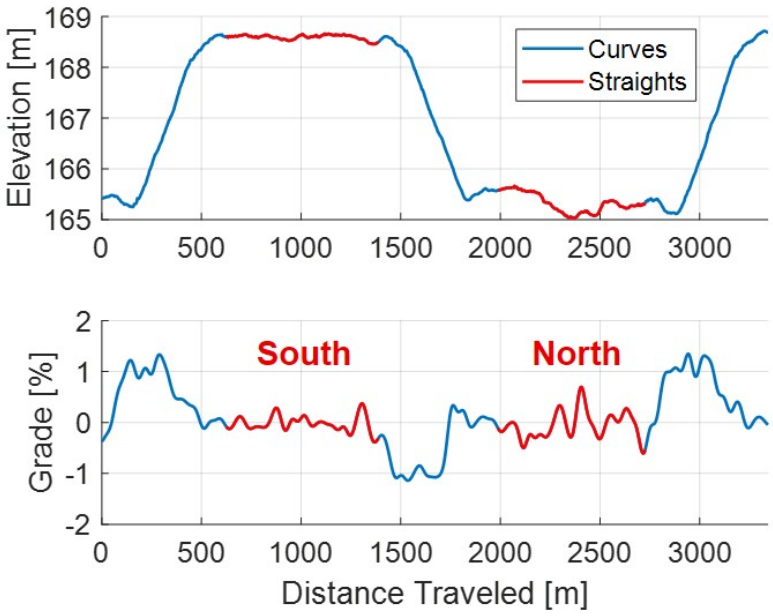

Figure 4.3: NCAT test track elevation.

The major limitation of the NCAT test track for coastdown testing is the speed limit. A high speed over 113 km/hr (70 mph) is typically desired for coastdown testing but this is well above the track speed limit of 76 km/hr (47 mph). This testing was completed with unloaded trailers so that the vehicles could operate above the speed limit to a speed of approximately 89 km/hr (55 mph).

4.1.3 Instrumentation

The fundamental coastdown analysis only needs position, velocity, and time information. The position and time information were collected from a GPS receiver and the velocity information was collected on-board the vehicle from the J1939 CAN bus. The CAN bus vehicle speed was first verified with a comparison to the GPS-based velocity. This data was processed and recorded by the CACC system on the vehicle. The GPS data and vehicle speed were recorded at 10 Hz and 40 Hz respectively. Additional data was collected from the CAN bus for post-processing. Specifically, the current gear was used to signal the beginning of the coastdown (i.e. when current gear in neutral) and brake status was used to ensure the coastdown speed segment did not include braking inputs.

An Airmar 220WX weather station [49] was placed track-side to collect ambient environmental conditions. In particular, the weather station collected GPS data, wind speed and direction, air temperature, and barometric pressure. The weather station's specifications are summarized in Table 4.2. The temperature and atmospheric pressure were used in the coastdown analysis to accurately calculate the local air density during a given test. The weather station data was time-aligned with the CACC system data using GPS time.

Table 4.2: Airmar weather station specifications [49].

Specification	**Range**	**Accuracy**	**Resolution**
Wind Speed	0-40 m/s	5% at 10 m/s	0.1 m/s
Wind Direction	0-359.9°	$\pm$ 3°at 10 m/s	0.1°
Temperature	-40 to 80°C	$\pm$ 1.1°C at 20°C	0.1 °C
Barometric Pressure	30-110 kPa	0.05 kPa at 25°C	0.01 kPa

The majority of testing was also completed with a weather station mounted on-board the lead vehicle. The on-board device was an Airmar 200WX weather station with the same specifications as the 220WX model and was installed on the single vehicle or platoon lead vehicle, depending on the test. The weather station was mounted behind the tractor cab, 0.69 m above the trailer fairing as shown in Figure 4.1. The combination of the track-side and on-board anemometry was collected to properly account for the local wind conditions during testing but was not completed as part of the analysis presented in this thesis because of time constraints.

4.1.4 Test Procedures

There are several published procedures for vehicle coastdown testing. The two most prominent documents are covered in SAE J1263 "Road Load Measurement and Dynamometer Simulation Using Coastdown Techniques" [50] and SAE J2263 "Road Load Measurement Using Onboard Anemometry and Coastdown Techniques" [51]. However, these SAE standards are defined for passenger vehicles and not for combination vehicles. The EPA's GHG Phase I and II documents provide the recommended practices for testing Class 8 vehicles and are based off the SAE standards [3], [6]. A standardized coastdown test procedure currently does not exist for heavy duty vehicles but SAE is in the process of developing J2978 [52].

The test procedure described here is a combination of the previously mentioned standards and documents. During this test campaign, a split speed range was used to complete the coastdown due to the track limitations. The split range coastdown uses a high speed segment, where the main resistive force is the aerodynamic drag, and a low speed range, where the dominant force is rolling resistance. This differs from other coastdown tests that require a full coastdown from the highest to lowest speed continuously. The split range is ideal for smaller test tracks where the full range cannot be completed because of length constraints. This testing was completed with a targeted high speed range of 89 to 72 km/hr (55 to 45 mph) and a low speed range of 24 to 8 km/hr (15 to 5 mph).

A single coastdown test is completed by coasting through the high speed segment and then the low speed segment. At the NCAT test track, the high speed segment was always completed on the South straight with minimal road grade and the low speed segment on the North straight. The high and low speed segments used at NCAT are illustrated in Figure 4.4. In this example, where travel is in the counter-clockwise direction, the coastdown vehicle prepares for the high speed segment by traveling approximately 80 km/hr (50 mph) in the West curve (far left of the figure). When exiting the curve, the vehicle accelerates starting at the red square to reach a target speed of 89 km/hr. The driver shifts the vehicle into neutral once at the high target speed (yellow circle) and coasts through the end of the South straight. The driver then applies braking through the East curve (far right) to slow the vehicle to the target speed for the low speed range,

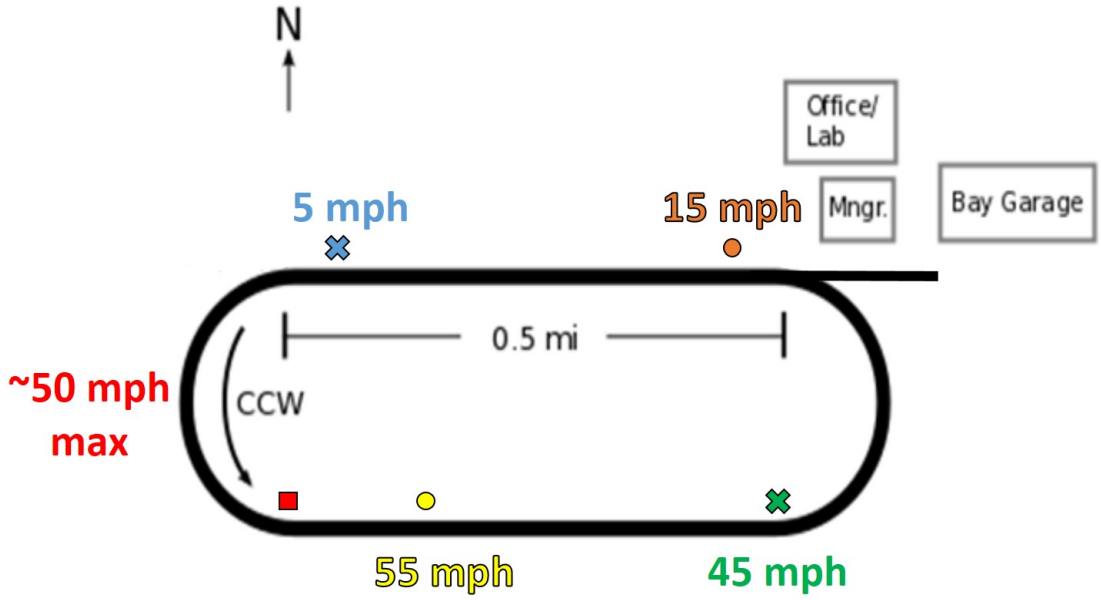

Figure 4.4: Coastdown procedure and target speeds at NCAT test track.

24 km/hr. Once at this speed on the North straight (orange circle), the driver continues to coast in neutral until the end speed of 8 km/hr is reached. One high and low speed pair constitutes a single coastdown test. This procedure was completed in both the counter-clockwise (CCW) and clockwise (CW) directions of the track. Regardless of direction, the South straight was used for the high speed range and the North straight for the low speed range.

The coastdown vehicle was warmed up for a minimum of 30 minutes before testing was completed. Additionally, checks were completed to ensure the doors and windows were closed and the vehicle maintained a fuel level over $7/8$ full. The tire pressures were not explicitly checked but were spot checked periodically to ensure the minimum pressure recommended. A full test procedure is defined in Appendix C.1.

Environmental conditions and road grade are important considerations for coastdown testing. The SAE J1263 wind speed limit is 16 km/hr average (10 mph), 20 km/hr peak (12.4 mph) and average crosswind of 8 km/hr (5 mph) [50]. The number of days for this testing was limited, and preliminary analysis of the track-side weather station shows winds that exceed these limits. Without including anemometry, it is assumed that traveling in opposite directions effectively cancels out the wind vector experienced by the vehicle. The implications of this approach

are expected to increase the scatter in the aerodynamic force and the resulting drag area. Additionally, J1263 recommends the road grade be less than 0.5% [50]. The South straight meets this requirement with a minimum and maximum grade of -0.15 and 0.29%. However, the North straight exceeds the grade limit with values of -0.49 and 0.70%.

4.2 High/Low Method

The analysis technique for the split speed range coastdown test is called the High/Low method. This method uses the two speed segments and models of the resistive forces to caclulate the coastdown coefficients. McAuliffe and Chuang compared the High/Low technique to the typical regression analysis and the resulting drag area values were within 0.2%, which suggests the High/Low method is a valid experimental procedure [33]. This section describes the modeling, solution method, and calculation of the aerodynamic drag reduction.

4.2.1 Modeling

The coastdown modeling includes the forces the vehicle experiences when coasting unpowered. The models used in this thesis are the same presented by McAuliffe and Chuang [33] which were used for tractor-trailer testing. The forces acting on a coasting vehicle are shown on the FBD in Figure 4.5. Applying Newton's 2nd Law, the governing Equation of Motion (EOM) is shown as

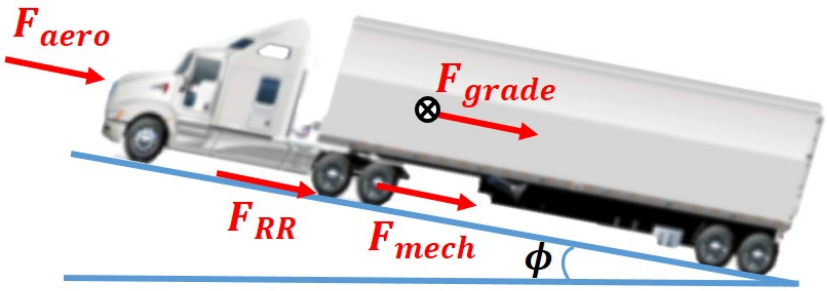

Figure 4.5: Coastdown vehicle Free Body Diagram.

$$m_e \frac{dv}{dt} = -F_{aero} - F_{RR} - F_{mech} - F_{grade} \tag{4.1}$$

where m_e is the effective mass, v is the speed, and F_i are the resistive forces modeled. The effective mass is a combination of the tractor and trailer mass plus the rotational inertia of the wheels.

The coastdown models and full EOM are developed in Appendix C.2 but a summary is provided here. The aerodynamic force is the resistive force the vehicle experiences when traveling through the air. This force is the primary interest for this study and is significant, especially for large vehicles. The force of rolling resistance results from tires interacting with the ground surface and is the second largest force since it is a function of weight and tractor-trailers are heavy vehicles. The mechanical force includes the bearing losses and rotational resistance in the driveline, such as the differential. Lastly, the force of road grade affects the vehicle motion up or down a road inclination, or grade. The full EOM, with the models described in the Appendix, is shown below in Equation (4.2).

$$m_e \frac{dv}{dt} = -\frac{1}{2}\rho U^2 C_D(\psi) A - C_{RRO} R_{RR}(v) \times W - (-.216v^2 + 13.2v) - W\frac{dh}{ds} \tag{4.2}$$

The aerodynamic force is described as a function of the air density, ρ, the relative wind speed, U, and the yaw angle, ψ, or the relative wind direction. In this analysis, the local air density is corrected using the local temperature and pressure during the test. Additionally, the on-board and track-side wind measurements can be incorporated in the model but were not used in this analysis. Therefore, the relative wind speed is assumed to be the vehicle speed, v, and the yaw angle is assumed to be zero. These assumptions infer the resulting drag area is the zero-yaw value even though it may represent conditions with ambient winds.

The coastdown model shown in Equation (4.2) includes a second order rolling resistance and mechanical resistance model. The second order rolling resistance model was developed with data from the EPA for "Smartway" verified, low rolling resistance tires and is valid to use since the test vehicle here also has Smartway verified tires. The EPA also provided data to

describe the estimated mechanical losses as a function of vehicle speed. McAuliffe and Chuang describe a second order model to fit this data, which is used in this analysis [33].

The parameters of interest in the coastdown model are the drag area (C_DA) and the coefficient of rolling resistance (C_{RR0}). The drag area is the drag coefficient, C_D, multiplied by the frontal area, A. Typically, the drag coefficient is used to describe how aerodynamic a vehicle is, but this requires knowledge of the vehicle's frontal area. The drag area can be re-written as $C_DA = F_{aero}/Q$ where Q is the dynamic pressure of the wind ($Q = \frac{1}{2}\rho U^2$). In this form, the drag area is independent of vehicle geometry and is a convenient measure of performance. The near-zero velocity component of the rolling resistance model, C_{RR0}, is also calculated from the coastdown analysis.

4.2.2 Solution Method

The coastdown EOM can be solved a number of ways. In this thesis, the High/Low method is used with two speed ranges and finite-difference approximations across those ranges to describe the physics. This method ignores the variation of a parameter, such as speed, within the range and is only concerned with the difference between the start and end of the segment. Thus, the derivatives become differences and the speed dependent forces are evaluated at the average velocity as

$$m_e\frac{\Delta v}{\Delta t} = -\frac{1}{2}\rho C_D(\psi)AU_{avg}^2 - C_{RRO}R_{RR}(v_{avg}) \times W + .216v_{avg}^2 - 13.2v_{avg} - W\frac{\Delta h}{\Delta s}. \quad (4.3)$$

Given two speed ranges, the high and the low segments, Equation (4.3) can be solved algebraically. The equations are re-arranged to isolate the two variables of interest. The resulting matrix equation is shown in Equation (4.4) and solves for the drag area and coefficient of rolling resistance. This process is detailed in Appendix C.3.

$$x = \begin{bmatrix} C_DA \\ C_{RRO} \end{bmatrix} = A^{-1}B \quad (4.4)$$

4.2.3 Drag Area Reduction

From the equations in the previous section, the variable of interest is the vehicle's drag area. The goal of the controlled coastdown testing is to quantify the reduction of drag area as a function of platoon gap distance. These results are a measure of the aerodynamic benefits which provide the improved fuel performance of truck platooning. In order to calculate the drag area reduction, tests must be completed for the single vehicle (baseline) and for the vehicle in various platoon configurations. The reductions are calculated in the same manner as the fuel saving results: the percent change of the average platoon tests to the baseline tests. The result uncertainty is also calculated using the same statistical approach presented by J1321 [28] and in Appendix B.2.

4.3 Test Configurations

Several different test configurations are needed in order to study the drag reduction from truck platooning. First, coastdown tests were completed with the single vehicle in order to quantify the baseline drag area without the effects of platooning. These tests were then used to compare to all other platooning tests.

When evaluating the truck platoon, there is a lead and following vehicle. The fuel saving results in Chapter 3 showed both the lead and following vehicles can benefit from truck platooning. Thus, it is important to study the controlled coastdown with the coastdown vehicle in both positions as well. As previously stated, A1 was the coastdown vehicle throughout testing. The coastdown testing was then completed with two different configurations: the lead vehicle position, or "regular" platoon, and in the following vehicle position, or "inverted" platoon. These two configurations are described in this section.

4.3.1 Regular Platoon

The regular platoon describes the nominal platooning scenario: the lead vehicle operates manually or in CC and the following vehicle operates in CACC. A1 is the lead vehicle in this

configuration, and the coastdown results are representative of the drag reduction of the platoon leader. This configuration is illustrated in Figure 4.6.

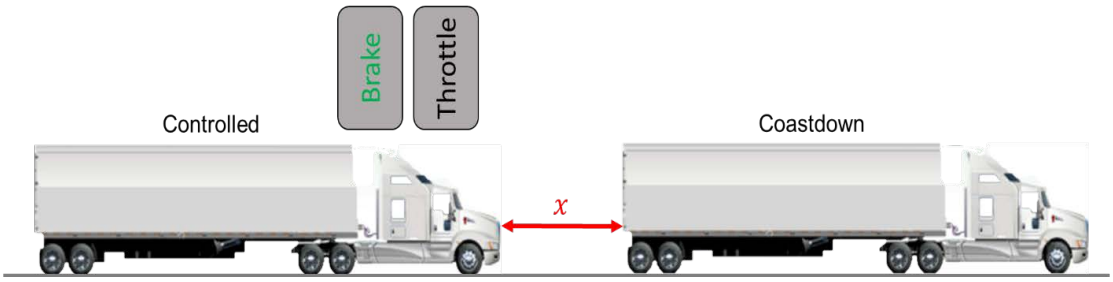

Figure 4.6: Regular platoon to quantify the lead vehicle's drag reduction.

While in this configuration, the CACC system operates normal by following the lead vehicle at a specified headway distance. The CACC system uses the same range estimation and control algorithms described in Chapter 2, where the range estimate is a filtered combination of DRTK range, RADAR, and wheel speed measurements. The lead vehicle shifts into neutral and the following vehicle, with a greater reduction in drag, begins to approach the lead vehicle. The main actuation of the controlled (following) vehicle is braking in order to keep the desired gap distance throughout the coastdown speed range.

4.3.2 Inverted Platoon

The following vehicle is evaluated by inverting the coastdown and controlled vehicles. In this case, A1 is still the coastdown vehicle but is the platoon following vehicle, as shown in Figure 4.7. The inverted platoon requires modification to the CACC system because it now operates on the lead vehicle to maintain the distance in front of the coastdown vehicle. The CACC system needs to control the position relative to its back bumper rather than the front bumper as in a regular platoon. The range estimate uses only DRTK range and wheel speed measurements because the forward facing RADAR does not return relevant information in this case. Also, the DRTK RPV must be properly resolved in 3D space in order to provide the same range measurement needed for the estimation algorithm. The range rate convention for the wheel speed update and the longitudinal controller error definition must flip, or multiply by -1,

for the system to achieve the same CACC behavior. The main actuation of the CACC control system is throttle in order to keep the desired gap distance as the following vehicle coasts down.

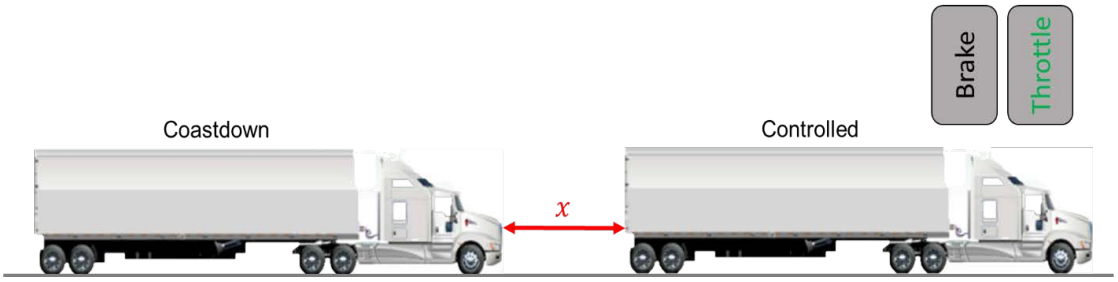

Figure 4.7: Inverted platoon to quantify the following vehicle's drag reduction.

4.3.3 Control Performance

The drag area reduction is presented as a function of platoon gap distance. Therefore, it is important to understand how well the control system maintained this desired distance. The CACC control performance is shown in Figure 4.8 for both the lead and following vehicle coastdown positions. The top plot shows both vehicles' speed, the middle plot shows the controller error, and the bottom plot shows the control commands during the coastdown. The lead vehicle coastdown (i.e. regular platoon) is shown in Figure 4.8a, and the following vehicle coastdown (i.e. inverted platoon) is shown in Figure 4.8b. In both positions, A1 accelerates in order to reach its target speed, as shown in the speed plot, and the control system responds to this transient behavior. These results show the error increases as A1 accelerates and the controller on A2 responds. This is because the CACC controller was originally designed for steady state operation and fuel performance, not tracking transients.

The LV and FV coastdowns have similar control performance for the high speed segment with the transient acceleration. In Figure 4.8a, the error is much larger for the high speed segment (time = 35-65 seconds) than for the low speed segment (time = 115-210 seconds). The high speed segment has a minimum and maximum error of -2.2 m and 4.1 m respectively. This behavior changes from the control performance of ± 1 m from the fuel test which was at a steady cruising speed. It is important to note that the only changes to the CACC controller where the ones necessary to allow for the coastdown configurations, specifically the inverted

platoon. This control system performance could be improved with an updated vehicle model or controller tuning for future testing.

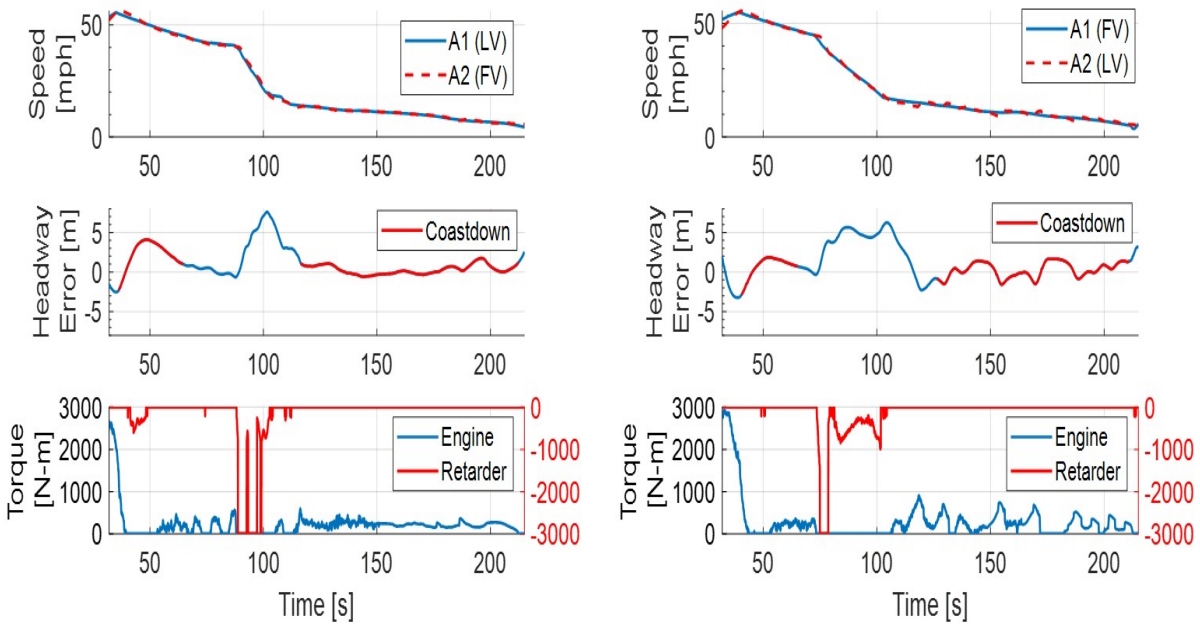

(a) Lead vehicle (LV) position.

(b) Following vehicle (FV) position.

Figure 4.8: CACC control performance during coastdown.

4.3.4 Test Matrix

A number of tests were completed with the coastdown vehicle in the single vehicle (SV), lead vehicle (LV), and following vehicle (FV) configurations. Multiple runs were completed in order to minimize environmental effects, average out road grade, and remove any outliers. Overall, two platoon following distances, 15.2 m (50 ft) and 45.7 m (150 ft), were selected to evaluate the platooning drag area reductions. These distances were selected to illustrate the platoon coastdown functionality and not meant to populate the entire curve as a function of platoon gap distance.

A target of 8 runs in each direction (16 total) was selected because J1263 recommends a minumum of 10 runs total [50]. The complete coastdown test matrix is shown in Table 4.3, and the target number of runs was not completed for all tests due to time constraints. The convention in the table is coastdown vehicle position, e.g. single, lead, or following vehicle (SV/LV/FV), and vehicle spacing. The table shows the number of runs in each direction, as well as the total

number of runs. During testing, tests were completed four at a time per direction traveled. For example, four tests were conducted in the CCW direction and then the direction was flipped and the corresponding four runs were completed in the CW direction.

Table 4.3: Coastdown test matrix.

Test	Coastdown Position	Spacing	Runs per Direction	Total Runs
SV-RF	Single vehicle	Reference, ∞	11	22
LV-S50	Lead vehicle	15.2 m (50 ft)	4	8
LV-S150	Lead vehicle	45.7 m (150 ft)	7	14
FV-S50	Following vehicle	15.2 m (50 ft)	8	16
FV-S150	Following vehicle	45.7 m (150 ft)	9	18

4.4 Results

The coastdown test results represent the aerodynamic benefits from truck platooning. In addition, the coefficient of rolling resistance is an additional result obtained from the coastdown test. First, the results are shown as a function of run number. These plots show the individually calculated values as points and the running average of the results as a solid line. The first half of the run numbers correspond to the CCW track direction and the second half are the CW direction. The results are then calculated using the J1321 analysis and represent an average with 95% CI error bars for the drag reduction [28]. The single vehicle baseline and platooning coastdown results are presented, and an estimated fuel saving is shown for the aerodynamic drag reduction.

4.4.1 Single Vehicle

It is important to study the single vehicle baseline results before the platoon coastdown. The single vehicle results represent the nominal behavior and drag area that is then compared to the platoon vehicle position and spacings. In total, 22 individual baseline tests were completed, 11 in each direction on the track. The calculated drag area and coefficient of rolling resistance are shown in Figure 4.9 for all baseline tests. The drag area results (top plot) are the most important for this study, and these results are consistent regardless of track direction. This is an important validation that the models, especially the road grade force which changes with

track direction, are sufficient to use in this analysis. The resulting drag area is 5.49 $\pm$ 0.80 m^2 for the baseline vehicle. As a comparison, these results are on the same order of magnitude (C_DA = 5.16 m^2) as the tractor-trailer testing in [33], which suggests this analysis and solution is valid.

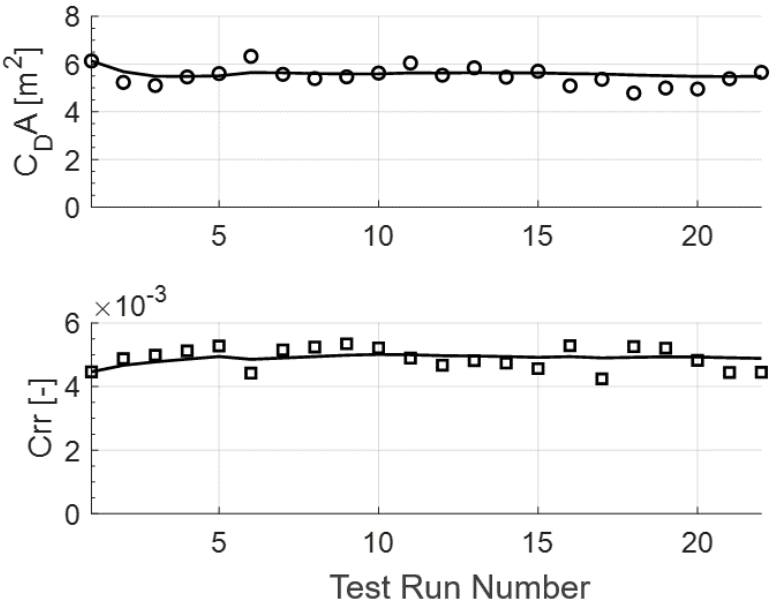

Figure 4.9: Single vehicle baseline coastdown test results.

The coefficient of rolling resistance is also calculated from the coastdown test, and the results are shown in the bottom plot of Figure 4.9. In this test setup, the coefficient of rolling resistance is more difficult to calculate accurately due to the higher variability in grade on the North side of the track. The coefficient of rolling resistance is still fairly consistent with baseline results of 0.0049 $\pm$ 0.0007. This parameter is important in the solution method, but it is not of primary interest for the platooning application. However, the calculated coefficient of rolling resistance can be used to improve a vehicle model. For example, the longitudinal vehicle model derived in Chapter 2 includes the force of rolling resistance. The new rolling resistance parameter can be used to improve the model fidelity and to update the feedforward term of the longitudinal controller.

The coastdown coefficients were then simulated with the full EOM to study how well the coastdown analysis models the dynamics. This was completed by inputting the average estimated coastdown C_DA and C_{RR0} values into the full differential equation, Equation (4.2), and

using the experimental coastdown start speeds as the model initial conditions. The model was then simulated using ODE45 in MATLAB and compared to the experimental data. The velocity as a function of time was used for comparison because it is the fundamental measurement (dv/dt) from the coastdown test to calculate the inertial force.

The resulting model simulation for a baseline run is shown in Figure 4.10. This simulation shows how well the calculated coefficients represent the physical system. From Figure 4.10a, these results show the model matches the experimental velocity quite well, especially for the high speed segment. The low speed segment, however, shows a small discrepancy where the model and experimental data do not align.

This discrepancy was investigated and found to be due to the road grade model assumption for finite-difference approximations: the road grade force is constant over the entire segment based on the start and end locations. For the experimental data, the vehicle has a very slight acceleration (time = 135 seconds) due to a negative road grade at that track location. Even with the difference in road grade, the low speed model and experimental data only differ by 1.2 mph at the end of the 93 second simulation. The model simulation verified with the road grade is shown in Figure 4.10b, where the model speed follows the experimental speed. The model simulation shows the analysis and calculated values are sufficient to capture the dynamics.

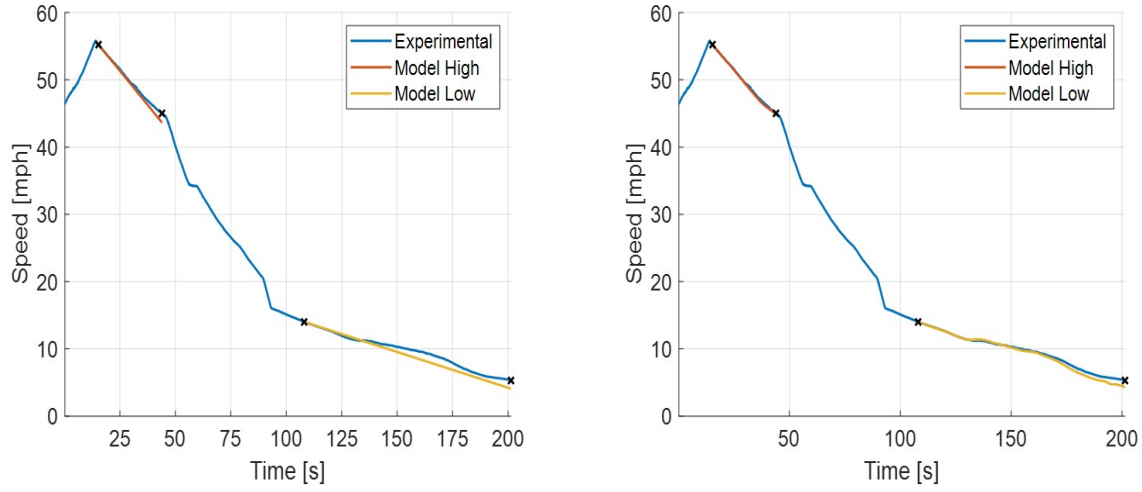

(a) Original model simulation.

(b) Model simulation with road grade.

Figure 4.10: Coastdown model simulation for validation.

4.4.2 Platoon Coastdown

The coastdown tests were completed with the coastdown vehicle in both platoon positions: the leader and follower. The results for the lead vehicle were evaluated and are shown in Figure 4.11 along with the baseline runs. The figure shows the individually calculated drag area values and running averages. The drag area results are similar for both platoon gap distances and the baseline test. These results represent the platoon "pushing" effect of the following vehicle on the lead vehicle, which is lower than the benefit experienced by the following vehicle. The main focus of this study was not on the lead vehicle since the magnitude is much less than the following vehicle at these distances.

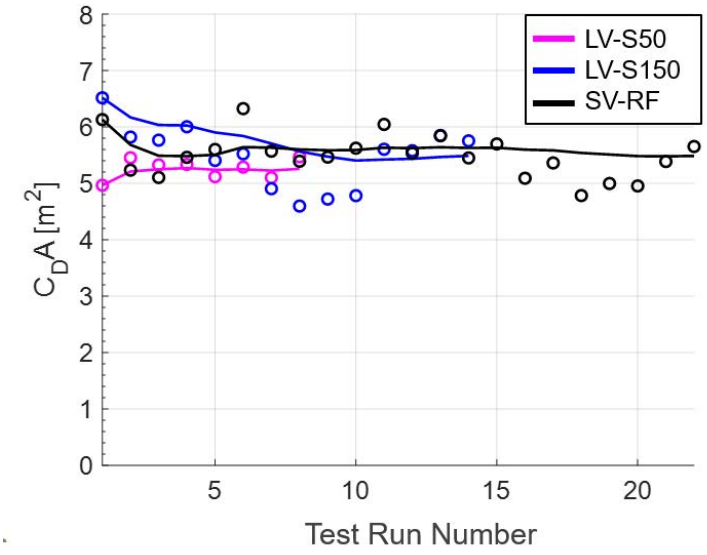

Figure 4.11: Platoon lead vehicle drag area results.

The platoon following vehicle experiences a relatively lower airspeed from the forward truck, resulting in a lower drag area. The follower vehicle results are shown in Figure 4.12, and these results show a distinct reduction in drag area at both platoon gap distances. These results also show a bigger distinction between the direction of travel on the track. As previously stated, the lower run numbers are the CCW direction and the higher run numbers are the CW direction. These results differ based on the track direction for the platoon following vehicle compared to the baseline runs. This may be caused by the increased variability of the inverted

CACC control system or the wind conditions that were not factored into these calculations. Despite the variability, these results are still valid but have an increased uncertainty due to the scatter. The platoon coastdown results were also verified with model simulations as described in Appendix C.4.

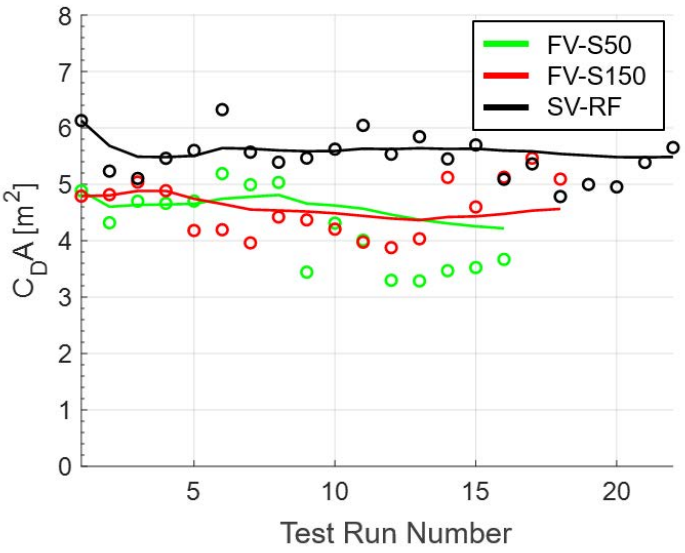

Figure 4.12: Platoon following vehicle drag area results.

The prior results show the individual calculations for each test run. These calculated results were then combined and analyzed for the overall drag reduction, similar to the fuel test analysis. The drag area reduction as a function of platoon gap distance is shown in Figure 4.13. These results show the aerodynamic benefit relative to the single vehicle baseline. The lead vehicle results show that there is no aerodynamic benefit at 45.7 m, and this result is consistent with the assumption that the lead vehicle is not influenced by the following vehicle at large following distances [39]. At the closer spacing of 15.2 m, the lead vehicle's reduction is $4.2 \pm 3.9\%$. This result shows there is a small, positive benefit at this gap distance.

As previously discussed, the following vehicle has significant aerodynamic benefits in the platoon. The follower's drag area reductions are $16.8 \pm 5.1\%$ and $23.1 \pm 7.2\%$ at 45.7 m and 15.2 m respectively. Although there are only two data points, these results follow the expected trend of increasing reduction with decreasing platoon gap distance. The magnitude of these results also suggests that the drag area reduction would persist at large following distances.

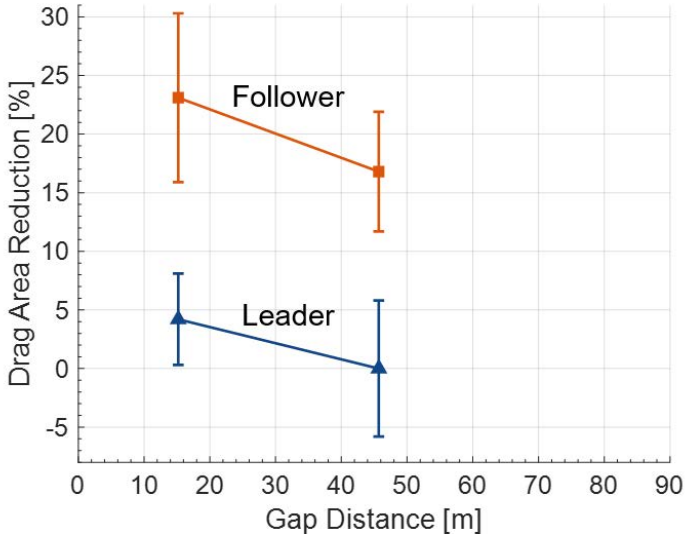

Figure 4.13: Platoon drag area reduction.

However, this study was limited in scope and more tests should be conducted to validate the benefits at closer and further gap distances.

A summary of the controlled coastdown test results is shown in Table 4.4. These results are similar to the constant-speed truck platoon drag results presented in [36]. McAuliffe showed the following vehicle drag reduction results of 12.5 $\pm$ 4.4% at 58 m and 20.4 $\pm$ 4.6% at 18 m [36]. These data points are not at the same platoon gap distance or tractor-trailer combination, but the magnitude and trends are the same as those presented here. In addition, the lead vehicle in [36] only showed drag reduction at distances less than 12 m. This result is consistent with the current study where little or no benefits were measured for the lead vehicle. Overall, this comparison supports that the controlled coastdown was completed effectively and can be used to quantify platoon drag area reduction.

Table 4.4: Coastdown test results.

Coastdown Position	**Spacing**	$\mathbf{C_DA[m^2]}$	$\mathbf{C_{RR}[-]}$	**Drag Area Reduction** [%]
Single vehicle	∞	5.49 $\pm$ 0.80	0.0049 $\pm$ 0.0007	-
Lead vehicle	15.2 m (50 ft)	5.26 $\pm$ 0.42	0.0050 $\pm$ 0.0010	4.2 $\pm$ 3.9
Lead vehicle	45.7 m (150 ft)	5.49 $\pm$ 1.19	0.0049 $\pm$ 0.0013	0.0 $\pm$ 5.8
Following vehicle	15.2 m (50 ft)	4.22 $\pm$ 1.46	0.0046 $\pm$ 0.0005	23.1 $\pm$ 7.2
Following vehicle	45.7 m (150 ft)	4.56 $\pm$ 1.04	0.0045 $\pm$ 0.0007	16.8 $\pm$ 5.1

4.4.3 Comparison to Fuel Test

The platoon coastdown test is representative of the aligned platoon during the fuel test. For reference, the aligned platoon described the nominal platooning scenario where the platooning vehicles had the best lateral alignment possible. In order to compare this aerodynamic evaluation to the fuel test, the drag area reductions were converted to an estimated fuel savings. The results are converted from the calculated coastdown results in Table 4.4 (with $C_{RR0,avg} = 0.0048$) and a road load model equivalent to the fuel test. The road load force, F_{RL}, is defined as $F_{RL} = F_{aero} + F_{RR} + F_{grade}$ where the resistive forces are the same as in Appendix C.2. The equivalent road load components are then calculated in Table 4.5 assuming $F_{grade} = 0$, $m = 29,500$ kg (65,000 lbs), $v = 105$ km/hr, and $\rho = 1.2$ kg/m^3 during the fuel test. From the coastdown coefficients and fuel test parameters, the average road load

Table 4.5: Equivalent road load during fuel test with coastdown test results.

Configuration	$\mathbf{F_{aero}}$[N]	$\mathbf{F_{RR}}$[N]	$\mathbf{F_{RL}}$[N]	% **Aerodynamic**
SV-RF	2800	1846	4646	60
LV-S50	2683	1846	4529	59
LV-S150	2800	1846	4647	60
FV-S50	2153	1846	3999	54
FV-S150	2329	1846	4176	56

is 58% aerodynamic force and 42% rolling resistance force. The coastdown results are converted assuming that the aerodynamic force is 58% of the overall road load. For example, an aerodynamic reduction of 20% would result in a fuel saving of 11.6%.

With the average aerodynamic percentage, Figure 4.14 shows the estimated fuel savings compared to the aligned platoon fuel test results (shown previously). The leader's estimated fuel savings follow the same trend previously described: little to no fuel saving benefit at either following distance. This result is consistent with the fuel test where a small, positive fuel saving of 3.3 $\pm$ 1.5% was measured at 15.2 m.

The follower's estimated fuel savings also follow the experimental trends but have a nominally higher magnitude. At 45.7 m, the follower's estimated fuel savings are 9.7 $\pm$ 3.0% and

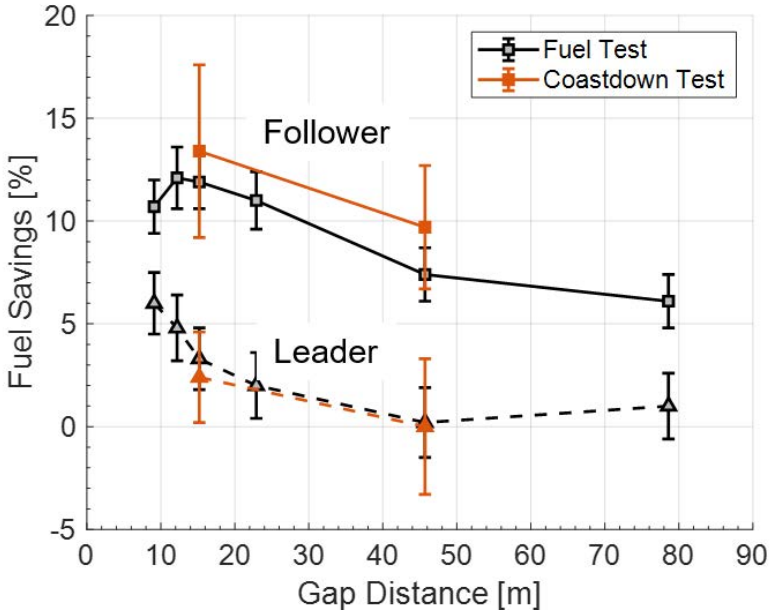

Figure 4.14: Estimated fuel savings from coastdown test compared to experimental fuel test.

the actual fuel test results were 7.4 $\pm$ 1.3%. At this distance, the coastdown test results predict a higher fuel savings of 2.3%. Similarly, the results at 15.2 m are 1.5% higher than the experimental test with estimated savings of 13.4 $\pm$ 4.2%.

It is important to note that all the estimated fuel savings and error bars overlap the corresponding values from the fuel test. The overlapping error bars suggest a common answer for the two tests, but it is interesting that the overpredicted fuel savings was also described in the constant-speed platoon analysis by McAuliffe [33]. McAuliffe described the same trend but with a higher overprediction of 2-5% and suggested a potential reason for this discrepancy are losses in the control strategy. The discrepancy shown here was smaller in magnitude, 1.5-2.3%, but further research is needed to address this result.

4.5 Conclusions

This chapter described a novel aerodynamic evaluation of truck platooning through the controlled coastdown method. The coastdown test was completed for a single vehicle and for platoon configurations using a CACC system to control the gap distance. The test configurations included the lead and following vehicle position and two platoon gap distances to quantify

the drag area reduction. This study was completed to show a proof of concept for the controlled coastdown test and serve as preliminary evaluation for future use. The results were calculated using a split range coastdown and the High/Low solution method. Although the results show some scatter, the drag area reductions for the following vehicle are distinct and significant in magnitude (16.8 - 23.1%). The lead vehicle reductions are less in magnitude, but these results agree with prior research that only showed aerodynamic benefits at distances lower than 12 m [36]. The drag area reductions were also converted to an estimated fuel saving for direct comparison to the previously described fuel test. The coastdown estimated savings agreed well with the corresponding fuel test which suggests two things: the main mechanism for platoon fuel savings is aerodynamic drag reduction and the controlled coastdown test can be used to quantify drag area reduction from platooning.

Chapter 5

Highway Fuel Test

In the prior chapters, the benefits of truck platooning were evaluated through a fuel test and an aerodynamic test. Both of these tests were completed on the controlled test track environment to increase repeatability and study different configurations. However, the test track results only represent some of the conditions a vehicle experiences on-road. It is important to study truck platooning in an on-road environment to understand the benefits vehicles, or fleets of trucks, can achieve from this technology.

Recently, prior research has introduced the idea that truck platoon benefits may differ on-road compared to the test track. [14] provides an overview and motivation for on-road truc-platoon testing, but their dataset and analysis was limited due to the lack of a control vehicle and gravimetric measurements. Other research suggests that truck platoons can be affected by the presence of other vehicles on the roadway [17], [21]. Much of this prior research motivated the "other traffic" cases studied during the Canada fuel test and in [44]. McAuliffe et al. evaluated the platoon fuel savings with a fixed upstream traffic pattern, a heavy duty truck, vehicle cut-ins, and dynamic vehicle passing on the test track [44]. In an on-road environment, a truck platoon can, and likely will, experience one or more of these effects, which may influence the achievable fuel savings. This chapter introduces a highway fuel test to study the complex on-road environment. The background, procedures, and analysis are discussed, and the basic gravimetric results are presented.

5.1 Background

The highway testing took place on Interstate 85 near Auburn, Alabama in the Fall of 2019. The testing was completed as a follow up to the limitations found in [14] and provide gravimetric results from on-road truck platooning. The vehicles and analysis are similar to the prior testing described, and this section provides the relevant background for the highway test.

5.1.1 Vehicles

The on-road testing was a two truck platoon with the same two Auburn Peterbilt 579 trucks previously described. All testing was completed in the same platoon order as the Canada fuel test: A1 was the lead vehicle and A2 was the platoon follower. There was not a control vehicle available for this testing, similar to [14], but the lead vehicle was used as a control truck as described later. The vehicle modifications described in the Chapter 4, including the fifth wheel position and extra antenna mounting, were the same for this testing as well.

The testing was completed with unloaded, 53' box trailers with side skirts. A1 pulled a 4000D-X Composite Utility trailer, and A2 pulled a Hyundai Translead trailer. The estimated GVWR is 16,000 kg (35,000 lbs) for each vehicle. It is important to note that the vehicle configurations can influence the fuel saving results. For example, the lower GVWR has an impact on the road load and fuel savings. McAuliffe et al. describe this effect and demonstrated a 1-2% higher fuel savings for an unloaded trailer (31,000 lbs) compared to a loaded trailer (65,000 lbs) [53]. In addition, the differing aerodynamic technology on the trailers has an impact on the aerodynamic drag and road load as well. In the same testing, McAuliffe et al. tested truck platoons with a standard trailer and aerodynamic trailer with side skirts and boat-tails. The results showed that the platoon following vehicles achieved a 0.5-2% higher fuel savings with the aerodynamic trailer compared to the standard trailer [53]. For this testing, these two effects are combined with the new environment (the highway with uncontrolled traffic) in order to quantify the fuel savings.

5.1.2 Test Route

The testing was completed on highway I-85 between Opelika and Tuskegee in Alabama. The test route is shown on the map in Figure 5.1 (created using [46]). The route began and ended at Exit 62 in Opelika, AL with a turn-around point at Exit 32. The test started on I-85 going South, and the total distance was 77.2 km (48 miles) long.

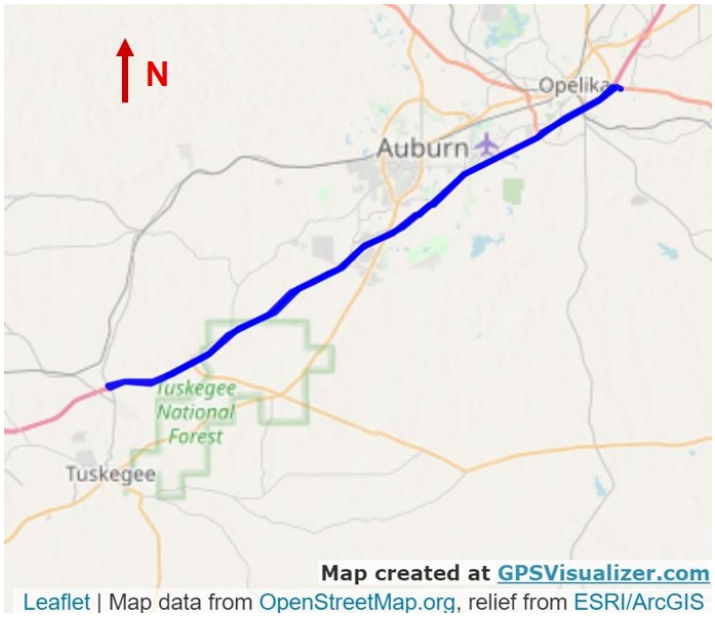

Figure 5.1: Test route for highway fuel test.

This highway route was selected for its length and proximity to Auburn. Overall, the route is a four-lane highway over rolling hills terrain. An example of the road grade is shown in Figure 5.2 for the South portion of I-85. The road grade reached $\pm$ 4% but much of the grade was between $\pm$ 2%. This environment has a much different grade profile than the test track and is more representative of a heavy duty truck drive cycle.

5.1.3 Instrumentation

Gravimetric fuel measurements were taken for this test campaign, like the Canada fuel test. External fuel tanks were mounted on the back of the tractor, between the fifth wheel and cab as shown in Figure 5.3. The fifth wheel was moved to its furthest back position to allow clearance between the trailer and fuel tank. The external tank is sitting on top of an aluminum

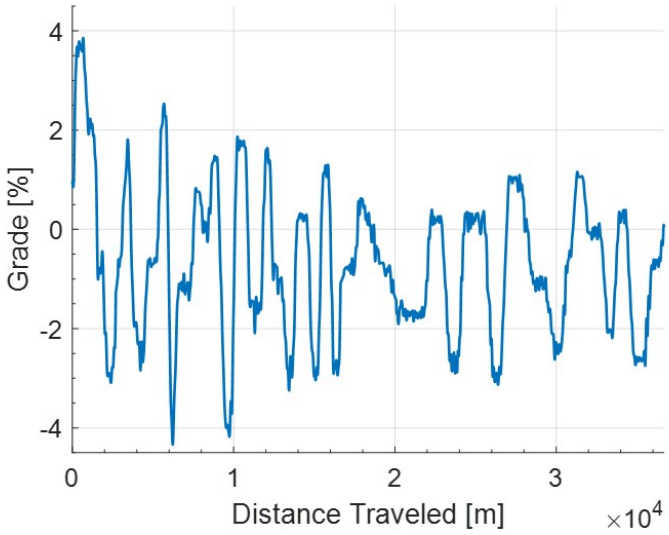

Figure 5.2: I-85 test route road grade.

Figure 5.3: External fuel tank for the highway test.

box for easy access and was held in place with straps connected to the truck frame. Quick connect fittings were used to easily attach and remove the fuel lines. Rather than connect the fuel lines directly to the fuel filter, alternative fuel lines were installed along with ball valves. A switch was then placed in the cab and wired to the ball valves. The switch position controlled which tank the fuel was drawn from; when the switch was off, the fuel was drawn from the vehicle's primary tank, and when the switch was on, the fuel was drawn from the external tank. The switch was used at the beginning and end of the test such that the fuel consumed was only from the test section of the route. A precision scale with an accuracy of 0.05 lbs was used to weigh the tanks before and after each test.

The CACC systems were used to collect and record data. The relevant information includes GPS position and time, CAN bus data, and CACC system data. It is important to note that no weather or wind speed measurements were taken during the highway test campaign.

5.1.4 Test Procedures and Analysis

Each test consisted of one lap on the route for a total distance of 77.2 km. The target speed of each test was 105 km/hr (65 mph), but the speed deviated from this when the platoon was affected by upstream traffic. For example, if the platoon approached a slower moving vehicle, the lead vehicle's ACC system would slow the platoon down. The truck platoon would pass slower moving traffic as needed to keep the set speed. The test procedure was simple: enter the highway, flip the fuel switch on (using signs for reference), complete the South part of the route, flip the switch off to turn around, flip the switch on once heading North bound, and flip the switch off at the end of the test. The gravimetric measurement represents only the fuel consumed during the on-highway portion of the test.

The SAE J1321 procedure [28] previously described was not strictly followed for this test campaign but used as a guide. The J1321 standard allows for on-road fuel testing and provides specific guidelines to complete testing this way. For example, the standard recommends each run should be greater than 100 miles for on-road testing and greater than 50 miles for test

tracks. At least 3 runs were used to calculate the savings for a given test configuration, similar to the track fuel testing. Additionally, some of the testing was completed with the J1321 recommended 1 hour warm-up, but a 15 minute warm-up was the minimum.

The fuel savings were calculated using the same process described in Appendix B.2 with fuel ratios of the test to control vehicle, T/C. This was completed to limit bias or error in the results for testing not completed simultaneously. The lack of control vehicle was the limiting factor in this testing, but the analysis was completed using the lead vehicle as the control vehicle. As described by Lammert et al., the lead vehicle is not influenced by the following vehicle at gap distances greater than approximately 25 m [39]. At these distances, the lead vehicle experiences conditions as if it were isolated and can be used as the control vehicle.

The T/C ratios were formed from the fuel weight measurements, with A2 being the test vehicle and A1 as the control. However, a portion of testing was completed with a known leak in A1's external fuel lines. These runs did not have a valid control vehicle weight, which is needed to use the corresponding test vehicle weight. A fuel rate calibration was completed for A1 using the fuel weight measurements after the leak was fixed to maximize the amount of data available. The fuel rate calibration, described in Appendix B.3, used 7 calibration points with the measured fuel weight and the calculated fuel volume (integrated from the CAN bus fuel rate). The fuel rate calibration is shown in Figure 5.4 , and the slope of the calibration line was

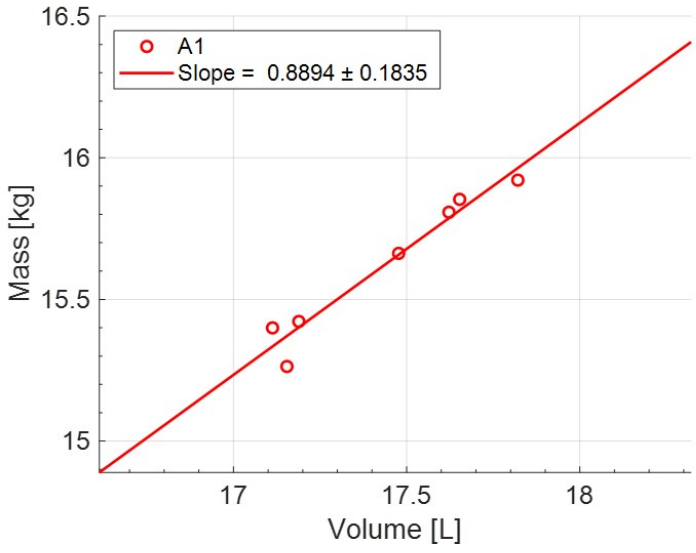

Figure 5.4: Fuel rate calibration for A1 during highway test.

calculated as C_f = 0.8894. Then, a calibrated fuel weight was calculated using the fuel volume and the calibration constant. This was completed for the runs with invalid measurements and produced a complete dataset to analyze. The results calculated with the calibrated fuel weight also have an additional error from the calibration. This error is incorporated into the result uncertainty and is assumed to be 0.5%. This is the same value calculated by Lammert et al., and the calibration constant is within 0.4% of the one from that testing [39].

5.2 Test Configurations

The on-road truck platoon was tested at two platoon gap distances: 22.9 m (75 ft) and 45.7 m (150 ft). The testing was a two-truck platoon with A1 operating ACC and A2 following with the CACC controller. The configuration was similar to the aligned platoon and mixed traffic scenarios tested during the Canada test campaign. This section describes the similarities of this test to the fuel test and presents the test matrix completed.

5.2.1 Comparison to Mixed Traffic

The Canada fuel test in Chapter 3 described several mixed traffic scenarios that a platoon could encounter on-road. Specifically, the platoon fuel savings were presented for a fixed traffic pattern of passenger vehicles and a forward heavy duty truck. In addition, McAuliffe et al. studied several other traffic related events in [44]. The other traffic events include vehicle cut-ins and vehicle passing events, and the results are summarized here to provide context for the current highway testing.

Cut-ins occur when a vehicle inserts itself between the two platooning vehicles. These events were experienced during the previous on-road testing in [14], and the CACC system has a cut-in detection system (previously described in Chapter 2) to detect and respond to vehicle cut-ins. Vehicle cut-ins were studied during the Canada fuel test at the platoon gap distance of 23 m. The results showed the fuel savings were completely negated by regular cut-ins. McAuliffe et al. show the following vehicle's behavior and describe the response depends on the control system implementation [44]. This is important to note in an on-road environment where it is possible for cut-ins to occur.

Another on-road scenario is dynamic vehicle passing. This event occurs when passenger vehicles or other heavy trucks pass the platoon in the neighboring lane. This scenario was recreated on the test track for the platoon following at 15 m gap distance, and the passing events only had an effect on the lead vehicle's fuel savings. The lead vehicle's savings had a 2% reduction in savings while the following vehicle retained the same savings when compared to the isolated platoon scenario. Overall, the highway is represented by a combination of the previously described configurations and others. For this reason, the highway testing is difficult to analyze with the transient and uncontrollable environment but is important to understand the expected benefits from platooning.

5.2.2 Test Matrix

A summary of the highway testing is shown in Table 5.1 which includes single vehicle baselines and two platoon gap distances. Each platooning test included two runs using the fuel-calibrated weight measurement previously described. Also, two of the three reference runs were completed with A1 and A2 simultaneously, with at least 160 m (0.1 mile) spacing. An additional reference run was completed right after one another with an hour between tests. It is assumed that the on-road conditions (traffic and weather) were the same during this time period. The final run totals included 3 baselines, 4 runs at 22.9 m, and 5 runs at 45.7 m.

Table 5.1: Highway test matrix.

Date	**Test**	**Spacing [m]**	**A1 Fuel Calibrated**
9/23/2019	Platoon	22.9	Yes
9/25/2019	Platoon	45.7	Yes
9/25/2019	Platoon	22.9	Yes
9/25/2019	Platoon	45.7	Yes
9/27/2019	A1/A2 Reference	∞	No
9/30/2019	Platoon	22.9	No
9/30/2019	A1 Reference	∞	No
9/30/2019	A2 Reference	∞	No
10/1/2019	Platoon	22.9	No
10/1/2019	Platoon	45.7	No
10/1/2019	Platoon	45.7	No
10/2/2019	Platoon	45.7	No
10/3/2019	A1/A2 Reference	∞	No

5.3 Results

The highway fuel test results are an example of the fuel savings a truck platoon may achieve on-road. The gravimetric results were calculated following the SAE J1321 procedure, and the savings are presented with the average and 95% CI error bars. In this analysis, the lead vehicle was used as the control vehicle for both gap distances. At 22.9 m, the lead vehicle may be influenced by the following vehicle as evident from the Canada mixed traffic platoon results with a minimal savings of 1.2%. Additionally, other research suggests the lead vehicle is not influenced by the following vehicle at this distance [36], [53]. Therefore, this analysis assumes the lead vehicle is not effected by the follower. This assumption adds an additional uncertainty in the results if the lead vehicle is actually affected. The uncertainty can be estimated using road load estimates at the two different configurations: the Canada fuel test with GVWR of 29,500 kg and the highway fuel test with GVWR of 16,000 kg. Using these road load estimates and the lead vehicle's fuel savings in Canada, and assuming the change in absolute aerodynamic drag is the same for the highway test, the additional uncertainty is estimated to decrease the following vehicle's savings up to 1.5%.

These results assume there is no fuel saving for the lead vehicle so only the following vehicle savings are calculated. The lead vehicle may experience savings from the nominal other traffic on the roadway, but the current dataset has no way to evaluate this with the lack of a separate control vehicle.

5.3.1 Gravimetric Results

The gravimetric fuel savings from the highway testing are shown in Figure 5.5 compared to the fixed traffic platoon from the Canada fuel test. For reference, the test track results represent the two-truck platoon following a 3 vehicle traffic pattern which is the closest comparison to the highway data. The highway results show a reduction in savings at both platoon gap distances tested. The results show a positive fuel saving of $4.6 \pm 2.2\%$ at the 22.9 m gap distance. This result dropped from the corresponding Canada test result of 8.4% at the same distance. At 45.7 m, the following vehicle does not have any fuel savings with the error bar crossing zero.

This test has a large error bar associated with the result, $\pm$ 4.2%, despite having the most test runs (5 runs). On the test track, an increase in the number of runs would typically reduce the result error bars, and this is an example of the highly variable on-road environment.

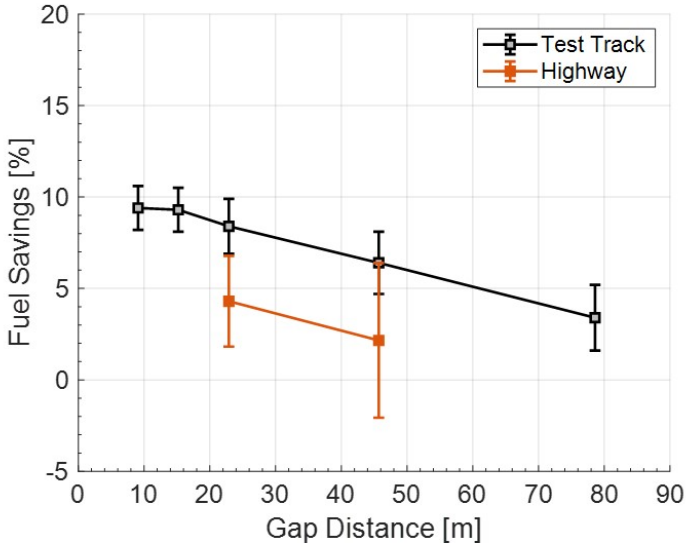

Figure 5.5: Highway test gravimetric fuel savings.

The reduction in fuel savings may be caused by a change in the drive cycle, transient traffic, or a number of other factors. These factors make these results difficult to analyze. As previously mentioned for the difference in the Canada and highway tests, the differing aerodynamic trailer technology suggests the highway results should be lower than the test track, but the lower GVWR for the highway test suggests the results should be higher than the test track, assuming the same drive cycle. The combination of these effects is also compounded with the different drive cycle, namely the more realistic road grade. The specific impact of the road grade on the truck platoon fuel savings has not been explicity studied and could also contribute to the reduced savings. However, it is important to note that the average fuel savings are positive in this preliminary study even under the variable circumstances. These results are limited in scope and more tests are needed to quantify and further study the fuel saving benefits of on-road platooning.

5.3.2 Highway Analysis

The highway platooning data was studied further to provide context for the gravimetric results. In particular, the control performance, amount of traffic, and number of other vehicle interactions were briefly studied. A summary of this analysis is shown in Table 5.2 with statistics about the longitudinal control performance and the estimated number of neighboring vehicles. The estimated number of neighboring vehicles is the same value described in [14] and is the number of vehicles the following vehicle's cut-in detection is tracking using the RADAR measurements. For reference, the RADAR has a 60 m range with $\pm$ 45° field of view (FOV). This value is a measure of the number of vehicles in the adjacent lane because the platoon leader is directly in front of the follower. The average number of neighbors represents the nominal traffic traveling in the RADAR's FOV throughout the duration of the test. The standard deviation of neighboring vehicles is a measure of the variation in the estimated traffic. For example, a higher standard deviation for the number of neighbors suggests there were periods with a higher or lower number of vehicles on the roadway.

Table 5.2: Highway test matrix.

Run #	**Run ID**	**Gap [m]**	**Avg Error [m]**	**Std Error [m]**	**Avg # Neighbor**	**Std # Neighbor**	**Speed Dist.**	**Cut -ins**	**Major Dist.**
1	F4	22.9	-0.17	2.95	0.70	0.73	5	0	1
5	F6	45.7	0.50	3.85	1.25	1.45	4	4	2
2	F7	22.9	-0.06	2.24	0.84	0.88	3	1	0
6	F8	45.7	-0.02	3.12	1.19	1.12	2	3	2
3	F14	22.9	0.03	1.78	0.73	0.85	5	2	1
4	F18	22.9	0.07	1.84	0.70	0.80	1	0	1
7	F19	45.7	-0.85	9.69	0.85	0.95	4	2	1
8	F20	45.7	0.09	2.27	0.98	0.99	1	1	2
9	F21	45.7	-0.59	6.69	0.98	1.00	2	1	1

The table also includes vehicle interactions during the testing and are grouped into three categories: speed disturbance, cut-ins, and major disturbance. Speed disturbances are a minor disturbance that occur when either platooning vehicles' speed deviated from the set speed by $\pm$ 5 mph. The speed disturbance typically occurred when the lead vehicle's ACC system detected a slower moving vehicle, slowing the platoon. The next category is cut-ins and occurred

when a vehicle inserts itself between the two platooning vehicles. The following vehicle detects and responds to the cut-in vehicle with the cut-in detection system, and the impact of this event depends on the cut-in vehicle's behavior [14]. The last category was major disturbances that caused significant impact on the truck platoon. Major disturbances included large amounts of traffic, merging traffic, or any other event that caused the driver to assume manual control. These events were infrequent but happened several times during the highway testing.

The nominal control performance was evaluated first without disturbances and is shown in Figure 5.6 for a platoon test at 45.7 m gap distance. These results show the expected on-road performance with more realistic road grade. The control performance decreases from the test track with an increase in the standard deviation. The longitudinal controller performs well on the highway with realistic road grade and no disturbances.

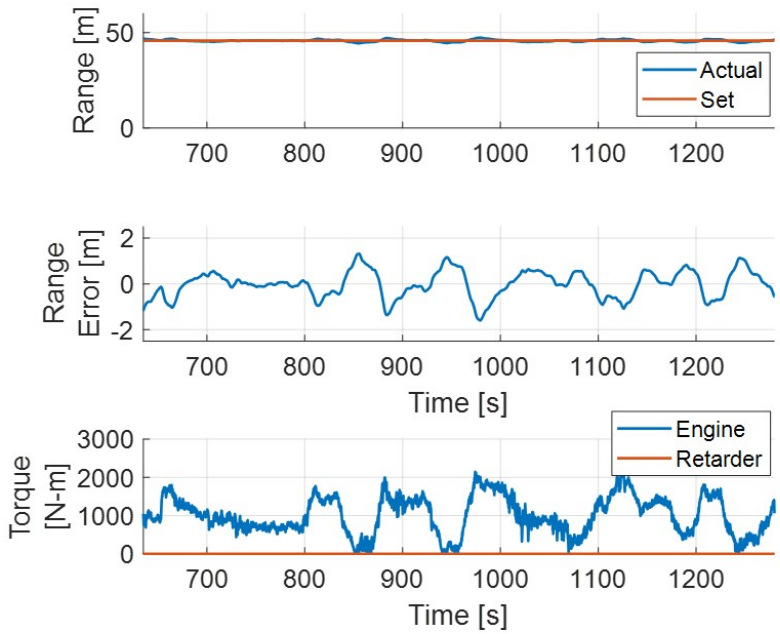

Figure 5.6: Control performance on highway with no disturbances.

The control performance was then studied for the duration of all test runs. The average and standard deviation (as error bars) of the controller error is shown in Figure 5.7, where blue is the 22.9 m test and orange is the 45.7 m test. These results show an average control error of approximately zero for all tests, which is expected, but the standard deviation differs

based on platoon gap distance. The standard deviation shows the impact disturbances have on the platoon following vehicle. In this testing, the standard deviation doubles at the larger gap distance, which suggests the traffic and other disturbances affected the platoon more at this following distance. At the closer gap distance, the following vehicle was able to follow more consistently, shown by the lower standard deviation.

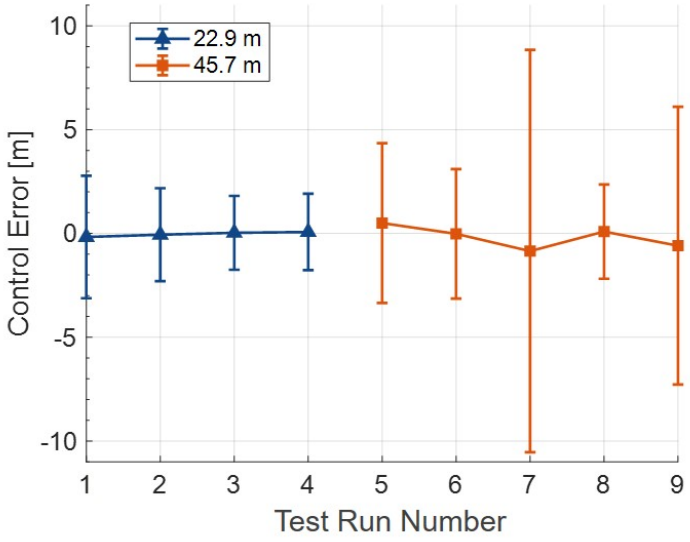

Figure 5.7: Control performance for highway platoon tests.

The amount of traffic and disturbances was then studied for the highway testing. These results are shown in Figure 5.8 with the estimated number of neighboring vehicles shown on top and the number of disturbances shown on bottom. The number of neighboring vehicles is used as an estimate of the amount of traffic on the roadway around the platoon, and these results are consistent for both platoon gap distances. The estimated amount of traffic is slightly higher at the larger following distance, but the results are similar. These results show the number of other vehicles on the highway likely did not cause the decrease in control performance at the larger following distance.

The number of platoon disturbances, separated by color, are shown in the bottom of Figure 5.8. These results show that speed disturbances were the most common disturbance with 3 or more events for nearly all test runs. The speed disturbances also occurred at both gap distances at a similar frequency. In contrast, there is a distinction between the two platoon gap

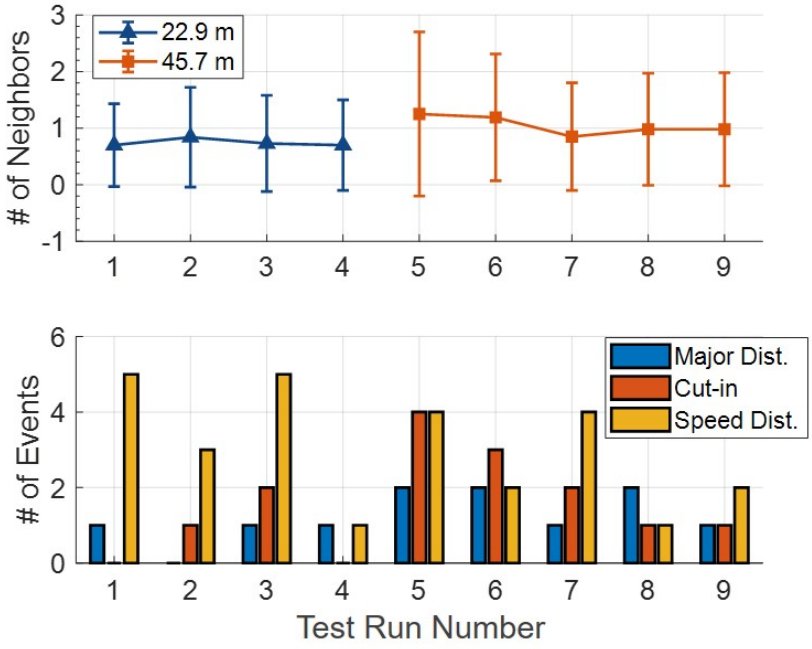

Figure 5.8: Traffic and disturbances for highway platoon tests.

distances for the remaining disturbances. The average number of major disturbances per run increased from 0.75 at 22.9 m to 1.60 at 45.7 m. This increase may be erroneous, but one reason may be due to the increased overall platoon length at the larger distance. For example, the platoon occupies more length of the highway with increasing gap distance and may be more susceptible to major disturbances. However, this is a hypothesis and would be difficult to quantify in the highly variable on-road environment.

The number of cut-ins also differed between the platoon gap distances. The average number of cut-ins per run was 2.20 at the larger following distance, which is nearly 3x the amount at the shorter distance, 0.75. This result is supported by [14] that suggested cut-ins are more likely to occur with increasing platoon gap distance. The cut-ins are more likely because there is more room in-between the platooning vehicles. It is interesting to note that the number of cut-ins increased even with a similar amount of traffic on the highway. The impact of the cut-ins on the fuel savings is not studied here but is expected to have a significant impact on the following vehicle with the current CACC system, as previously described in [44]. McAuliffe et al. contrast the CACC cut-in system to a stock ACC system and the vehicles' respond quite

different. Furthermore, cut-ins were also studied as part of another test-track study and were shown to have minimal effect on the platoon fuel savings [17]. It is important to note that the loss of fuel savings for this test campaign is likely due to the control system, and the CACC control system can be improved for better performance. The cut-ins could also be further studied using the CAN bus fuel rate analysis, as done in Chapter 3, and can provide insight into the effects of cut-ins for the on-road platoon.

The number of disturbances during the highway platoon testing affected the control performance, especially for the following vehicle. However, it is difficult to quantify the types of disturbances and their specific impact on the platoon fuel savings. This supports track fuel testing where a scenario, such as the fixed traffic platoon, can be tested and the independent impacts can be studied in a more controlled fashion. Overall, the total dataset included 52 total disturbances for all tests, or approximately 1 disturbance every 8 miles traveled. The CACC system also operated for over 400 miles of highway with other traffic. Although there were disturbances and other uncontrollable factors, this testing supports that CACC systems can be developed for on-road use. Further testing and data analysis is needed to study the benefits and potential issues from on-road truck platooning.

5.4 Conclusions

This chapter described a series of on-road highway tests to examine the fuel savings of truck platooning in a realistic environment. This testing is important to understand the achievable benefits of truck platooning, as compared to those evaluated on a test track. Gravimetric measurements were taken for a two truck platoon on a highway route to study the fuel savings. The J1321 analysis showed a fuel savings of $4.6 \pm 2.2\%$ at 22.9 m platoon gap distance, a reduction from a similar test completed on the track during the Canada fuel testing. At the larger distance of 45.7 m, there were no measurable savings for the following vehicle. The platoon control performance and interactions with surrounding traffic were then studied and showed an increase in disturbances from the closer gap distance. These interactions and their variable nature cannot be represented on a test track and are difficult to quantify. In particular, the effect

of cut-ins was studied in prior research and likely caused a decrease in the fuel savings during this testing. This CACC system's cut-in detection is not optimized for fuel economy and should be improved for better on-road performance. The highway test campaign was limited in scope but showed that fuel savings can still be achieved. However, more testing is required to understand all the effects, such as road grade and platoon disturbances, truck platoons may experience on-road.

Chapter 6

Conclusions and Future Work

6.1 Conclusions

The evaluation of new vehicle technology is critical to understand widespread benefits and impacts. Heavy duty trucks are of particular interest for their importance to the economy and relative inefficient fuel consumption and GHG emissions. This thesis presented a Cooperative Adaptive Cruise Control (CACC) truck automation system that allows two vehicles to benefit from traveling in close proximity to each other, or platooning. The CACC system was introduced and the individual components were described. Prior research demonstrated Auburn University's platooning system implementation and feasibility through testing on test tracks and on-road. The remainder of this thesis focused on the evaluation of a two truck platoon to study the fuel savings of truck platooning in a variety of configurations.

The Auburn University CACC platooning system was evaluated through a formal SAE Type II fuel test with gravimetric measurements on a Canadian test track. The Canada fuel test studied a variety of platoon configurations, such as the nominal, aligned platoon and mixed traffic platoon, with inter-vehicle gap distances from 9.1 to 78.6 m. The aligned platoon results were similar in magnitude and trends to prior research. The lead vehicle demonstrated monotonically increasing savings with decreasing platoon gap distance. The following vehicle had much higher savings from 6.1 $\pm$ 1.3% at the furthest distance to 10.7 $\pm$ 1.3% at the closest with a maximum of 12.1 $\pm$ 1.5% at 12.2 m. This dip in the following vehicle's savings with decreasing gap distance was not explained in this thesis, but is consistent with prior research.

Additional tests were conducted to replicate the traffic conditions a truck platoon may experience in an on-road environment. These tests showed that a single truck achieved 4.6 - 7.4% nominal savings, and the fixed traffic platoon demonstrated that platooning is still effective with these nominal savings removed. The fuel savings were not only retained but were additional (not directly additive) to the nominal savings with the presence of other traffic. This is important to understand what trucks on-road might experience rather than on a test track. The mixed traffic also provided insight that the platoon lead vehicle and its control system are important to the overall platoon's efficiency. The ACC system, target detection, and system response performed differently with a forward SUV and heavy duy truck. As a result, the lead vehicle can be particularly important with the presence of other traffic on the roadway.

As an alternative evaluation, aerodynamic testing was completed for the two truck platoon using a first of its kind, controlled platoon coastdown test. The coastdown test and its procedure were described and provided a novel aerodynamic evaluation of truck platooning. The CACC system was modified to allow for coastdown of the lead and following vehicle to quantify the platoon's drag area reduction. The coastdown tests were completed on a test track and showed a proof of concept for the controlled coastdown. The drag area reductions were demonstrated for two platoon gap distances, and the results agreed well with similar prior research. The calculated drag area reductions were also converted to an estimated fuel savings for comparison to the Canada fuel test and the results were within the uncertainty of each other. This confirmed that platoon fuel savings are predominantly aerodynamic in nature and that the platoon controlled coastdown can effectively quantify drag area reduction.

Finally, an on-road fuel test was conducted to provide insight into the achievable fuel savings for truck platooning in an uncontrolled environment. Although the testing was limited, two platoon gap distances were evaluated using gravimetric measurements on a 48 mile highway route. There was not a separate control vehicle for the testing, but the lead vehicle was used as the control with the assumption the lead vehicle is not influenced by the follower. The following vehicle showed a fuel saving of $4.6 \pm 2.2\%$ at the 22.9 m gap distance, which was a reduction from a similar configuration on the test track. An analysis of traffic and the platoon's interaction with other vehicles was completed and provided context for the reduced control

performance of the following vehicle. This analysis showed major platoon disturbances and vehicle cut-ins occurred 2x and 3x more often at the 45.7 m gap spacing compared to 22.9 m. These results highlight the importance of the CACC system to handle a variety of scenarios and future work is needed to understand the expected on-road fuel saving of platooning.

Overall, this thesis provided the relevant background and motivation for improving the fuel efficiency and GHG emissions of heavy duty trucks. An overview of evaluation techniques was provided, and three separate evaluations were provided for the two-truck platoon with this CACC system. Fuel testing was used as a common evaluation for truck technology, and the controlled coastdown was a novel method to evaluate the aerodynamic benefits from truck platooning. In conclusion, these evaluations provide relevant information and describe some of the potential benefits for widespread adoption of CACC platooning for heavy duty trucks.

6.2 Future Work

The conclusions in this thesis lead to future work to further understand heavy duty truck platooning. Specific future work is discussed for the CACC system, fuel testing, coastdown testing, and on-road evaluation of truck platooning.

The CACC system has a number of improvements which should be investigated to handle more scenarios and achieve higher performance. The control system performance here was adequate, but higher levels of performance, especially tracking transients, may require a new implementation. Future work can be completed to include optimal engine control or road grade information into the control architecture. The platoon's interactions with other traffic can also be improved. For the lead vehicle, a new system can be designed to replace the stock ACC system. This could include an optimal cruise controller and a "cut-in" detection system. This new system would allow for more development and control on the lead vehicle, which was shown to be important in Chapter 3. For the following vehicle, the cut-in detection system can be further tuned for a better control response.

Future work can also be completed for fuel testing of heavy duty truck platooning. In this thesis, a two truck platoon was studied for the fuel testing, and this work can be extended by studying a 3 or 4 truck platoon. Similarly, work can be completed in mixed tractor-trailer

combinations that may provide optimal platoon configurations based on vehicle shape or trailer load. Fuel testing should be completed at more platoon gap distances to study the trade-off between fuel savings, safety, and implementation as these systems are developed and deployed.

The use of the controlled coastdown should be studied further to provide insight into the aerodynamics of platooning. This thesis developed and proved the viability of the platoon coastdown test, and more testing should be completed with more platoon gap distances at a facility where a higher speed can be achieved. Additionally, anemometry should be incorporated into the coastdown analysis to provide higher quality results and the drag area as a function of yaw angle. The CACC system controller can also be improved for better performance during the controlled coastdown. This could include an updated vehicle model, control design, or simple tuning of the current system.

A significant amount of future work can be completed in terms of on-road platoon testing. This testing is important to provide feedback for the CACC system design and improvement as well as provide context for the fuel saving potential of on-road platooning. Further analysis should be completed for the on-road testing completed in this thesis, but more data is likely needed to quantify effects from the highly variable highway environment. Ultimately, this testing could drive commercialization of this technology and inform potential consumers of the potential benefits or drawbacks.

References

[1] U.S. Department of Commerce, "The Logistics and Transportation Industry in the United States." https://www.selectusa.gov/logistics-and-transportation-industry-united-states. Accessed: 2020-03-05.

[2] Federal Motor Carrier Safety Administration, "2019 Pocket Guide to Large Truck and Bus Statistics," Technical Report, U.S. Department of Transportation, Jan. 2020.

[3] Environmental Protection Agency and Department of Transportation, *Greenhouse Gas Emissions Standards and Fuel Efficiency Standards for Medium- and Heavy-Duty Engines and Vehicles*. USA, Sept. 2011. Vol. 76, No. 179.

[4] Federal Highway Administration, "Annual Vehicle Distance Traveled in Miles and Related Data - 2018 by Highway Category and Vehicle Type," Highway Statistics Table VM-1, U.S. Department of Transportation, 2018. Revised November 2019.

[5] T. E. Reinhart, "Commercial Medium- and Heavy-duty Truck Fuel Efficiency Technology Study - Report 1," Report DOT HS 812 146, Southwest Research Institute, June 2015. Revised Octover 2015.

[6] Environmental Protection Agency and Department of Transportation, *Greenhouse Gas Emissions and Fuel Efficiency Standards for Medium- and Heavy-Duty Engines and Vehicles - Phase 2*. USA, Oct. 2016. Vol. 81, No. 206.

[7] J. Katz, "Aerodynamics of race cars," *Annual Review of Fluid Mechanics*, vol. 38, no. 1, pp. 27–63, 2006.

[8] M. Belloli, S. Giappino, F. Robustelli, and C. Somaschini, "Drafting Effect in Cycling: Investigation by Wind Tunnel Tests," *Procedia Engineering*, vol. 147, pp. 38 – 43, 2016. The Engineering of SPORT 11.

[9] X.-Y. Lu and J. Hedrick, "Practical string stability for Longitudinal Control of Automated Vehicles," *Vehicle System Dynamics*, vol. 41, Jan. 2004.

[10] P. A. Ioannou and C. C. Chien, "Autonomous intelligent cruise control," *IEEE Transactions on Vehicular Technology*, vol. 42, pp. 657–672, Nov 1993.

[11] G. J. L. Naus, R. P. A. Vugts, J. Ploeg, M. J. G. van de Molengraft, and M. Steinbuch, "String-Stable CACC Design and Experimental Validation: A Frequency-Domain Approach," *IEEE Transactions on Vehicular Technology*, vol. 59, pp. 4268–4279, Nov 2010.

[12] SAE International, *J3016: Taxonomy and Definitions for Terms Related to Driving Automation Systems for On-Road Motor Vehicles*, June 2018.

[13] S. Tsugawa, S. Jeschke, and S. E. Shladover, "A Review of Truck Platooning Projects for Energy Savings," *IEEE Transactions on Intelligent Vehicles*, vol. 1, pp. 68–77, March 2016.

[14] P. Smith and D. Bevly, "Analysis of On-Road Highway Testing for a Two Truck Cooperative Adaptive Cruise Control (CACC) Platoon," in *COMVEC*, SAE Paper 2020-01-5009, SAE International, 2020.

[15] W. G. Apperson, "Design and Evaluation of Cooperative Adaptive Cruise Control System for Heavy Freight Vehicles," Master's thesis, Auburn University, 2019.

[16] P. Smith, J. Ward, J. Pierce, D. Bevly, and R. Daily, "Experimental Results and Analysis of a Longitudinal Controlled Cooperative Adaptive Cruise Control (CACC) Truck Platoon," in *Dynamic Systems and Control*, DSCC2019-9135, Oct. 2019.

[17] B. McAuliffe, M. Lammert, X.-Y. Lu, S. Shladover, M.-D. Surcel, and A. Kailas, "Influences on Energy Savings of Heavy Trucks Using Cooperative Adaptive Cruise Control,"

in *WCX World Congress Experience*, SAE Paper 2018-01-1181, SAE International, Apr. 2018.

[18] B. R. McAuliffe and A. S. Wall, "Aerodynamic Performance of Flat-Panel Boat-Tails and Their Interactive Benefits with Side-Skirts," in *SAE Int. J. Commer. Veh.*, vol. 9(2), pp. 70–82, SAE International, Sept. 2016.

[19] B. McAuliffe and M. Ahmadi-Baloutaki, "A Wind-Tunnel Investigation of the Influence of Separation Distance, Lateral Stagger, and Trailer Configuration on the Drag-Reduction Potential of a Two-Truck Platoon," in *SAE Int. J. Commer. Veh.*, vol. 11(2), pp. 125–150, SAE International, June 2018.

[20] K. Salari and J. Ortega, "Experimental Investigation of the Aerodynamic Benefits of Truck Platooning," in *WCX World Congress Experience*, SAE Paper 2018-01-0732, SAE International, Apr. 2018.

[21] B. McAuliffe and M. Ahmadi-Baloutaki, "An Investigation of the Influence of Close-Proximity Traffic on the Aerodynamic Drag Experienced by Tractor-Trailer Combinations," in *SAE Int. J. Adv. & Curr. Prac. in Mobility*, vol. 1(3), pp. 1251–1264, SAE International, Apr. 2019.

[22] H. Humphreys and D. Bevly, "Computational Fluid Dynamic Analysis of a Generic 2 Truck Platoon," in *SAE 2016 Commercial Vehicle Engineering Congress*, SAE Paper 2016-01-8008, SAE International, Sept. 2016.

[23] P. Vegendla, T. Sofu, R. Saha, M. Madurai Kumar, and L.-K. Hwang, "Investigation of Aerodynamic Influence on Truck Platooning," in *SAE 2015 Commercial Vehicle Engineering Congress*, SAE Paper 2015-01-2895, SAE International, Sept. 2015.

[24] M. Ellis, J. I. Gargoloff, and R. Sengupta, "Aerodynamic Drag and Engine Cooling Effects on Class 8 Trucks in Platooning Configurations," in *SAE Int. J. Commer. Veh.*, vol. 8(2), pp. 732–739, SAE International, Sept. 2015.

[25] M. Siemon, P. Smith, D. Nichols, D. Bevly, and S. Heim, "An Integrated CFD and Truck Simulation for 4 Vehicle Platoons," in *WCX World Congress Experience*, SAE Paper 2018-01-0797, SAE International, Apr. 2018.

[26] D. Bevly, C. Murray, A. Lim, R. Sesek, and et al., "Heavy Truck Cooperative Adaptive Cruise Control: Evaluation, Testing, and Stakeholder Engagement for Near Term Deployment: Phase Two Final Report," Technical Report, Auburn University, Apr. 2014.

[27] M. P. Lammert, A. Duran, J. Diez, K. Burton, and A. Nicholson, "Effect of Platooning on Fuel Consumption of Class 8 Vehicles Over a Range of Speeds, Following Distances, and Mass," in *SAE Int. J. Commer. Veh.*, vol. 7(2), pp. 626–639, SAE International, Oct. 2014.

[28] SAE International, *J1321: Fuel Consumption Test Procedure - Type II*, Feb. 2012.

[29] P. Gururaja, "Wind-Averaged Drag Determination for Heavy-Duty Vehicles Using On-Road Constant-Speed Torque Tests," in *SAE 2016 Commercial Vehicle Engineering Congress*, SAE Paper 2016-01-8153, SAE International, Sept. 2016.

[30] A. Ragatz and M. Thornton, "Aerodynamic Drag Reduction Technologies Testing of Heavy-Duty Vocational Vehicles and a Dry Van Trailer," Tech. Rep. NREL/TP-5400-64610, National Renewable Energy Laboratory, Oct. 2016.

[31] M. Moomen, M. Rezapour, A. M. Molan, and K. Ksaibati, "Assessing Road Load Coefficients of a Semi-Trailer Combination Using a Mechanical Simulation Software with Calibration Corrections," in *SAE Int. J. Commer. Veh.*, vol. 12(1), pp. 31–43, SAE International, 2019.

[32] S. Hausberger, M. Rexeis, J. Blassnegger, and G. Silberholz, "Evaluation of fuel efficiency improvements in the Heavy-Duty Vehicle (HDV) sector from improved trailer and tire designs by application of a new test procedure," Tech. Rep. Report No. I-24/2011 Hb-Em 18/11/679, Institute for Internal Combustion Engines and Thermodynamics, Dec. 2011.

[33] B. R. McAuliffe and D. Chuang, "Coast-down and constant-speed testing of a tractor-trailer combination in support of regulatory developments for greenhouse gas emissions," Tech. Rep. LTR-AL-2016-0019-R, National Research Council Canada, May 2017.

[34] P. Hong, B. Marcu, F. Browand, and A. Tucker, "Drag Forces Experienced by Two, Full-Scale Vehicles at Close Spacing," in *International Congress & Exposition*, SAE Paper 980396, SAE International, Feb. 1998.

[35] M. Duoba and A. Fernandez Canosa, "On-Track Measurement of Road Load Changes in Two Close-Following Vehicles: Methods and Results," in *WCX SAE World Congress Experience*, SAE Paper 2019-01-0755, SAE International, Apr. 2019.

[36] B. McAuliffe, "Aerodynamic Drag Reduction of Heavy Trucks using a Cooperative Adaptive Cruise Control System," in *Presentation only at SAE COMVEC*, 18-AERO-0006 Session, 2018. https://www.researchgate.net/publication/340273961_Aerodynamic_Drag_Reduction_of_Heavy_Trucks_using_a_Cooperative_Adaptive_Cruise_Control_System.

[37] K. Steudle and N. Annelin, "Buckendale lecture series: Transformational technologies reshaping transportation—a government perspective," in *COMVEC*™, SAE International, Sept. 2018.

[38] SAE International, *J1939: Vehicle Application Layer - J1939-71*, Apr. 2014.

[39] M. P. Lammert, B. McAuliffe, P. Smith, A. Raeesi, M. Hoffman, and D. Bevly, "Impact of Lateral Alignment on the Energy Savings of a Truck Platoon," in *WCX SAE World Congress Experience*, SAE Paper 2020-01-0594, SAE International, Apr. 2020.

[40] M. Quigley, K. Conley, B. P. Gerkey, J. Faust, T. Foote, J. Leibs, R. Wheeler, and A. Y. Ng, "ROS: an open-source Robot Operating System," in *ICRA Workshop on Open Source Software*, 2009.

[41] W. Travis and D. M. Bevly, "Trajectory duplication using relative position information for automated ground vehicle convoys," in *2008 IEEE/ION Position, Location and Navigation Symposium*, pp. 1022–1032, May 2008.

[42] D. Baum, C. D. Hamann, and E. Schubert, "High Performance ACC System Based on Sensor Fusion with Distance Sensor, Image Processing Unit, and Navigation System," in *Vehicle System Dynamics: International Journal of Vehicle Mechanics and Mobility*, vol. 28, pp. 327–338, 1997.

[43] R. C. Coulter, "Implementation of the Pure Pursuit Path Tracking Algorithm," Tech. Rep. CMU-RI-TR-92-01, Carnegie Mellon University, Pittsburgh, PA, January 1992.

[44] B. McAuliffe, A. Raeesi, M. Lammert, P. Smith, M. Hoffman, and D. Bevly, "Impact of Mixed Traffic on the Energy Savings of a Truck Platoon," in *WCX SAE World Congress Experience*, SAE Paper 2020-01-0679, SAE International, Apr. 2020.

[45] PMG Technologies, "High Speed Oval - BRAVO." `https://www.pmgtest.com/facilities/tracks`. Accessed: 1-14-2020.

[46] A. Schneider, "GPS Visualizer." `https://www.gpsvisualizer.com/about.html`. Accessed: 1-14-2020.

[47] NCAT Test Track. Twitter, Aug. 2018. `pavetrack.com`.

[48] M. E. Heffernan, "Simulation, Estimation, and Experimentation of Vehicle Longitudinal Dynamics that Effect Fuel Economy," Master's thesis, Auburn University, 2006.

[49] Airmar, "220WX WeatherStation®Instrument." `http://airmartechnology.com/weather-description.html?id=153`. Accessed March 21, 2020.

[50] SAE International, *J1263: Road Load Measurement and Dynamometer Simulation Using Coastdown Techniques*, Mar. 2010.

[51] SAE International, *J2263: Road Load Measurement Using Onboard Anemometry and Coastdown Techniques*, Dec. 2008.

[52] Surface Vehicle Recommended Practice - Work in Progress, *J2978: Road Load Measurement Using Coastdown Techniques*. SAE International, 2017. http://standards.sae.org/wip/j2978/.

[53] B. R. McAuliffe, M. Croken, M. Ahmadi-Baloutaki, and A. Raeesi, "Fuel-economy testing of a three-vehicle truck platooning system," Technical Report No. LTR-AL-2017-0008, National Research Council Canada, Apr. 2017.

[54] M.-D. Surcel and J. Michaelsen, "Fuel Consumption Tests for Evaluating the Accuracy and Precision of Truck Engine Electronic Control Modules to Capture Fuel Data," in *SAE 2009 Commercial Vehicle Engineering Congress & Exhibition*, SAE Paper 2009-01-1605, SAE International, May 2009.

Appendices

Appendix A

CACC Controller

A.1 Control Gains

As previously mentioned, the controller gains are in terms of the longitudinal model parameters. The controller gains are re-calcualted everytime the system starts or stops. An example of the controller gains used for the Canada fuel test are shown in Table A.1. It is important to note the negative sign is due to the controller error convention. For example, a negative error means the following vehicle is further away from the reference and produces a positive torque.

Table A.1: Example controller gains with m = 29,792 kg and τ = [12.5, 6.25, 2.5] seconds.

Gear	$\mathbf{k_P}$	$\mathbf{k_I}$	$\mathbf{k_D}$	$\omega_{\mathbf{BW}}$ **[rad/s]**
1	-69.95	-3.29	-205.95	0.341
2	-71.37	-3.36	-230.05	0.370
3	-83.92	-3.95	-361.09	0.527
4	-106.37	-5.01	-530.52	0.643
5	-127.93	-6.02	-675.33	0.693
6	-172.41	-8.11	-956.32	0.739
7	-235.65	-11.09	-1340.87	0.763
8	-322.08	-15.16	-1856.69	0.776
9	-470.56	-22.14	-2733.69	0.784
10	-594.46	-27.97	-3462.16	0.786

The controller gains for each gear all use the same time constants. This is the current implementation, but the time constants could differ for each gear if desired. The closed loop bandwidth is also shown in the table for this configuration as well.

Appendix B

Fuel Test and Analysis

B.1 Test Procedures

This section describes the test procedures that were used for the Canada fuel test campaign. Before any testing, the professional drivers visually inspected each vehicle. All vehicles then completed a 1 hour warm-up to ensure the vehicle is in proper condition for testing. Note, additional warm-ups were completed as needed if the next test did not begin within 30 minutes of the last test ending. After the warm-up, the vehicles were parked in the staging area in the correct order: A1, A2, and control vehicle.

Each test was completed following the procedure in Table B.1. This procedure is specific to the platooning test runs, but a similar procedure was used for the baselines as well. The only difference between the platooning and baseline runs was the appropriate delay/start of truck 2 and control vehicles, in order to have all three vehicles run isolated simultaneously. After completion of the test procedure, the fuel tanks were removed and the weights were recorded.

Table B.1: Test Procedure for platooning test runs.

Platooning Test Procedure	
Truck 1/2	Key on the vehicle and check system, start logging systems
Truck 1/2	Simultaneously start ignition of platooning vehicles
Truck 1/2	Idle for 1 minute, check that the CACC system is ready
Truck 1/2	Countdown and both platooning vehicles depart staging area
Truck 1/2	Truck 1/2 get up to speed in East curve
Truck 1	Set ACC in North straight and signal with vehicle flashers
Truck 2	Engages platooning
Platoon completes approximately $1/3$ of a lap	
Control	Key on the vehicle and check system, start logging systems
Control	Start ignition and idle for 1 minute
Control	Countdown and depart staging area
Control	Get up to speed and set ACC
Platoon and control vehicle are approximately half track length apart	
Platoon and control vehicle complete 13 laps of test	
Truck 1/2	After West curve, disengage control systems, switch into neutral and coast
Truck 1/2	Apply service brakes as needed, stop vehicles at staging area
Truck 1	Idle after parking vehicle
Truck 2	Idle for 1 minute after parking vehicle
Truck 1/2	Turn off engine, end of test
Control	After West curve, disengage ACC, switch into neutral and coast
Control	Apply service brakes as needed, stop at staging area
Control	Idle for 1 minute after parking vehicle
Control	Turn off engine, end of test

B.2 J1321 Gravimetric Fuel Analysis

The Society of Automotive Engineers (SAE) provides a procedure to determine the impact of various technologies on fuel consumption. This document is the SAE J1321 standard titled "Fuel Consumption Test Procedure - Type II". The purpose of the document is to provide a standard test procedure to determine the change in fuel consumption by "adding, removing, or modifying a vehicle component or system" [28]. In the context of this paper, truck platooning, i.e. two vehicles traveling in close proximity to each other, is the vehicle modification to be evaluated. The standard describes the test procedures, requirements/limitations, and important

parameters for a result to classify as a "J1321-Type II" test result. This appendix describes how to calculate a J1321 fuel result using gravimetric, or weight, fuel measurements.

The J1321 calculations are based off the ratios of fuel consumed for a test to control vehicle. The test vehicle is the vehicle being evaluated, and the control vehicle is used to compare all measurements to. In order to compare the measurements, the control vehicle always operates unchanged, isolated and at the same time as the test vehicles. The control vehicle is used to reduce run to run variations from the environment, control system, and human error. The fuel mass ratio of test vehicle (T) to control vehicle (C) is then:

$$\frac{T}{C} = \frac{m_{f,test}}{m_{f,control}} \tag{B.1}$$

Where m_f is the weight fuel measurement for a given vehicle and run. The results for a single run are the fuel weights and the calculated T/C ratio. This result is specific to a single vehicle and the given test configuration, such as the lead vehicle of the aligned platoon at *x* meter gap spacing. In order to calculate the fuel savings for a vehicle, two items are needed:

- A minimum of 3 valid baseline, or reference, run measurements
- A minimum of 3 valid test run measurements

In this test campaign, the reference measurements represent a single vehicle operating while not in platoon configuration. The reference runs are used to compare to the test configurations. Then, the test measurements include when a vehicle was in a platoon at a given configuration. The result of a platooning *test* are the T/C ratios for the lead and following vehicles. After completion of all testing, the T/C ratios are calculated for all reference and test runs, for each vehicle. The fuel savings are defined as the percent change in fuel usage as:

$$\Delta F = \frac{\overline{(\frac{T}{C})}_{baseline} - \overline{(\frac{T}{C})}_{test}}{\overline{(\frac{T}{C})}_{baseline}} \tag{B.2}$$

Where $\overline{(\frac{T}{C})_i}$ is the average of the 3 or more T/C ratios for the baseline or test segment. The resulting ΔF quantity is the percent fuel savings for a given test configuration. An Excel

spreadsheet is provided with the J1321 standard to calculate the T/C ratios and fuel savings. In addition, the standard provides a measure of uncertainty for each fuel result. The uncertainty is derived using a 95% Confidence Interval (CI) and is shown in Appendix B of [28]. The final J1321-Type II result is then:

$$\Delta F \pm \delta f \tag{B.3}$$

Where δf is the 95% CI for the fuel result.

B.3 Calibrated Fuel Rate

Another method of fuel analysis can be completed using fuel volume measurements. The fuel rate signal is readily available on most vehicles or can be obtained by installing a fuel flow meter. A fuel volume can then be calculated by integrating the fuel rate signal:

$$V_{calculated} = \int \dot{v}_f dt \tag{B.4}$$

Where $\dot{v}_f$ is the fuel rate signal, and $V_{calculated}$ is the volume calculated from the fuel rate integration.

In this test campaign, the J1939 fuel rate signal was read and recorded for this analysis. However, prior research suggests that the Electronic Control Modules fuel rate signal can differ from the true fuel consumption [54]. Lammert et al. describe a method to handle this discrepancy by calibrating the fuel rate signal with gravimetric fuel measurements [39]. This section describes the process used to calibrate the fuel rate signals. In order to calibrate the fuel rate, a scaling factor is needed to relate the measured fuel weight, $m_{measured}$, and the calculated fuel volume, $V_{calculated}$. The scaling factor, C_f is calculated as:

$$C_f = \frac{m_{measured}}{V_{calculated}} = \frac{m_{measured}}{\int \dot{v}_f dt} \tag{B.5}$$

Any number of calibration data points can be used as long as a test run has gravimetric and fuel rate data. C_f is then found using a linear regression on the calibration data, as shown in Figure B.1.

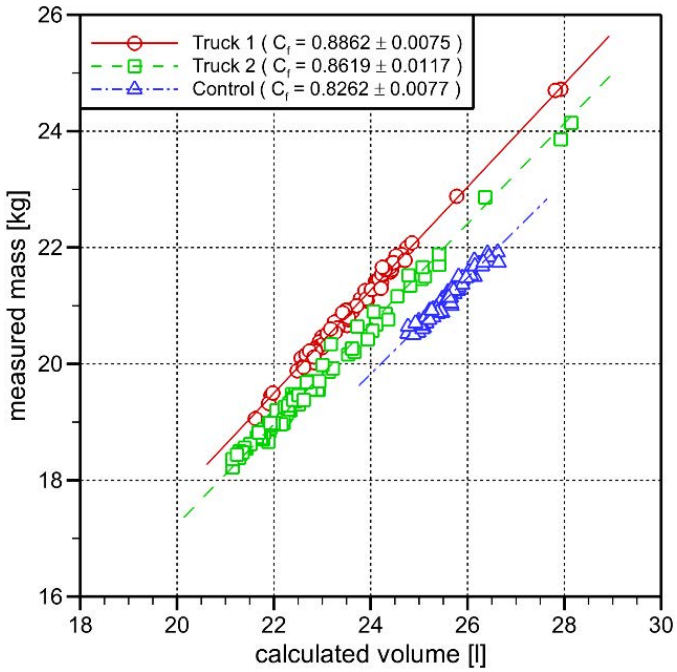

Figure B.1: Fuel rate calibration. Reprinted with permission from [39]. ©SAE International; National Renewable Energy Laboratory; National Research Council Canada.

The calibrated fuel rate measurement can be used in the same analysis described by the J1321 standard. For example, the calibrated fuel rate T/C ratio would look like:

$$(\frac{T}{C})_{segment} = \frac{C_{f,i} \int_{t_{start,i}}^{t_{end,i}} \dot{v}_{f,i} dt}{C_{f,C} \int_{t_{start,C}}^{t_{end,C}} \dot{v}_{f,C} dt} \tag{B.6}$$

Where the subscript i represents the test vehicle, either the lead or following vehicle, and C is the control vehicle. The $segment$ and corresponding time interval, t_{start} to t_{end}, subscripts are used to describe a portion of a test that is desired to study. For example, Lammert et al. shows how the straight and curved segments were extracted as part of the fuel consumption analysis [39]. The calibrated fuel rate analysis is powerful because portions of a test can be isolated and studied, which is not possible with gravimetric measurements.

B.4 Sample SAE J1321 Calculation

SAE 1321 Data Analysis - Fuel Economy Improvement Testing

Baseline Segment			
Gallons or Lbs			
Run	Test	Control	T/C
1	22.00	21.34	1.0309
2	22.46	22.08	1.0172
3	21.96	21.58	1.0176
4	21.46	21.50	0.9981
5	20.76	20.54	1.0107
6	20.86	20.52	1.0166
7	20.68	20.50	1.0088
8	20.90	20.70	1.0097
9			
10			
11			
12			
13			
14			
15			

Test Segment			
Gallons or Lbs			
Run	Test	Control	T/C
1	18.94	21.00	0.9019
2	18.98	20.86	0.9099
3	18.88	20.86	0.9051
4			
5			
6			
7			
8			
9			
10			
11			
12			
13			
14			
15			

Test Result			
	Nominal	Confidence Interval	
Fuel Saved	10.66%	±	1.29%
Improvement	11.93%	±	1.44%

Summary Stats		
	Baseline	Test
Mean T/C	1.0137	0.9056
Number of Data Points	8	3
Standard Deviations	0.0094	0.0040
Variances	0.0000892	0.0000161
Difference in Means	0.1081	

F-Test for Equal Variances	
Baseline T/C Variance	0.00009
Test T/C Variance	0.00002
F test stat (test/baseline)	0.18056
F low	0.02541
F high	6.54152
Are Variances Equal ?	yes

T-Test with Equal Variances (2-tailed)	
Pooled St dev	0.00854
t-crit	2.262
t-stat	18.694
Is Fuel Economy Improved ?	yes
P-value	0.0000
lower CI bound	0.095001
upper CI bound	0.121160

T-Test with Unequal Variances (2-tailed)	
df (nu)	8.482
t-crit	2.283
t-stat	26.597
Is Fuel Economy Improved ?	yes
P-value	0.0000
lower CI bound	0.098802
upper CI bound	0.117360

	CI t-critical	2.262
	CI std err term	0.00578

Description

This worksheet provides an analysis for the comparison of mean fuel consumption between a Test and Control vehicle. The chosen confidence level is 95%. The outcome of an f-test for equal variance is used to choose the appropriate t-test for difference in means.

Instructions

1) Conduct a minimum of 3 Baseline segment runs entering Test and Control fuel consumption values, in the Test and Control columns of the Baseline table. T/C values are computed in the gray column.

2) Conduct a minimum of 3 Test segment runs entering Test and Control fuel consumption values, in the Test and Control columns of the Test table. T/C values are computed in the gray column.

3) Review the F-test results - if variances are equal - the information shown in the T-Test with equal variance results table are used. If variances are unequal - the information shown in the T-Test with unequal variance results table are used.

4) For statistically justified fuel economy improvement,the appropriate t-test must show a "YES" in the box for "Is Fuel Economy Improved?" question.

5) Now review the Test Result box at the top of the worksheet.

The nominal value is determined from an analysis of the measured fuel consumption data only and reflects the measured change in fuel consumed resulting from the modification to the test vehicle. The confidence interval value is determined from the variation (scatter) in the measured fuel consumption data, relative to the nominal value, and the number of data values obtained. The confidence interval is shown as a ± value about the nominal value. A confidence interval is a range around the nominal value that conveys how precise the nominal value is and indicates the reliability of the nominal value.

A desirable result is to have the confidence interval column value that is significantly less than the nominal value column. A Nominal positive value for Fuel Saved or Improvement is only valid if the minimum value is also positive.

Figure B.2: Sample J1321 calculation using SAE provided spreadsheet in [28].

B.5 Fuel Test Gravimetric Results

The gravimetric fuel saving results from the Canada fuel test are summarized in Table B.2. The first surrounding vehicle traffic uses the new traffic baselines to evaluate the savings, and the second surrounding vehicle traffic test uses the isolated vehicle baselines for the reference.

Table B.2: Gravimetric fuel saving results from SAE J1321 testing and analysis.

Test	**Separation Time [s]**	**Separation Distance [m]**	**Lead Vehicle Savings [%]**	**Following Vehicle Savings [%]**
Aligned	0.32	9.1	6.0 ± 1.5	10.7 ± 1.3
	0.42	12.2	4.8 ± 1.6	12.1 ± 1.5
	0.53	15.2	3.3 ± 1.5	11.9 ± 1.3
	0.79	22.9	2.0 ± 1.6	11.0 ± 1.4
	1.58	45.7	0.2 ± 1.7	7.4 ± 1.3
	2.71	78.6	1.0 ± 1.6	6.1 ± 1.3
Surrounding Vehicle Traffic (New Traffic RF)	0.32	9.1	5.7 ± 1.7	9.4 ± 1.2
	0.53	15.2	2.7 ± 1.5	9.3 ± 1.2
	0.79	22.9	1.2 ± 2.9	8.4 ± 1.5
	1.58	45.7	1.0 ± 1.7	6.4 ± 1.7
	2.71	78.6	2.1 ± 2.8	3.4 ± 1.8
Surrounding Vehicle Traffic (Isolated Vehicle RF)	0.32	9.1	11.2 ± 1.5	13.9 ± 0.8
	0.53	15.2	8.3 ± 1.5	13.7 ± 0.8
	0.79	22.9	6.9 ± 1.8	12.9 ± 1.3
	1.58	45.7	6.7 ± 1.4	10.9 ± 0.8
	2.71	78.6	7.7 ± 1.8	8.1 ± 1.4

Appendix C

Coastdown Test and Analysis

C.1 Test Procedures

This section describes the test procedures that were used for the coastdown testing at NCAT. Before any testing, the professional drivers visually inspected each vehicle. The coastdown vehicle completed at least a 30 minute warmup prior to testing. Each test was completed following the procedure in Table C.1. This procedure was used for the baselines and the platoon coastdowns. During the testing, four coastdowns were completed in a single direction and then the tests were repeated in the opposite direction.

Table C.1: Test procedure for coastdown test.

Coastdown Test Procedure	
Coastdown/Controlled	Travel in the correct configuration (single vehicle, platoon leader, platoon follower) in the desired track direction at 80 km/hr
Controlled	Move to proper distance from coastdown vehicle; engage CACC system at specified gap distance for test
Once CACC system is engaged, coastdown vehicle controls the rest of the test	
Coastdown	When entering curve on the North side of the track, maintain 80 km/hr through curve
Coastdown	At exit of curve and on the South straight, accelerate to 89 km/hr for beginning of test
Coastdown	Once high target speed is reached, driver lets foot off the throttle, shifts into neutral
Start high speed segment	
Coastdown	Coast through high speed segment until 72 km/hr is met or end of straight segment
End high speed segment	
Coastdown	Through opposite curve, apply braking to slow vehicle speed to prep for low speed range
Coastdown	Once at target speed on North side of the track, remove foot from pedals (no braking, neutral gear still)
Start low speed segment	
Coastdown	Coast through low speed segment until 8 km/hr
Coastdown	Put back into drive
End low speed segment	
Coastdown/Controlled	Prepare for next coastdown test

C.2 Coastdown Modeling

The coastdown test involves a vehicle coasting un-powered through a speed range, modeling the resistive forces, and calculating vehicle parameters from the test. In particular, the coastdown is used to solve for a vehicle's drag area ($C_D A$) and coefficient of rolling resistance (C_{RRO}). This section describes the models used for the coastdown, which are the same as defined by McAuliffe and Chuang [33]. First, the Free Body Diagram is used with Newton's 2nd law to model the coasting vehicle as

$$m_e \frac{dv}{dt} = -F_{aero} - F_{RR} - F_{mech} - F_{grade}. \tag{C.1}$$

where m_e is the effective mass, v is the speed, and F_i are the resistive forces. The effective mass is a combination of the tractor and trailer mass plus the rotational inertia of the wheels. The effective mass in kg can be approximated by Equation (C.2) as

$$m_e = m_{vehicle} + (56.7 \times n) \tag{C.2}$$

where n is the number of tires. These tractor-trailers have 18 tires, so $n = 18$ in this calculation. Now, models of the resistive forces are used to complete the full EOM.

The aerodynamic force is the main focus of the coastdown test. This is the resistive force the vehicle experiences when traveling through the air. The aerodynamic force (F_{aero}) is defined as

$$F_{aero} = \frac{1}{2}\rho U^2 C_D(\psi) A \tag{C.3}$$

where ρ is the air density, U is the relative wind speed, $C_D(\psi)A$ is the drag area as a function of yaw angle. The drag area is the drag coefficient (C_D) multiplied by the frontal area, A, but can also be written as $C_D A = F_{aero}/Q$ where Q is the dynamic pressure of the wind ($Q = \frac{1}{2}\rho U^2$). In this form, the drag area is a convenient measure of aerodynamic performance that is independent of vehicle geometry.

The force of rolling resistance is a result of the vehicle's tires interacting with the ground surface. This force depends on a number of factors such as road surface, tires, loading, and vehicle speed. The force of rolling resistance is defined as

$$F_{RR} = C_{RR}(v) \times W \tag{C.4}$$

assuming that the force of rolling resistance is only impacted by the vertical load on the tires. In low grade scenarios, the vertical load on the tires is the vehicle weight, W. The coefficient of rolling resistance, C_{RR}, is velocity dependent and can be expanded shown by

$$F_{RR} = C_{RRO} \times R_{RR}(v) \times W \tag{C.5}$$

where C_{RRO} is the near-zero velocity component and $R_{RR}(v)$ is a velocity dependent component. The EPA provided data for "Smartway" verified tires such that the velocity dependence is shown as [33]:

$$R_{RR} = \frac{C_{RR}}{C_{RRO}} = (1.33 \times 10^{-4})v^2 + (7.96 \times 10^{-3})v + 1.0 \tag{C.6}$$

where v has units of m/s. This model is sufficient to use for this testing because the Peterbilt trucks have Smartway verified tires.

The mechanical resistance force includes the rotational resistance and bearing losses of the driveline, such as the differential. Again, the EPA provided data for the estimated mechanical loss as a function of speed. McAuliffe and Chuang describe a second order model, Equation (C.7), that fits this data and is used here [33]. Again, the vehicle speed, v, has units of m/s.

$$F_{mech} = F_{mech}(v) = -.216v^2 + 13.2v \tag{C.7}$$

The road grade can be a significant force depending on the road grade angle, ϕ. The force of road grade is shown in Equation (C.8). This force can also be written in terms of the change in height, or elevation, divided by the distance traveled.

$$F_{grade} = W \times \sin(\phi) = W \times \frac{dh}{ds} \tag{C.8}$$

Combining the previous forces and substituting into Equation (C.1) results in the full EOM as

$$m_e \frac{dv}{dt} = -\frac{1}{2}\rho U^2 C_D(\psi) A - C_{RRO} R_{RR}(v) \times W - F_{mech}(v) - W\frac{dh}{ds}. \tag{C.9}$$

C.3 High/Low Solution Method

This section describes the solution method to solve the coastdown EOM given two speed ranges, a high speed and a low speed segment, using the High/Low method. The High/Low method assumes finite difference approximations across a speed range and ignores the variation within the range. This replaces the derivatives with differences and uses average values for the

resistive forces that are a function of speed, v. These forces include the force of air drag, rolling resistance, and mechanical resistance. The full EOM with finite differences is then shown as

$$m_e \frac{\Delta v}{\Delta t} = -\frac{1}{2}\rho C_D(\psi) A U_{avg}^2 - C_{RRO} R_{RR}(v_{avg}) \times W - F_{mech}(v_{avg}) - W\frac{\Delta h}{\Delta s}. \tag{C.10}$$

This equation can then be re-arranged in order to isolate the terms with the variables of interest: the drag area and coefficient of rolling resistance. This is shown in Equation (C.11).

$$\frac{1}{2}\rho U_{avg}^2 C_D(\psi) A + C_{RRO} R_{RR}(v_{avg}) \times W = -F_{mech}(v_{avg}) - W\frac{\Delta h}{\Delta s} - m_e \frac{\Delta v}{\Delta t} \tag{C.11}$$

After the model is re-arranged, the variables $C_D A$ and C_{RRO} are then factored out of their respective terms. Given a high and speed range, a system of equations can be formed with one equation from the high speed segment and one from the low speed. These two equations can be written in matrix form as

$$\begin{bmatrix} \frac{1}{2}\rho U_{avg,HI}^2 & R_{RR}(v_{avg,HI})W \\ \frac{1}{2}\rho U_{avg,LO}^2 & R_{RR}(v_{avg,LO})W \end{bmatrix} \begin{bmatrix} C_D A \\ C_{RRO} \end{bmatrix} = \begin{bmatrix} -F_{mech}(v_{avg,HI}) - W\frac{\Delta h}{\Delta s} - m_e \left(\frac{\Delta v}{\Delta t}\right)_{HI} \\ -F_{mech}(v_{avg,LO}) - W\frac{\Delta h}{\Delta s} - m_e \left(\frac{\Delta v}{\Delta t}\right)_{LO} \end{bmatrix} \tag{C.12}$$

where the first row is Equation (C.11) evaluated at the high speed and the second row is for the low speed. Now, Equation (C.12) is in the matrix equation form of

$$Ax = B \tag{C.13}$$

which can then be solved used matrix operations. The final solution to the coastdown equation is given as:

$$x = \begin{bmatrix} C_D A \\ C_{RRO} \end{bmatrix} = A^{-1}B. \tag{C.14}$$

This solution method was used to solve each individual coastdown test, with a high and low speed range, for the drag area and coefficient of rolling resistance. These results were then

used across a number of runs in order to determine the overall values with an average and 95% CI, like the fuel saving results.

C.4 Model Simulation

The coastdown coefficients were calculated for a number of runs in a given configuration. These coefficients were then simulated with the full EOM differential equation to validate the parameters. An example of the model simulation is shown in Chapter 4 for the baseline vehicle parameters. The model matches well, but there is a difference in the low speed model because of the un-modeled road grade in the simulation. This is shown in Figure C.1 where the model simulation is shown with and without the road grade. In the figure, the start and the end of the speed segments are shown with black X's. For the low speed segment, there is a continuous negative grade which causes the model and experimental velocities to differ. In Figure C.1b, the simulation follows the same trend as the experimental velocity for the low speed segment. These results show that the road grade causes this difference and the coefficients are valid for the analysis.

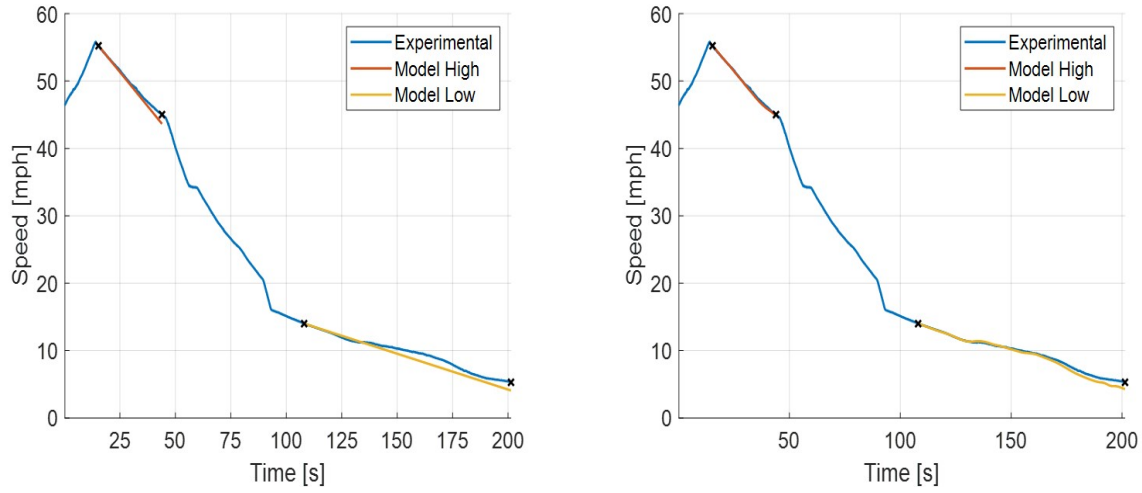

(a) Original model simulation.

(b) Model simulation with road grade.

Figure C.1: Baseline coastdown model simulation with road grade.

The model was also simulated with the coastdown parameters from the platoon coastdown. These results are shown in Figures C.2 and C.3 for the lead and following vehicle coastdown

respectively. These results also match the model well and show the same effect with the road grade.

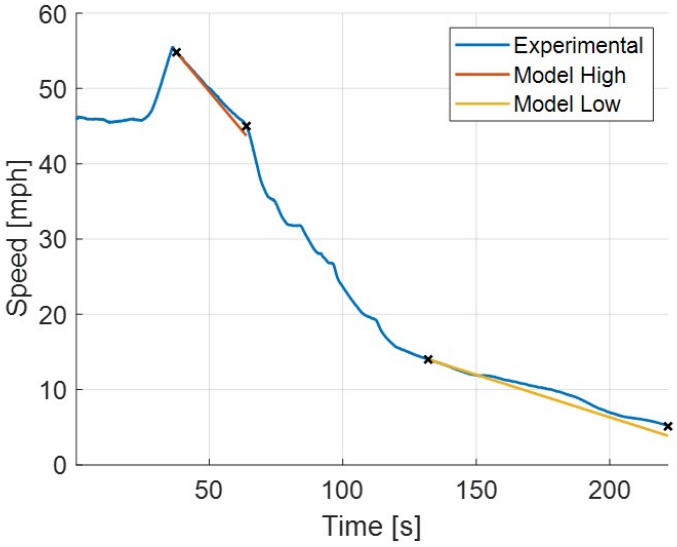

Figure C.2: Lead vehicle coastdown model simulation.

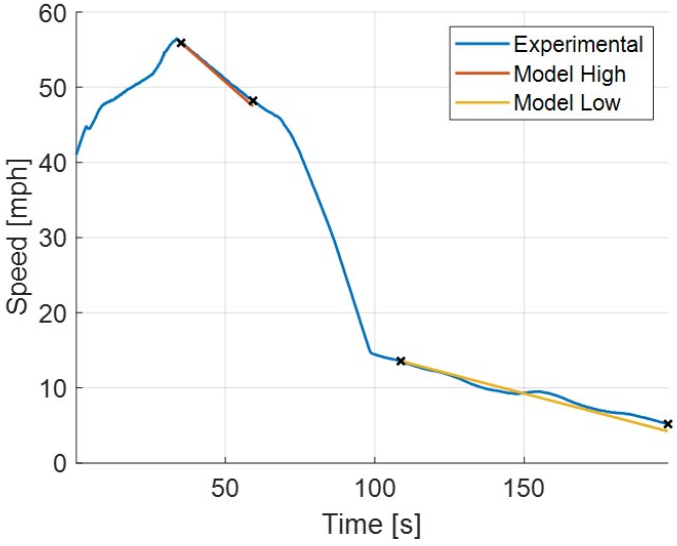

Figure C.3: Following vehicle coastdown model simulation.